PALAEOENVIRONMENTAL RECONSTRUCTION AND PROVENANCE STUDIES OF BARAIL SEDIMENTS, WEST OF KOHIMA TOWN, NAGALAND

A. Moalong Kichu

DEPARTMENT OF GEOLOGY
Nagaland University
2019

NAGALAND UNIVERSITY

May 2019

DECLARATION

I, A. Moalong Kichu, hereby declare that the subject matter of this thesis is the record of work done by me, during the period May 2014 to November 2018. That the content of this thesis has not provided the basis for the award of any previous degree to me, or to the best of my knowledge, to anybody else, and that the thesis has not been submitted by me for any research degree in any other University/Institute.

This thesis is submitted to the Nagaland University in partial fulfilment for the degree of Doctorate in Philosophy in Geology under the supervision of Dr. S.K. Srivastava of Nagaland University.

Date: 17th May, 2019
Place: Department of Geology
Nagaland University,
Kohima Campus, Meriema

A. MOALONG KICHU
Ph.D. Scholar
Department of Geology
Reg. No. 587/2014 (20th May, 2014)

Head

Professor B.V. Rao
Department of Geology
Nagaland University
Kohima Campus, Meriema

Supervisor

Dr. S.K. Srivastava
Department of Geology
Nagaland University
Kohima Campus, Meriema

NAGALAND UNIVERSITY

Dr. S.K. Srivastava
Assistant Professor
Department of Geology

Email: *sksrivastava@nagalanduniversity.ac.in*
sanjaikohima@yahoo.co.in

CERTIFICATE

The thesis presented by Mr. A. Moalong Kichu, M.Sc., bearing registration No.587/2014 dated 20.05.2014 embodies the results of investigations carried by him under my supervision and guidance.

I certify that this work has not been presented for any degree elsewhere and that the candidate has fulfilled all conditions laid down by the University.

Date: 17.05.2019

(S.K.SRIVASTAVA)
Supervisor

Acknowledgement

I have been fortunate to work under the guidance of my supervisor, Dr. Sanjai K. Srivastava and I am deeply grateful for him. He provided continuous support throughout the duration of my Ph.D. study and his extensive knowledge, unyielding patience and countless words of advice and encouragement were invaluable.

I would like to express my sincere appreciation to theHead of Department, Geology, Nagaland University, for laying the foundation necessary for me to be successful in this field; without their support and the support of all the faculty and staff in this Department, I would not have been paired with an accomplished supervisor, placed among brilliant peers, and provided with the laboratory and instruments needed for my research.

I must extend my gratitude to Mrs. Priti Srivastava and Mr. Yash Srivastava for believing in me and also for how graciously they welcomed me into their home. The time I spent with the family was always comfortable and the support they provided me throughout the years will always be appreciated.

Special thanks to Mrs. Aien Ngullie, my field partner. From the day I started this work to the very end, she was a constant source of support and help. Always a valued friend and colleague, I could have not asked for a better partner to work and learn alongside with.

I was surrounded by many talented individuals who each provided valuable contributions towards the completion of this study. I want to thank my Ph.D. colleagues, Miss. Anettsüngla and Miss J.N. Moiya in particular, for the countless stimulating conversations and for their diligence while we worked and studied together. Their supports were irreplaceable, and each one of them helped me out in their own unique way. I love them a lot.

I would like to thank Dr. Maibam and associates in the Department of Earth Sciences, Manipur University for the pulverization of samples and Dr. Jayanta Jivan Lashkar at Gauhati University for their help during the course of the work. Thanks to Mr.SupongtemjenJamir for providing me with a digitized map of Kohima district.

I would also like to acknowledge the contributions of Wadia Institute of Himalayan Geology for XRF analysis; IIT, Guwahati for SEM photography and Department of Geological Sciences, Gauhati University, Assam for XRD analysis.

I would like to extend my sincere thanks to the villagers of Jotsoma, Khonoma and Mezoma for their generosity and for providing unrestricted access to their lands in order to collect samples and study the areas necessary for completion of my work.

Coming into my life like a flash of brilliant light is Ms. Katrina McKee. My thesis work became so much easier with her encouragement and eagerness to help. Her optimism and curiosity is infectious, and has been a constant source of strength for me.

I thank Mr. Ngongo Ngullie and all my friendsand my relatives who have helped me in their own way, including everyone who has accompanied me to the fieldworks. Their constant prayers and support were invaluable and are deeply appreciated.

Lastly, but not the least, the trust, confidence, love and patience shown by my parents and siblings towards me has always been consistent throughout my life, and it mattered even more so throughout the course of this work. I dedicate this small work to this loving family.

(A. Moalong Kichu)

PARTICULARS OF THE CANDIDATE

NAME OF THE CANDIDATE	: A. Moalong Kichu
DEGREE	: Ph.D.
DEPARTMENT	: Geology
TITLE OF THE THESIS	: **Palaeoenvironment Reconstruction and Provenance Studies of Barail Sediments, West of Kohima Town, Nagaland**
DATE OF ADMISSION	: 2nd September, 2013
APPROVAL OF RESEARCH PROPOSAL	: 16th June 2014
REGISTRATION NUMBER & DATE	: 587/2014 (20th May, 2014)

Head of the Department

Biodata of the Candidate

I. PAPERS PUBLISHED

1. Srivastava, S.K.; Vadeo, K. and **Kichu, A.M.** (2015): Petrography of the Palaeogene Sandstones, south of Kohima town, Nagaland, India, *Inter. Jour. Earth Sci. and Eng.*, **8(5):**2025-2032.
2. **Kichu, A.M.** and Srivastava, S.K. (2018): Diagenetic environment of Barail Sandstones in and around Jotsoma village, Kohima district, Nagaland, India, *Jour. Of Geosciences Research*, **3(1):**31-35.
3. **Kichu, A.M.**; Srivastava, S.K. and Khesoh, K. (2018): Trace fossils from Oligocene Barail sediments in and around Jotsoma, Kohima, Nagaland – implications for palaeoenvironment, *Jour. Palaeo. Soc. India*, **63(2):**197-202.

II. ABSTRACT PUBLISHED/ORAL PRESENTATION

1. Trace fossils from Oligocene Barail sediments in and around Jotsoma, Kohima, Nagaland: Implications for palaeoenvironment, National Seminar on Geology, Geochemistry, Tectonics, Energy and Mineral Resources of NE India, Department of Geology, Nagaland University (9^{th} – 11^{th} November, 2016). Abstract Volume, p. 29.
2. Major oxide geochemistry of Oligocene Barail Sandstones, West of Kohima town, Nagaland, National Seminar on Chemistry in Interdisciplinary Research, Department of Chemistry, Nagaland University (9^{th} – 10^{th} November, 2018). Abstract Volume, p.39.

III. WORKSHOP/TRAINING ATTENDED

1. Regional workshop for Young Earth Scientists on 'Tectonics, Sedimentation and Geohazards with special reference to NE India' organized by the Department of Geology, Nagaland University (16-21 November, 2015).
2. Workshop on 'Course on Palaeontology with emphasis on the biostratigraphy and palaeoenvironmental interpretation' organized by GSI, RTI, Shillong (2-6 July, 2018).
3. National workshop on 'Sequence Stratigraphy and Basin Analysis' organized by Nagaland University and Oil India Ltd. at Department of Geology, Nagaland University (26^{th} – 30^{th} November, 2018).

Preface

This study is an attempt to reconstruct the palaeoenvironment and also to search for provenance of the Barail sediments lying west of Kohima town. Study area is approximately 40 sq. km and is spread through Jotsoma, Khonoma and Mezoma villages of Kohima District, Nagaland. The results of the present study are presented in 7 chapters, dealing with the different aspects of the study.

The **first chapter** introduces the study area, the objectives and scope of the research and the methodology adopted. Stratigraphic and tectonic framework of the study area is discussed in the **second chapter,** including regional stratigraphy and geologic setting.

The **third chapter** deals with the various lithology and sedimentary structures observed in the study area, their relationship to one another and the facies scheme developed basing on the various facies parameters. Grain size analysis and related parameters are discussed in **chapter four**, along with their geological interpretations. Textural maturity and the palaeocurrent have also been discussed in the same chapter. The **fifth chapter** discusses the petrography, diagenetic features and major oxide geochemistry of the sediments of the study area and suitable inferences are drawn. Reconstruction of palaeoenvironments and depositional history of the area is discussed in **chapter six**. The tectonic provenance and transport/dispersal mechanism of the sediments of the study area are also discussed here. The **seventh chapter** presents the summary and the conclusions of the present study.

Each of the individual chapters is arranged with all texts appearing first and the relevant tables, plates and figures following in that order.

As not much published data available on these rocks, it is expected that this thesis will provide a comprehensive document and also open new frontier for further research, especially Naga Hills.

List of tables

List of plates

List of figures

CONTENTS

CHAPTER 1

INTRODUCTION

1.1 GENERAL

Amongst the Cenozoic orogenic belts of Indian sub-continent, Himalaya is the one where stratigraphic records of collision have been studied in detail following plate tectonic paradigm. But for Assam-Arakan orogenic belt, not much data is available; though in recent times, many attempts were made to understand the tectonic complexities of the region. The Naga Hill sector is an ideal setting to examine the geodynamic processes involved in the evolution of Assam-Arakan orogenic belt through Mesozoic-Cenozoic periods. Tectonic evolution of northeastern India including the Naga Hills is directly correlated with the movement of Indian plate and its interaction with the Burmese plate in the east. It is a classic example of transformation of a passive margin set up (Kumar and Naik, 2006) into an active margin setting through time in response to the changing plate interaction and evolution of north-east south-west trending foreland basin. According to Mathur and Evans (1964), the Naga Hills can be divided into 3 distinct linear zones into Schuppen Belt, the Inner Fold Belt, and the Ophiolite Belt. Naik (1994) has suggested an oblique collision and tectonic wedge model for the region.

1.2 STUDY AREA

An area, a part of Inner Fold Belt, comprising of well-developed Oligocene Barail sediments, west of Kohima town, has been identified for the study. It is bounded between latitudes 25°36’00” N and 25°41’00” N and longitudes 94°00’00” E and 94°05’00” E of the topographic sheet no. 83 K/2 and covers an area of nearly 40 sq. km (**Fig. 1**).

1.3 GEOMORPHIC FEATURES

The average height of the area is 1350 meters above MSL, being limited by higher ranges towards south, where peaks attain heights ranging between 1700 meters to more than 1900 meters. The entire area is dissected by a prominent northerly flowing *Dzüdza* River which forms the main drainage system in the area, the *Hapuma*, *Dzütre*, *Khü* and *Dieru* rivers being the important tributaries. The higher altitudes are comprised of hard,

resistant Barail sandstones whereas splintery Disang shales constitute the low lying areas. According to Dasgupta (1977), the geomorphic features present in the area are the direct manifestations of topographic inversion.

1.4 REVIEW OF PREVIOUS LITERATURES

Much of the information on the structures and tectonics of Naga Hills and stratigraphy come from the works of Oil and natural Gas Corporation Ltd., the Directorate of Geology and Mining, Government of Nagaland and the Geological survey of India. Not much was known of the stratigraphy of Naga-Lushai-Patkai hill ranges before the pioneering surveys of F. R. Mallet (1876) of the Geological Survey of India. Evans (1932) and Mathur and Evans (1964) have also added important information to this knowledge in masterly contributions which have withstood the test of time. Brunnschweiler (1966); Bhandari *et al.* (1973); Desikachar (1974); Rangarao (1983); Ganju and Khar (1985); and Chakravarti and Banerjee (1988) have attempted regional correlation. Srivastava *et al.*, (2004) and Srivastava and Pandey, (2005) have worked on the evolution and the depositional mechanism of the Palaeogene sediments at Disang-Barail Transitional Sequences (DBTS) of Kohima district, Nagaland. Srivastava and Pandey (2011) have also worked on the provenance of the Oligocene Barail sandstones in and around Jotsoma village of Kohima district.

1.5 OBJECTIVES AND SCOPE OF PRESENT INVESTIGATION

The proposed study is an attempt to understand the un-roofing history of the source area using petrographic and geochemical characteristics, which can be correlated to the geodynamics and subsequent sedimentation history of the region. Attempts have also been made to develop a lithofacies scheme for reconstruction of the depositional environment of the Oligocene sediments of the study area. The outcome of the present research work would increase our understanding of the geodynamics and sedimentation history of the region.

The study has been carried out with the following objectives:

1. Interpretation of the depositional environment using facies analysis technique.

2. Source rock characterization using petrography, heavy minerals and geochemical properties.

1.6 HYPOTHESIS

The available literatures pertaining to the geology of this region indicate that the thick sedimentary deposits are the result of continuous sedimentation in a northeast-southwest trending linear trough formed due to sub-duction of Indian plate below the Burmese plate where huge quantities of sediments were deposited. During this period, sedimentation kept pace with subsidence and at intervals, there were periods of slight emergence which allowed coal to form. Due to the continuous subduction of the Indian plate, sediments of the Naga Hills are highly folded and faulted. The proposed study area, a part of Kohima Synclinorium, is comprised of Barail Group of sediments having a transitional/gradational contact with underlying sediments. There is not much published sedimentological data available on the study area except that of Srivastava and Pandey (2011).

1.7 METHODOLOGY

The present study shall advance along the following lines:

FIELD INVESTIGATIONS

a. Collection of random and oriented samples from suitable rock exposures both in time and space.
b. Measurement of vertical profile sections.
c. Recording and identification of Sedimentary structures including biogenic.
d. Identification of lithofacies.

LABORATORY ANALYSIS

a. Petrography and Modal analysis
b. XRD analysis for clay minerals
c. Major element analysis
d. SEM of freshly broken rock surfaces

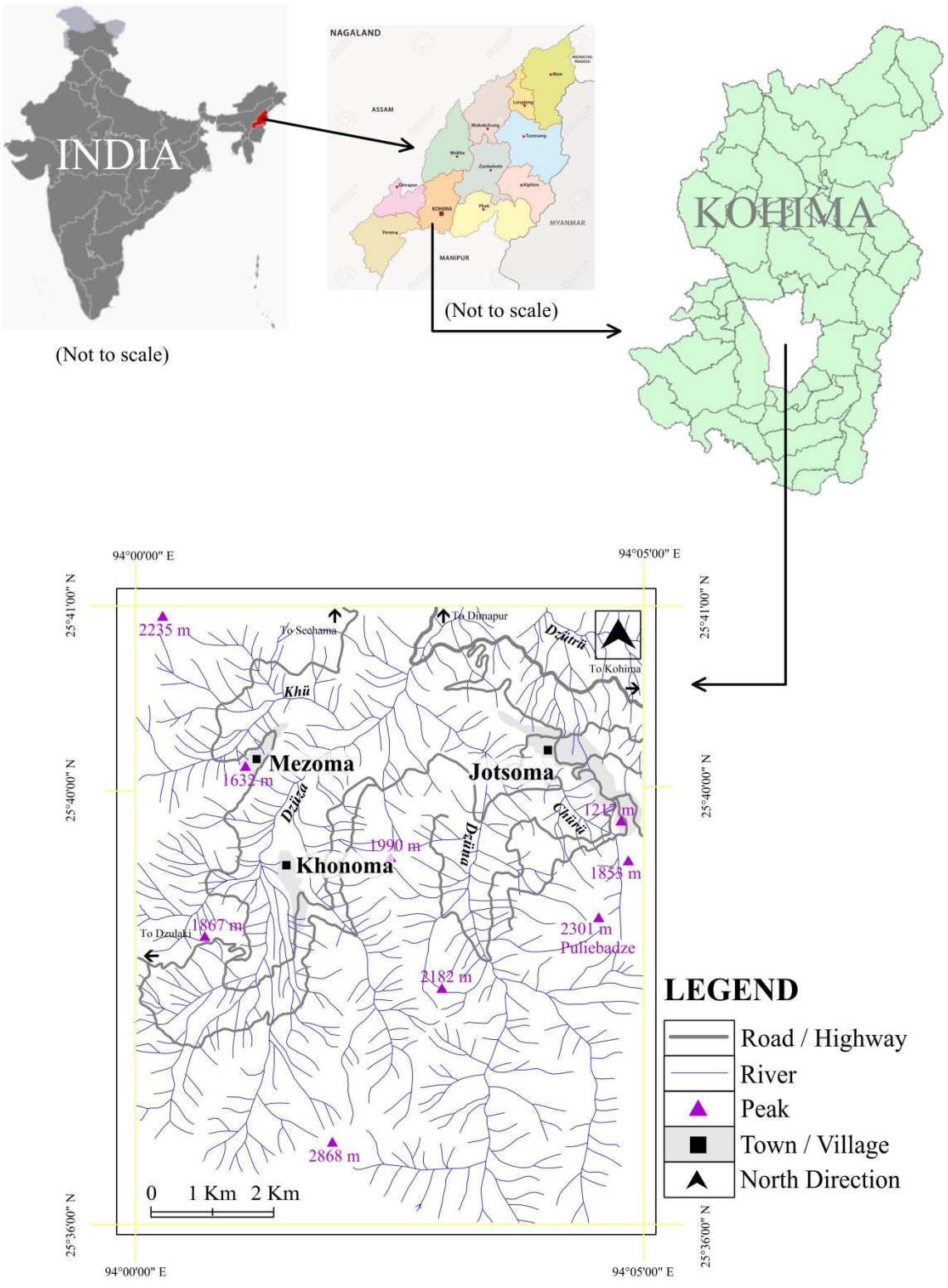

Fig. 1: Location map of the study area.

CHAPTER 2

STRATIGRAPHIC AND TECTONIC FRAMEWORK

2.1 GENERAL

Along the eastern margin of North-East India, bordering Myanmar occur spectacular NE-SW trending domain of Himalaya's cousin named Naga Hills. Owing to its location towards the northern extension of Indo-Burman Ranges (IBR; also known as AAOB), Naga Hills connects the Himalayas to the Andaman Nicobar island arc and provide an ideal setting to examine the geodynamic processes involved in the evolution of North East Indian crustal block through Mesozoic-Cenozoic period.

2.2 GEOLOGIC SETTING

The Naga Hills form a part of the northern extension of the Arakan Yoma Flysch (in Myanmar) and is bounded on the western side by the Pre-Cambrian Mikir Massif and Tertiary Shelf Sediments of Assam; and in the eastern side by the tectonic sediments of Myanmar. The early deposits of Nagaland belong to the geosynclinal facies with its northern and southern parts forming two separate major tectonic units known as the Patkai Synclinorium and the Kohima Synclinorium respectively. The three distinct morphotectonic units of the Naga Hills (**Fig. 2**) are discussed below briefly.

2.2.1 THE SCHUPPEN BELT:

The Belt of Schuppen which follows the boundary of the Assam valley alluvium for a distance of 350 km along the flank of the Naga-Patkai Hill ranges, has been defined as a narrow linear belt of imbricate thrust slices. It is postulated that this belt comprises eight or more over thrusts along which the Naga Hills has moved north-westward. It is estimated that all these thrusts together have moved horizontally approximately 200 Km. The Belt of Schuppen is marked by the Halflong-Disang thrust in the East and Naga Thrust in the West. The Belt of Schuppen is characterized by the Eocene-Oligocene and Plio-Pleistocene sediments with complete absence of Disang sediments.

2.2.2 THE INNER FOLD BELT:

The Inner Fold Belt, a part of which constitutes the study area, occupies the central part of the Naga Hills. The geological setting of this belt is characterized by Disangs, Barails as well as Disang-Barail Transitional Sequences (Srivastava, 2002). The Inner Fold Belt is represented by a series of anticlines and synclines which are confined within two major tectonic features *viz.* Halflong-Disang Thrust in the west and the Ophio-Disang Thrust in the east. This belt is occupied by Kohima Synclinorium in the South and Patkai Synclinorium in the North and the culminating point is Mokokchung and its adjoining areas. In Kohima Synclinorium, the younger Surma rocks are developed in its core (DGM, 1978). Oligocene sediments exposed in the study area have been designated as Laisong Formation of Barail Group by Geological Survey of India (Unpublished report, 1975).

2.2.3 THE NAGA OPHIOLITE BELT:

The northeast-southwest trending Ophiolite Belt runs nearly 90 Km along the Myanmar border. It is represented by tectonic slices of serpentines, volcanics and cumulates. Cherts and limestones are the associated pelagic sediments. They are often bedded with the volcanics. The bedded chert contains siliceous microfossil radolaria. An Upper Cretaceous to Lower Eocene age for the Ophiolites have been suggested on the basis of fossil assemblages from the limestone interbands. These Ophiolite suites of rocks are unconfomably overlain by an Ophiolite derived volcaniclastics with an open marine to pelagic sedimentary cover which has been designated as the Phokphur Formation by the Geological Society of India (GSI, 1975).

2.3 REGIONAL STRATIGRAPHY

The stratigraphic framework of Nagaland (**Table 1,** after Mathur and Evans, 1964; Agarwal and Ghose, 1986; and Srivastava *et al.*, 2004) consists of the following litho-units which are briefly described below.

2.3.1 NAGA METAMORPHICS:

The Naga Metamorphics were christened by Brunnschweiler (1966) mainly for the meso-grade metamorphic rocks occurring towards the Myanmar side of the Indo-Burman Ranges. It mostly consists of Proterozoic crystalline rocks. It is represented in the Naga Hills by quartzite, marble, mica schist, gneisses, etc. The base of this formation is not exposed but it is tectonically juxtaposed against or even overlay the Ophiolites as well as the Phokphur Formation. Recent studies of less deformed members of this formation have not yielded any fossil. It is regarded as Pre-Mesozoic in age by Brunnschweiler (1966).

2.3.2 NIMI FORMATION:

This lies on the eastern fringe of Nagaland and is probably a detached part of Pre-Tertiary Burmese continental crust. It stretches over 216 km, and is assumed to be of Pre-Mesozoic age. This formation consists of crystalline quartzite, phyllite, carbonaceous phyllite, quartzite-sericite schist and granites.

2.3.3 ZEPUHU FORMATION:

This formation, probably of Pre-Mesozoic age, occupies the eastern fringe of Nagaland and consists of crystalline limestone schist and schistose granite.

2.3.4 DISANG GROUP:

The Disang Group was first describe by Mallet in 1876 from the type section of the Disang river, wherein the lower part of the sequence, dark grey, finely laminated shales were predominant, but flaggy sandstones of variable thickness occur higher up in the sequence. The thickness varies between 2000 to over 3000 m. It has yielded Cretaceous fauna from the lower part and Late Eocene *Nummulites* from the upper part. The Disang Group of rocks is the oldest exposed sedimentary rock of central Naga Hills comprising the Lower Disang Formation and Upper Disang Formation, which consist of monotonous and thick successions of splintery grey shales and dark to black carbonaceous shales, shales-siltstone and sandstone rhythmities.

The surface extents of Disang Group are tectonically limited to the west by the Disang Thrust and to the east by the Naga Ophiolite complexes. The basal part of the Disang Group is not exposed anywhere but the argillaceous bed with limestone inter-bands was considered earlier to represent the Lower section of the formation because of

associated older fauna. It conformably passes upward onto the Barail Group through Disang-Barail Transitional Sequences (DBTS).

2.3.5 THE DISANG-BARAIL TRANSITIONAL SEQUENCES (DBTS):

This comprises of heterogeneous succession of alternating sand-mud lithology. The mud is made up of colored shale, ferruginous shale, and sandy shale ranging in thickness between 0.3 m and 1 m. A general decline in the thickness is observed at the higher stratigraphic levels. They display gradational base and erosional top. The sand-silt unit in the succession exhibits numerous alternations of thin, flaggy, fine grained sandstone and silty/sandy shale. Thickest beds of sandstone are nearly 1m. The sedimentary structures present in the fine sand-silt units are micro-hummocky cross stratification, cross and parallel laminations, wave ripples and gently dipping fine laminations. The contact between sand and shale is usually found to be erosional (Srivastava *et al.*, 2004).

2.3.6 BARAIL GROUP:

It was Mallet in 1876, who first studied the rock succession of this Group. But later, it was Evans (1932) who coined the name Barail and accorded the status of ‘series’ to the similar rock associates exposed in the Barail range. Barail Group is represented by the oldest Laisong Formation, the middle Jenam Formation and the youngest Renji Formation in the Assam shelf and in the Schuppen Belt, but in the Inner Fold Belt, it is undifferentiated. The upward section consists of medium grained sandstones with intercalation of shale and thin coal bands. A seismic survey (GSI, 1975) conducted in *Dhansiri* valley shows that Barail Group of rocks (Upper Eocene to Oligocene) continues with a reduced thickness in the sub thrust block of the Naga Hills.

The sedimentary structures present in the Barail lithology include ripples marks, plane laminations, channel structures and small to medium scale planer cross beddings. They are exposed in the south of Kohima town, the eastern parts of Nagaland and all along the western margin of the state.

The three formations of the Barail Group are briefly discussed below:

1) Laisong Formation: In Schuppen Belt, the Laisong Formation is the oldest litho unit recorded. It consists of hard compact and well bedded sandstones. The

sandstone show different shades of color from white to grey and becomes reddish brown and pink on weathering. The thickness of the formation measured along Dimapur-Kohima road section is 1730 m (Rangarao, 1983). Along Mokokchung-Mariani road section, a 200 m sequence of current bedded sandstones on the upthrust block of the Chungliyimsen Thrust has been recorded. This is referred to as Laisong Formation on the basis of lithological characters. In Borjan Coal Belt, the sequence of thin bedded sandstones with alternation of shale and streaks of coal has been designated as Nagaon Formation, and this is usually considered to be homotaxial to Laisong Formation. The Laisong Formation have yielded *Nummulites* and *Dictyoconoids* of Middle and Upper Eocene affinity in the north-east of Ngalwa (Acharyya, 1982) and *Operculina sp., Nummulites chavanessa* of Upper Eocene affinity from Hening Kungwla (Rangarao, 1983). Laisong Formation, in the Inner Fold Belt, gradationally overlies the Disang sediments in different synclinal troughs of Konya, Mokokchung, Zunhebuto and Kohima Syncline. It consists of medium to fine grained, well bedded, hard, light grey laminated sandstone alternating with minor grey and sandy shale with siltstone.

2) Jenam Formation: In the southern part of the Schuppen Belt, it is represented by a predominantly argillaceous sequence of dark siltstone, shale, thin sandstone bands, carbonaceous bands and a number of coal seams. The thickness of this formation along Dimapur-Kohima road section is about 800 m (Rangarao, 1983). Jenam Formation of Schuppen Belt is equated with Baragolai Formation of Upper Assam and lower part of Tikak Parbat Formation is correlated with upper units of Jenam Formation and the lower units of Renji Formation. Evans (1932) synthesized that Jenam Beds within Schuppen Belt are argillaceous in the upper part, thus forming a transition into the overlying Renji stage.

3) Renji Formation: A great thickness of ferruginous sandstone defines the top of Barail Group in the Schuppen Belt. The thickness of Renji rocks in the different tectonic slices of Schuppen Belt varies widely due to changes in depositional environment and unconformable overlap of Surma rocks. The best exposure of

Renji formation is seen in the Changki unit where it can be traced continuously from Moilang to north of Tuli, with a thickness of about 400-500 m.

Based on available palaeontological records (Acharyya, 1982; Rangarao, 1983), it is interpreted that Barail sedimentation commenced in Upper Eocene period, but in absence of diagnostic fossil beds, the period of Oligocene sedimentation is yet to be precisely confirmed. Renji Formation, the uppermost unit of the Barail Group, is conspicuously developed in the cliffs and peaks of *Japfü*, rising almost to 10,000 ft. above sea level. Evans (1932) described this unit as "a great thickness of hard, ferruginous, usually massive sandstone occurring above the soft Jenam Beds". It is made up of very thick multistoried sandstone units with a number of grit beds (2000 m).

2.3.7 JOPI FORMATION:

It is considered to be the equivalent to Barail Group. The Jopi Formation rests unconformably over the Naga Ophiolite suite of rocks, occupying different topographic levels. It consists of a thick pile of alternating and repeated sequence of polymictic conglomerate-grit-pebbly and cobble-like sandstone, greywacke and shale. The individual cycles varies in thickness from less than a meter to over 10 m, the overall thickness of the formation being more than 600 m. The basal conglomerate unit contains angular to sub rounded boulders, cobbles and pebbles derived from the underlying ophiolite suite and embedded in reworked tuffaceous/siliceous cement. The succession grades upward into grit, lithic greywacke, siltstone, sandstone and shale. The sandstone gradually becomes arkosic towards the top.

2.3.8 SURMA GROUP:

These rocks are exposed in the Belt of Schuppen in the form of a number of long, narrow strips running along almost the entire length of Nagaland on the western margin. They gradually thin out towards the north. The rocks of this group are also reported to be in the core of the Kohima Synclinorium (DGM, 1978). Alternating succession of grey laminated shale, sand and conglomerate comprises the Surma rocks in Nagaland and are of Lower Miocene age. The overall thickness of this group varies from 300-1250 m.

2.3.9 TIPAM GROUP:

A group of massive sandstones that are highly friable and contain subordinate clay and shale, known as the Tipam, unconformably overlie the Surma rocks. However, in Nagaland, the unconformity is not clear and the contact between the Tipam and Surma is usually thrusted. The molasses sediments are of Mio-Pliocene age and are massive and very friable due to improper compaction and cementation. These rocks are generally coarse grained, occasionally gritty and ferruginous and characterized by multi storied, channelled false-bedded sandstones. Because of the presence of chlorite, they are commonly green in colour but are found to be weathered to different shades of brown. The Tipam is made up of two Formations, *i.e.* the older Tipam Sandstones and the younger Girujan Clays. Tipam Sandstones are exposed along the western fringe of Nagaland in the Schuppen Belt as long, narrow strips due to strike faulting. The Girujan Clay Formation is dominated by thick sequence of mottled and varied clays with a few silt and sandstone beds.

2.3.10 NAMSANG BED:

The Namsang Beds, which belong to the Dupitila Group, lie unconformably over Girujun Clays and are confined towards the northern part of the Schuppen Belt. These beds of Mio-Pliocene age consist of sandstone, lignite pebbles, conglomerate, grit, mottled clay and lenticular seams of lignite. Thickness varies between 400-1080 m.

2.3.11 DIHING GROUP:

These consist mainly of thick pebbles beds, with clays and sands resting unconformably on the Tipam Group and Namsang beds. Rocks of Dihing Formation are well developed in Nagaland along the western margin of the Belt of Schuppen.

2.4. LITHOLOGIC UNITS, THEIR DISTRIBUTION AND FIELD RELATIONSHIPS

The geological map of the study area (**Fig. 3**) shows the distribution of various litho-units belonging to Disang Group, Barail Group and Disang-Barail Transition. Locations of rock samples and vertical profile sections have been shown in **Fig. 4**. The exposed arenaceous Barail sediments of Oligocene age in the study area, lies above mixed lithology of Disang-Barail Transition (DBTS, Srivastava, 2002; **Table 2**). The

Barail Group of rocks is represented by multistoried fine to medium sandstone with minor intercalations of shales. Wave, interference and bifurcating ripples, plane/ cross laminations and channels of varied dimensions are the sedimentary structures encountered in the study area. Coal streaks and leaf impressions are quite common. The Oligocene Barail sequences in the area also exhibit varied tectonic signatures, the most important being normal faults, anticlinal structures and shear zones. The area has been traversed by almost North-South, Northeast-Southwest and Northwest-Southeast striking faults. At places, anticlinal valleys have also been observed.

Age (approx.)	**Group**	**Outer & Intermediate Hill Ranges**	**Eastern High Hill Ranges**
Recent and Quaternary		Alluvium and high level terraces	Alluvium and high level terraces
Pleistocene		Dihing Beds	
~~*Unconformity*~~~~~~~~~~			
Mio-Pliocene		Namsang Beds	
~~*Unconformity*~~~~~~~~~~			
Miocene	Tipam	Girujan Clay Formation Tipam Sandstone Formation	
~~*Unconformity*~~~~~~~~~~			
Miocene	Surma	Bokabil Formation Bhuban Formation	
~~*Unconformity*~~~~~~~~~~			
Oligocene	Barail	Tikak Parbat Formation Baragoloi Formation Naogaon Formation	
----------*Gradational Contact*----------*Disang-Barail Transitional Sequence*--------			
Upper Cretaceous-Eocene	Disang	Disang	

Table 1: Lithostratigraphy of Naga Hills (after Mathur and Evans, 1964; Agarwal and Ghose, 1986 & Srivastava *et al.*, 2004)

Sequence	Lithology	Age	Reference
Barail Group	Sandstones with minor Shales	Oligocene	Krishnan (1982)
DBTS (Disang-Barail Transitional Sequence)	Sand silt and shale alternations	Upper Eocene	Pandey and Srivastava (1998)
Disang Group	Shale with minor sandstones	Upper Cretaceous to Middle Eocene	Krishnan (1982)

Table 2: Lithostratigraphy of the study area

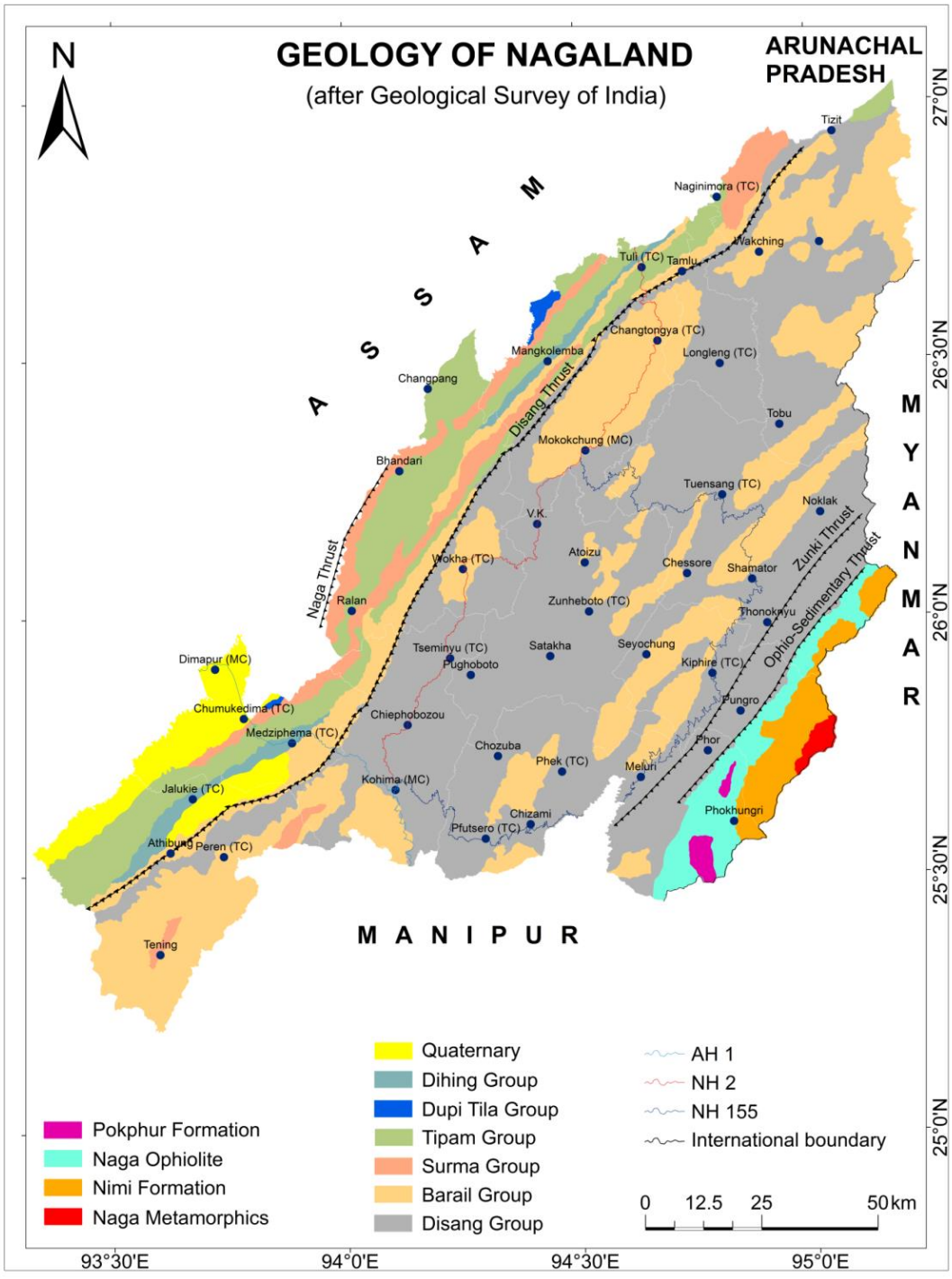

Fig. 2: Geological map of Nagaland (after GSI, 2011)

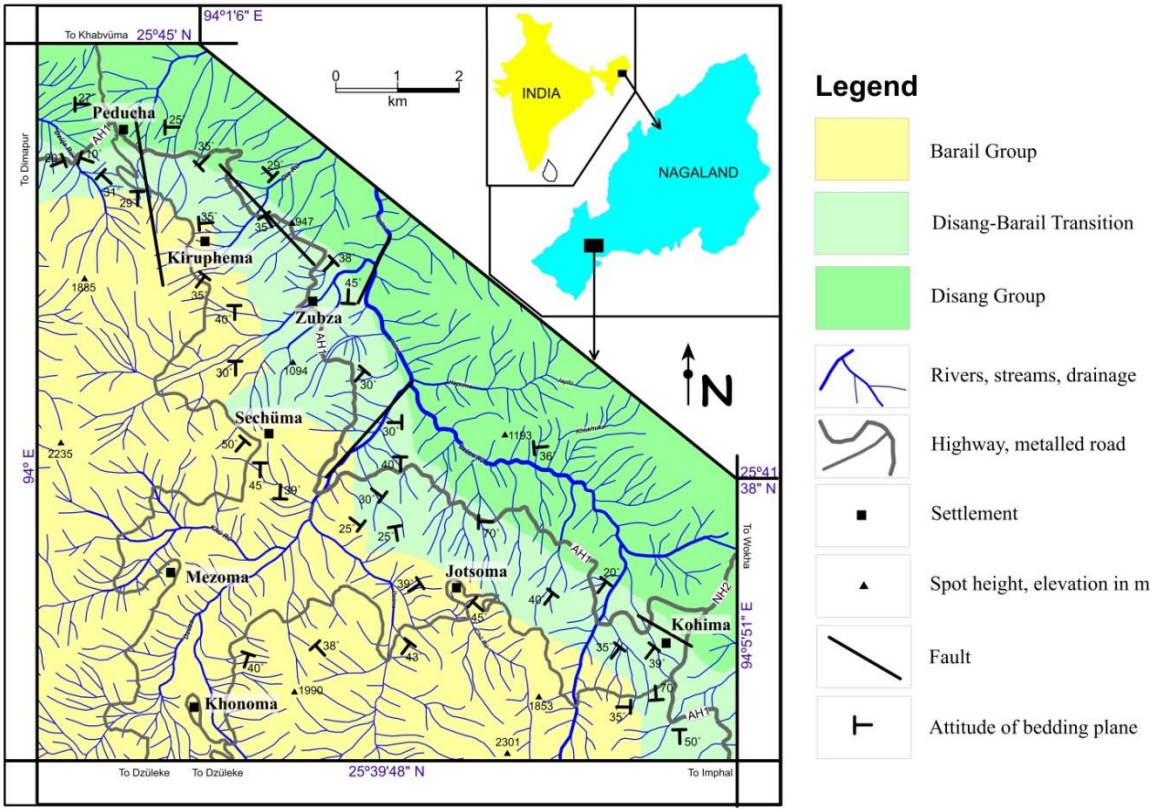

Fig. 3: Geological map of the study area (modified after Srivastava, 2002)

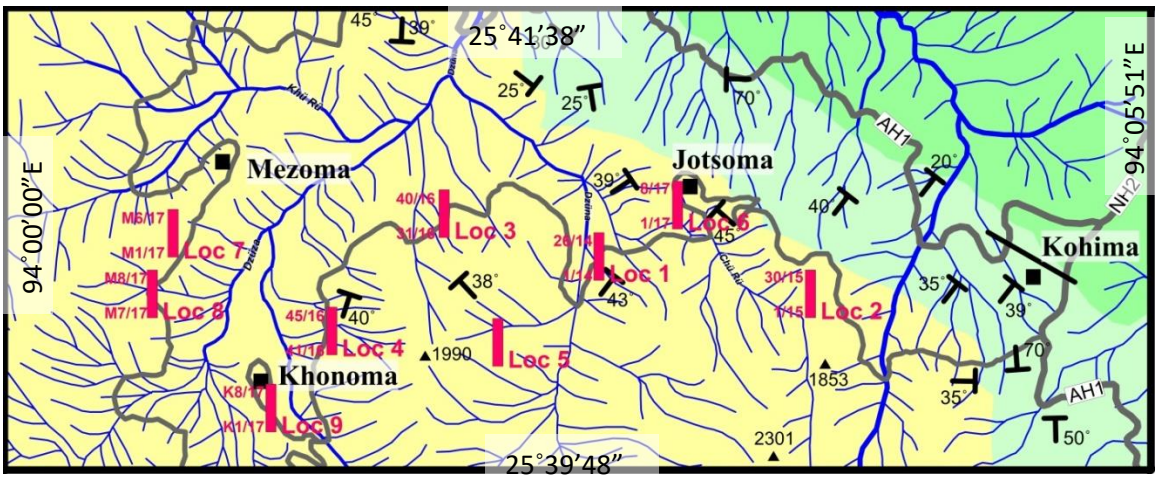

Fig. 4: Location of rock samples and Vertical Profile Sections

CHAPTER 3

LITHOLOGIC DISTRIBUTION, VERTICAL PROFILE SECTIONS AND LITHOFACIES

3.1 GENERAL

To understand the lithologic variability in stratigraphic succession, it is necessary to describe and categorize what is seen in the outcrop. Meticulous recording of the details of outcrops in stratigraphic sections in time and space in combination with facies analysis would lead to palaeoenvironmental interpretations. This was first recognized by Walther (1894) and he suggested that changes of lithofacies in space and time are a sensitive indicator of depositional environment. Study of modern sedimentary environments (Reineck and Singh, 1980) has enhanced the application of facies studies in understanding the ancient sedimentary record. Such studies have also been considered by Visher (1965), LeBlanc (1972), Selley (1976) and Reading (1978).

3.2 PARAMETERS OF SEDIMENTARY FACIES

The five parameters of sedimentary facies (Selley, 1970; 1976), for clastic sedimentary rocks, include - bed geometry, lithology including grain-size, primary sedimentary structures, palaeo-current patterns, and biogenic remains, if any. These parameters have been considered as diagnostic characters of depositional environment.

3.2.1 GEOMETRY

Shape of a sedimentary facies is an important criterion in distinguishing the depositional sedimentary environment. Mackenzie (1972), LeBlanc (1972) and Allen (1982) have provided significant data on the geometry of sedimentary facies. In the study area, exposures of various litho-units in vertical sections at various locations form the basis for description of lithofacies in two and, sometimes, in three-dimensional plan view.

3.2.2 LITHOLOGY AND GRAIN-SIZE

Using mineralogy and texture of a clastic sedimentary rock, the nature of source terrain, mechanism of transportation and the environment of deposition can be interpreted. There have been numerous attempts to utilize grain size attributes of siliciclastics as environmental indicators. However, the reliability and effectiveness of grain parameters as environmental indicator have been questioned (Pettijohn, 1975; Selley, 1976; Friedman and Sanders, 1978; Walton, Stephens and Shawa, 1980; Reineck and Singh, 1980).

The grain-size variations within the Barail sediments in the study area range between silt and very fine to medium sand size; and generally display a coarsening upward trend. The mineralogical composition of constituent litho-units also varies from greywackes near the base through lithic arenite to quartz arenite near the top.

3.2.3 SEDIMENTARY STRUCTURES

Sedimentary structures are important features of the sediments and sedimentary rocks as they not only provide hydraulic conditions but also reflect the process which has produced them (Allen, 1982; Collinson and Thompson, 1994).

In the study area, a wide variety of primary and post depositional features including biogenic have been observed. Primary sedimentary structures, observed in the study area include fine cross laminations, parallel lamination, wave ripple, interference ripples, bifurcating ripples, linguoid ripples, channels, and bioturbated mud layers. These features provide unique opportunity for understanding the depositional processes responsible for Barail sedimentation.

3.2.4 PALAEOCURRENTS

One of the basic requirements of palaeoenvironmental studies is the determination of palaeoflow directions from primary sedimentary structures and various scalar attributes of the rock. Allen (1966, 1967) and Selley (1968) have provided basic information on the palaeocurrent for specific and general environments; and their utility in environmental reconstructions.

In the present study, an attempt has been made to infer the palaeocurrent directions from the suitable sedimentary structures as well as with the help of scalar attributes.

3.2.5 BIOGENIC STRUCTURES/ FOSSILS

Biogenic sedimentary structures provide significant information for interpretation of depositional environmental with respect to water depth, salinity, energy level, oxygenation, *etc.* Trace fossils become more valuable especially where body fossils are absent (Frey, 1975). In the study area, many groups of trace fossils have been recognized. Intensely bioturbated mud is found to be overlying sandstones. Faunal yield of Barail sediments in the study area could not be proved, though their presence in the mud rocks cannot be ruled out.

3.3 DESCRIPTION OF SEDIMENTARY STRUCTURES

In the study area, a number of primary sedimentary structures, varying in scale and geometry, were recognized and were placed into four categories of sedimentary structures; namely erosional, depositional, post-depositional and biogenic (Tucker, 1993).

3.3.1 EROSIONAL SEDIMENTARY STRUCTURES

The common structures of this group include scoured surfaces and channels:

3.3.1(A) Scoured Surfaces

These are characterized by the cutting of underlying strata, truncation of underlying laminae and the presence of coarser sediments. The scoured surfaces observed in the study area display both, the sharp and irregular outline with some relief as well as smooth outline (**Plate 1a**).

3.3.1(B) Channels

Channels are recognized by their cross-cutting relationship with underlying sediments. Channels are large-scale structures measuring and show a concave-up profile (**Plate 1c**, **1d**, **1e** and **1f**). Channeled sediments are generally coarser than the sediments below or adjacent. Cross-bedded sandstones were seen infilling some of the channels. Lateral accretion of the channels has also been observed.

3.3.2 DEPOSITIONAL SEDIMENTARY STRUCTURES

Depositional structures found on the upper surface of beds and also within them. This group of sedimentary structures, in the present context, includes bedding, lamination, ripple marks, cross-stratifications, mud cracks and rain imprints.

3.3.2(A) Bedding

Bedding represents changes in the sedimentation pattern. Thickness of a bed in a succession is an important and useful parameter to measure. The Barail sediments in the study area exhibit all variations of bed thickness, ranging from a few cm to 2 m (very thinly bedded to very thickly bedded; after Tucker, 1993). A systematic upward decrease as well as increase in bed thickness was recorded during the course of measurements (**Plate 2a**, **2b** & **2c**).

3.3.2(B) Lamination

Laminations are internal structures where sedimentation units are less than 1 cm. in thickness. This occurs both in sandstones as well as mud dominated layers. One basic type, namely plane laminations (**Plate 2e**), could be recognized. These are typically few millimeters in thickness and at places display rhythmic patterns.

3.3.2(C) Cross-Stratification

It is an internal organization of most sedimentary rocks that comprises stratification at an angle to the principal bedding direction. For the most part of the study area, cross-stratification may be considered as an uncommon feature. Nevertheless, their preservation at places is spectacular and forms the basis for interpretation of changing energy conditions through time (**Plate 2d**, **2f** & **2g**).

3.3.2(D) Ripple Marks

Ripples are most common sedimentary structures and are found mainly in sand to medium silt size sediments. Their migration under conditions of net sedimentation, give rise to various types of cross-stratification. Wave ripples (**Plate 3a**, **3b**, **3c** & **3e**) , common in the study area, are observed both in mudstones as well as in sandstones and are bifurcating at many places (**Plate 3d**) whereas current

ripples (**Plate 3f**) and interference ripples (**Plate 3h**) are restricted to the upper stratigraphic horizons only.

3.3.3 POST-DEPOSITIONAL SEDIMENTARY STRUCTURES

This group of sedimentary structures includes soft sediment deformation which might occur at the time of deposition or shortly thereafter. In the study area, such structures include load casts (**Plate 1b**), mud cracks (**Plate 3g**) and intraclasts (**Plate 4b**).

3.3.4 BIOGENIC SEDIMENTARY STRUCTURES/FOSSILS

This group is characterized by the disruption of sediment due to the activity of organisms (bioturbation, **Plate 4d**, **4e**, **4f** & **4g**) and also feeding structures, carbonized plant materials, leaf imprints and resting traces (**Plates 4a**, **4c**, **7e** & **7f**). The bioturbation index, after Tucker (1989), grades from 2 to 5 in the study area. Most of the identified trace fossils belong to the *Skolithos* and *Cruziana* ichnofacies.

Following are the descriptions of the identified trace fossils in the study area:

Chondrites isp (**Plate 5a** & **5b**), a three dimensional systems of branching cylindrical tunnels, with individual tunnel segments are generally straight and do not intersect each other. Diameter is varying between 0.5 and 5 mm. These are found to be associated with dominantly mud lithology showing full relief.

Gyrochorte comosa **Heer, 1865** (**Plate 5c** & **5d**): These are unbranched, winding, plaited, bilobed trails separated by a median furrow with obliquely aligned sediments, preserved as ridges in positive epirelief. This is in agreement with generic characters of *Gyrochorte comosa* Heer (Haentzschel, 1975).This ichnospecies is very common in siltstone /fine grained sandstone.

Ophiomorpha nodosa **Lundgren 1891** (**Plate 5e** & **5f**): Burrow walls are consisting predominantly of dense pelletal horizontal burrows. Burrow material is different than the sediments it is found associated with. Exterior surface lined with ridges covering the tube. One side of the tube is slightly acute whereas other end is rounded in shape showing full relief. This ichnospecies is very common in fine to medium grained sandstone lithology.

***Skolithos linearis* Haldeman, 1840** (**Plate 6a**, **6b** & **6c**): *Skolithos linearis* is one of the most common trace fossil reported from the massive sandstone facies of the study area. These are straight, unbranched structures showing full relief. Straight and unbranched trace fossils have a diameter between 1-15 mm.

Planolites isp (**Plates 6f**, **7a** & **7b**) are generally horizontal; and are straight to gently curved and commonly overlap one another. These are unbranched cylindrical or sub-cylindrical in filled burrows and show a circular or elliptical shape in cross section. Burrow fills are generally structure less. In the present study area, they have been reported from fine grained sand-mud lithologies.

***Thalassinoides horizontalites* Woodward**, **1830** (**Plates 6d**, **6e**, **7c** & **7d**): *Thalassinoides horizontilites* consists of three dimensional structures with horizontal network, generally swollen at Y-shaped junction. These are found to be associated with very fine sandstones as well as in mudstones.

3.4 FACIES SCHEME

Utilizing observations made through the study of nine vertical profile sections a lithofacies scheme has been envisaged for the first time to describe the lithologic variations within Barail sediments. The scheme includes description of seven lithofacies types, based on their grain size and contained sedimentary structures. **Table 3** lists these lithofacies together with their respective codes. Some of the facies codes have been taken from Miall (1990).

3.5 DESCRIPTION OF LITHOFACIES IN THE STUDY AREA

1. Fine to medium massive sandstone facies **(*Sm*)**: This facies is characterized by fine to medium grained sandstone. Thickly bedded massive sandstones are found associated with vertical burrows. Other features of this facies include channels of varying dimension, leaf impression, and intraclasts (**Plate 4b**). The thickness of sandstone beds varies between 1 to 4 metres. Vertical burrows are very common. Trace fossils recorded from this facies includes *Skolithos*.

2. Plane laminated fine to very fine sandstone facies (***Sl***): This facies is characterized by very fine to fine grained sandstones. Plane laminations, ripples, horizontal bedding showing colour variations, horizontal traces, and moderate bioturbation are common in this facies. Its thickness ranges between a few centimetres to a meter. This facies is represented by *Gyrochorte comosa* and *Ophiomorpha* isp.

3. Fine cross laminated sandstone facies (***Fx*)**: Fine to medium sandstones possessing fine cross lamination with occasional small scale channels are the main characteristics of this facies. Its thickness ranges between 5 cm to 40 cm. *Gyrochorte comosa* and *Thalassinoides horizontalitis* have been recorded from this lithofacies.

4. Shale-silt facies (***Fsm***): Strong bioturbation with burrows marks are prominent features of this facies. Thickness varies from 2.5 to 20 cm. This facies (**Plate 4h**) is represented by *Chondrites* and *Gyrochorte comosa* trace fossils.

5. Mudstone facies (***Fl***): This facies is represented by mud lithology showing alternating clay-silt layers. Plane laminations, ripple marks, intra-clasts and intense bioturbations are the other features recorded from this facies. Thickness of beds ranges from few cm to a meter.Horizontal traces are very common in this facies.

6. Rippled sandstone facies (**Sr**): This facies is represented by fine to medium sandstones lithologies. Interference and linguoid ripples with mud drapes are the characteristic features of this facies. This facies is recorded at higher stratigraphic levels only where linguoid ripples with mud drapes has been recorded.

7. Wave rippled fine to medium sandstones facies (**Sr_w**): This facies is represented by fine to medium sandstone lithologies having wave ripples with occasional bifurcation.

3.6 DESCRIPTION OF VERTICAL PROFILE SECTIONS (VPS)

To establish the time and spatial distribution relationships of various lithofacies, a total of nine vertical profile sections were measured and carefully studied at various locations, in the field. All the sections thus studied are described briefly in the following

subsections. The reference symbols used in constructing the vertical profile sections (**Fig. 6 to 14**) are shown in **Fig. 5**.

3.6.1 VPS 1 SW OF JOTSOMA (25° 39' 46.04" N, 94° 03' 14.15" E)

This VPS was measured southwest of Jotsoma along the Jotsoma-Khonoma road. It is characterized by the presence of *Sm, Sl, Sr*$_w$*, Fx, Fsm* and *FI* facies and displays an overall coarsening upward trend. The total thickness measured, corresponds to 21 m (**Fig. 6**).

3.6.2 VPS 2 NEAR SAZOLIE COLLEGE (25° 39' 33.48" N, 94° 04' 33.48" E)

This vertical profile section was measured south of Sazolie College, Jotsoma. In a total thickness of 39 m, all 7 facies are represented in the section. An overall coarsening upward trend characterizes the facies succession (**Fig. 7**).

3.6.3 VPS 3 JOTSOMA-KHONOMA ROAD (25° 40' 10.98" N, 94° 03' 02.48" E)

An 8 m thick vertical profile section was measured on Jotsoma-Khonoma road. It consists of *Sm, Sl, Fsm* and *Fl* facies and exhibits a fining upward trend (**Fig. 8**).

3.6.4 VPS 4 JOTSOMA-KHONOMA ROAD (25° 40' 14.45" N, 94° 02' 25.66" E)

This is a road section along the Jotsoma-Khonoma road. The 6 m thick section shows *Sm, Sr*$_w$ and *Sl* facies. It also displays a fining upward trend (**Fig. 9**).

3.6.5 VPS 5 OPPOSITE *LOVERS' PARADISE* (25° 39' 45.08" N, 94° 03' 44.46" E)

This vertical profile section was measured opposite the *Lovers' Paradise* viewpoint in Jotsoma. The thickness of the vertical profile section is 7 m which includes *Sm, Sr*$_w$ and *Sl* facies. In this vertical profile section a fining upward trend was observed (**Fig. 10**).

3.6.6 VPS 6 NEAR JOTSOMA (25° 40' 09.26" N, 94° 03' 34.47" E)

This vertical profile section was measured less than 1 km from Jotsoma along the Jotsoma-Khonoma road. It has a thickness of 38 m. The *Sm, Sl, Sr*$_w$ and *Fl* facies together comprise the section and present a coarsening upward trend (**Fig. 11**).

3.6.7 VPS 7 SOUTH OF MEZOMA (25° 39' 50.98" N, 94° 00' 42.82" E)

This 24 m section has been measured just south of Mezoma village along Khonoma-Mezoma road. The facies present are *Sm*, *Sl*, *Fsm* and *Fl*. It displays an overall coarsening upward trend (**Fig. 12**).

3.6.8 VPS 8 KHONOMA – MEZOMA ROAD (25° 39' 43.63" N, 94° 00' 37.34" E)

This Vertical profile section was measured along Khonoma-Mezoma road. The total thickness measured corresponds to 12 m. The lithofacies *Sm* and *Fl* are well represented here. A coarsening upwards trend is well displayed (**Fig. 13**).

3.8.9 VPS 9 AT KHONOMA VILLAGE (25° 39' 06.65" N, 94° 01' 23.99" E)

This section is measured at Khonoma village below the village bus stand. The total thickness is 11 m. It consists of *Sm*, *Sl* and *Fl* facies and has alternating fining upward and coarsening upward sequence (**Fig. 14**).

Facies code	Lithofacies	Sedimentary structures	Interpretation
Sm	Fine to medium massive sandstones	Thickly bedded massive sandstones with vertical burrow marks and channels, leaf impression, intraclasts	Tidal channel fill, High energy upper shore face
Sl	Very fine to fine sandstones	Plane laminations, ripples, Horizontal bedding showing colour variations, horizontal traces	Inter-distributaries bay, Levees deposits, Lower shoreface
Fx	Fine to medium sandstones	Fine cross laminations, small dimension channels, burrows	Beach face, upper shore face
Fsm	Siltstones-shale	Laminations, Bioturbation	Low energy, lower shore face
Fl	Mudstone	Plane laminations, Bioturbation, intraclasts	Delta front, offshore transition, low energy
Sr	Fine to medium sandstones	Interference and Linguoid ripples with mud drapes	Tidal sand waves, Upper shoreface
Sr_w	Fine to medium sandstones	Wave ripples/ bifurcating ripples	Wave processes, upper shoreface

Table 3: Lithofacies scheme for the Barail sediments of the study area

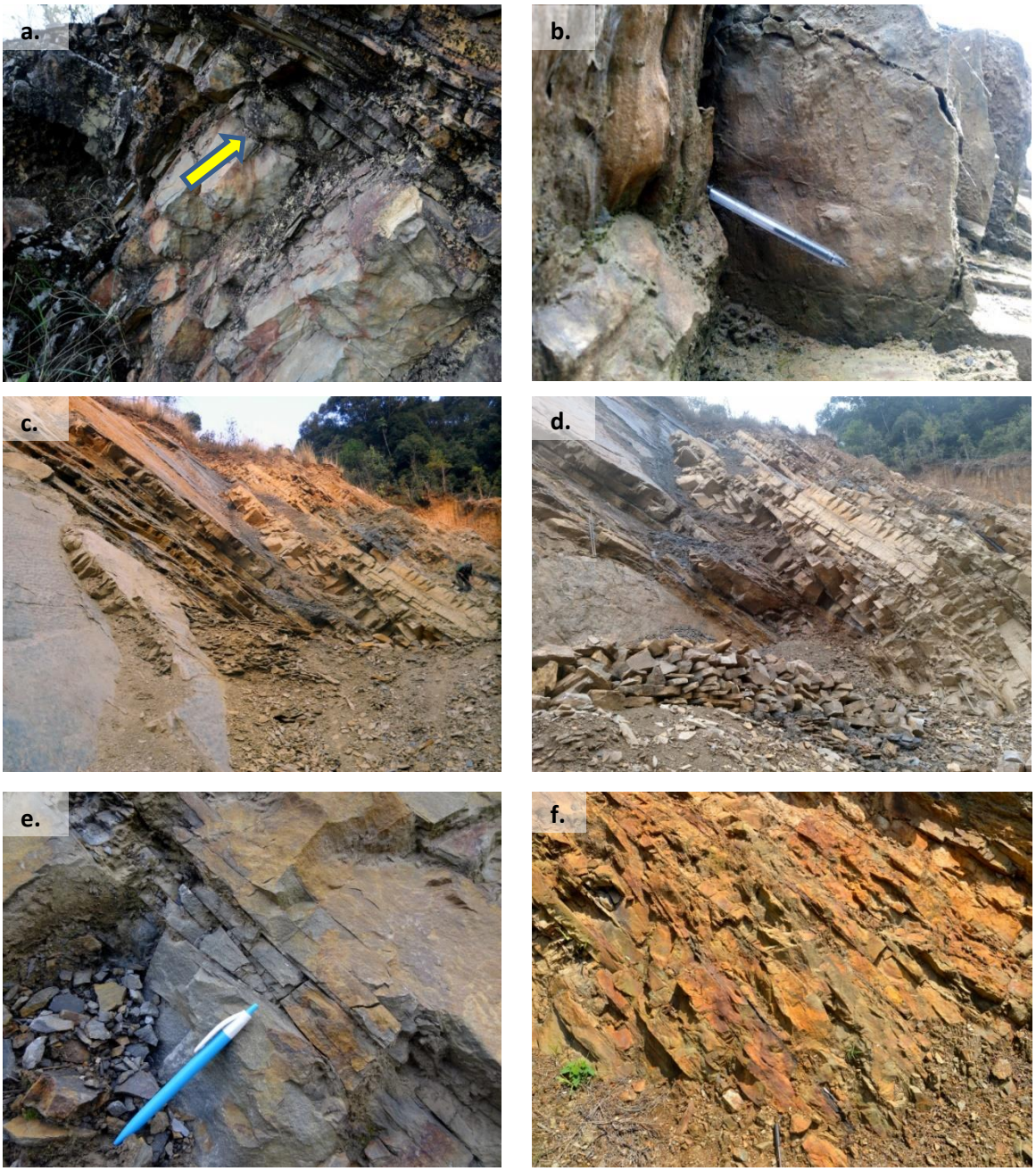

Plate 1: Field photographs showing - **a**) Scour faces **b)** Load cast **c**), **d**), **e**) & **f**) Channels

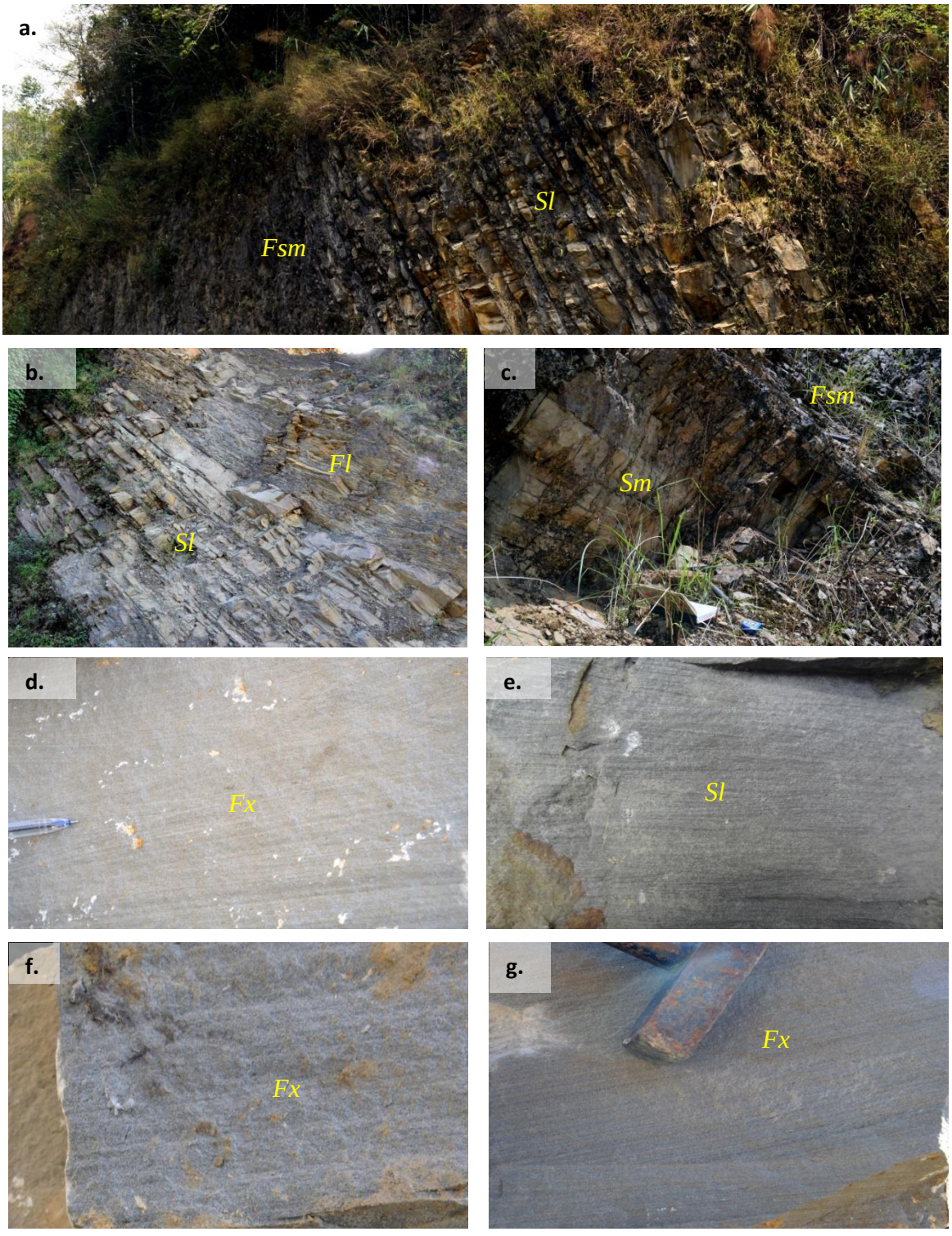

Plate 2: Field photographs showing - **a**) Coarsening upwards sequence **b**) & **c)** Fining upward sequence **d**) Low angle cross stratification (*Fx*) **e**) Plane laminations (*Sl*) **f)** & **g)** Cross stratification (*Fx*)

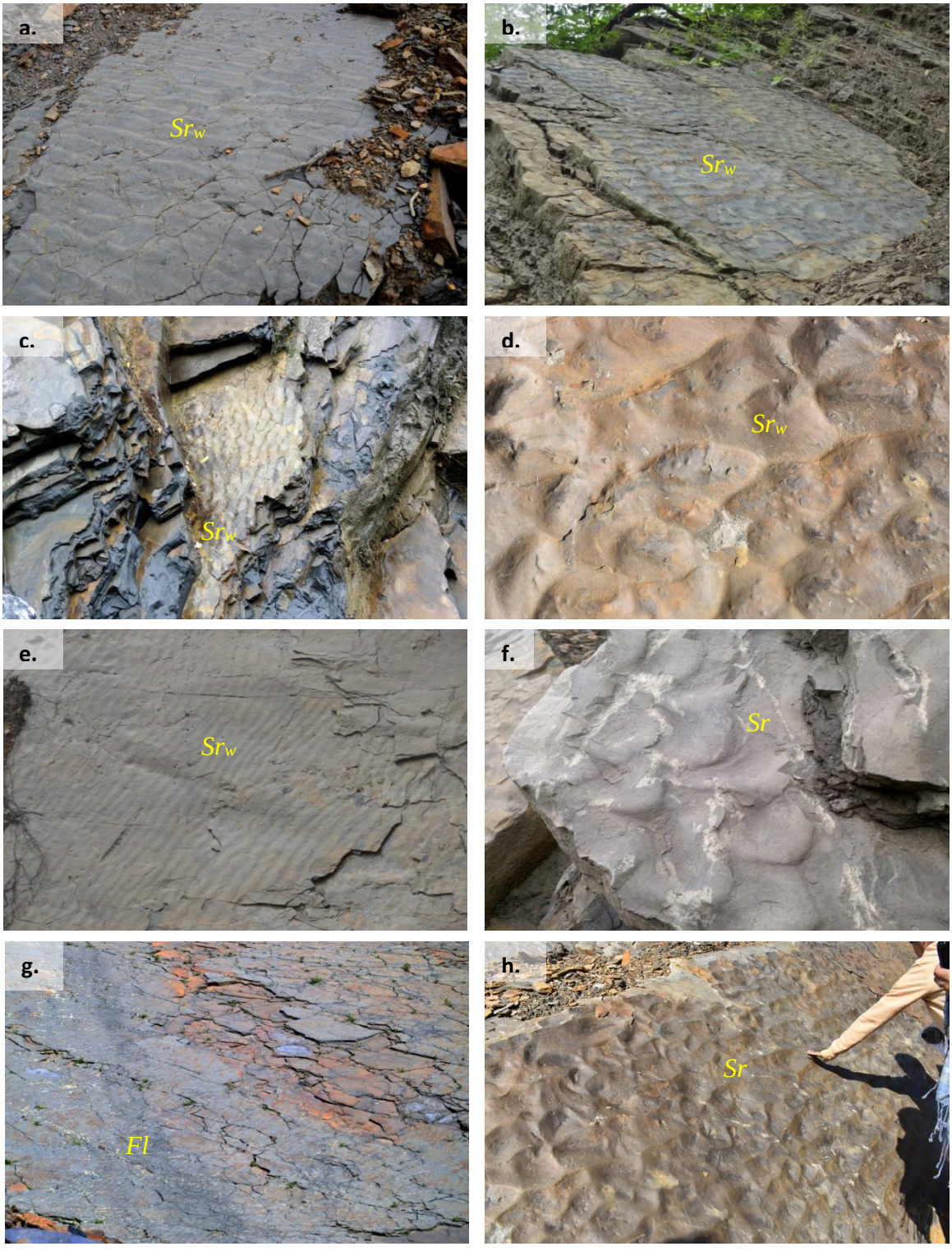

Plate 3: Field photographs showing - **a**), **b**) & **c)** Wave ripples (Symmetrical, Sr_w) **d**) Bifurcating ripples (Sr_w) **e**) Wave ripples (Sr_w) **f)** Linguoid ripples (*Sr*) **g)** Mud cracks with symmetrical ripples (*Fl*) **h)** Interference ripples (*Sr*)

Plate 4: Field photographs showing - **a)** Leaf imprints (*Sm*) **b)** Intraclasts (*Sm*) **c)** Carbonised plant material in sandstones (*Sm*) **d**) Bioturbated sandstone (*Sm*) **e**) Bioturbated sandstone with symmetrical ripples (*Sl*) **f)** Bioturbated mudstone (*Fl*) **g)** Bioturbated mudstone (*Fl*) **h)** Laminated silt-shale alternation (*Fsm*)

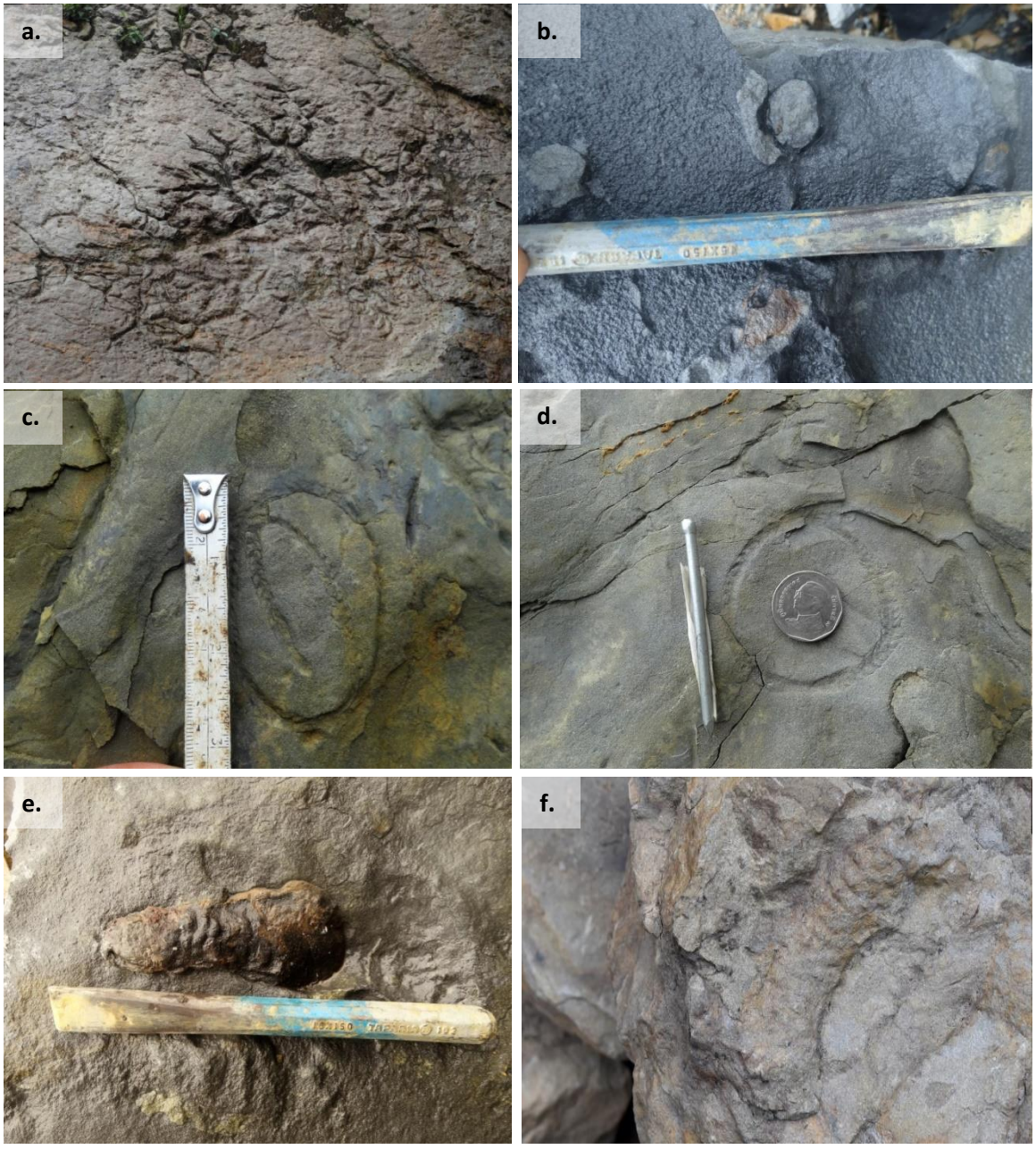

Plate 5: a) *Chondrites* **b)** *Chondrites* and *Skolithos linearis* **c)** *Gyrochorte comosa* **d)** *Gyrochorte comosa* **e)** *Ophiomorpha nodosa* **f)** *Ophiomorpha nodosa*

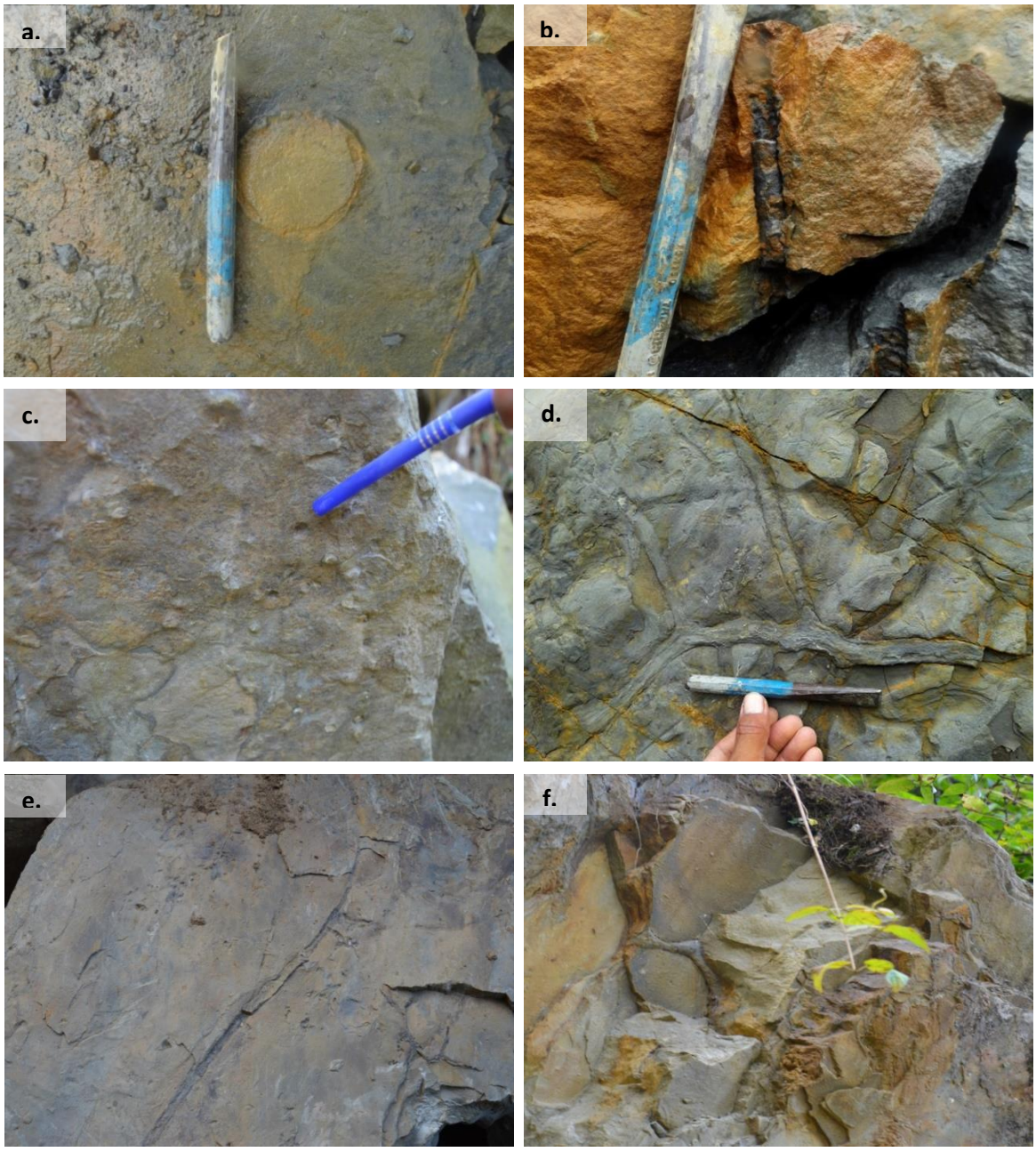

Plate 6: a) *Skolithos linearis* **b)** *Skolithos linearis* **c)** *Skolithos linearis* **d)** *Thalassinoides horizontalites* **e)** *Thalassinoides horizontalites* **f)** *Planolites*

Plate 7: a) *Planolites* **b)** *Planolites* **c)** *Thalassinoides horizontalites* **d)** *Thalassinoides horizontalites* **e)** Resting traces **f)** Resting traces

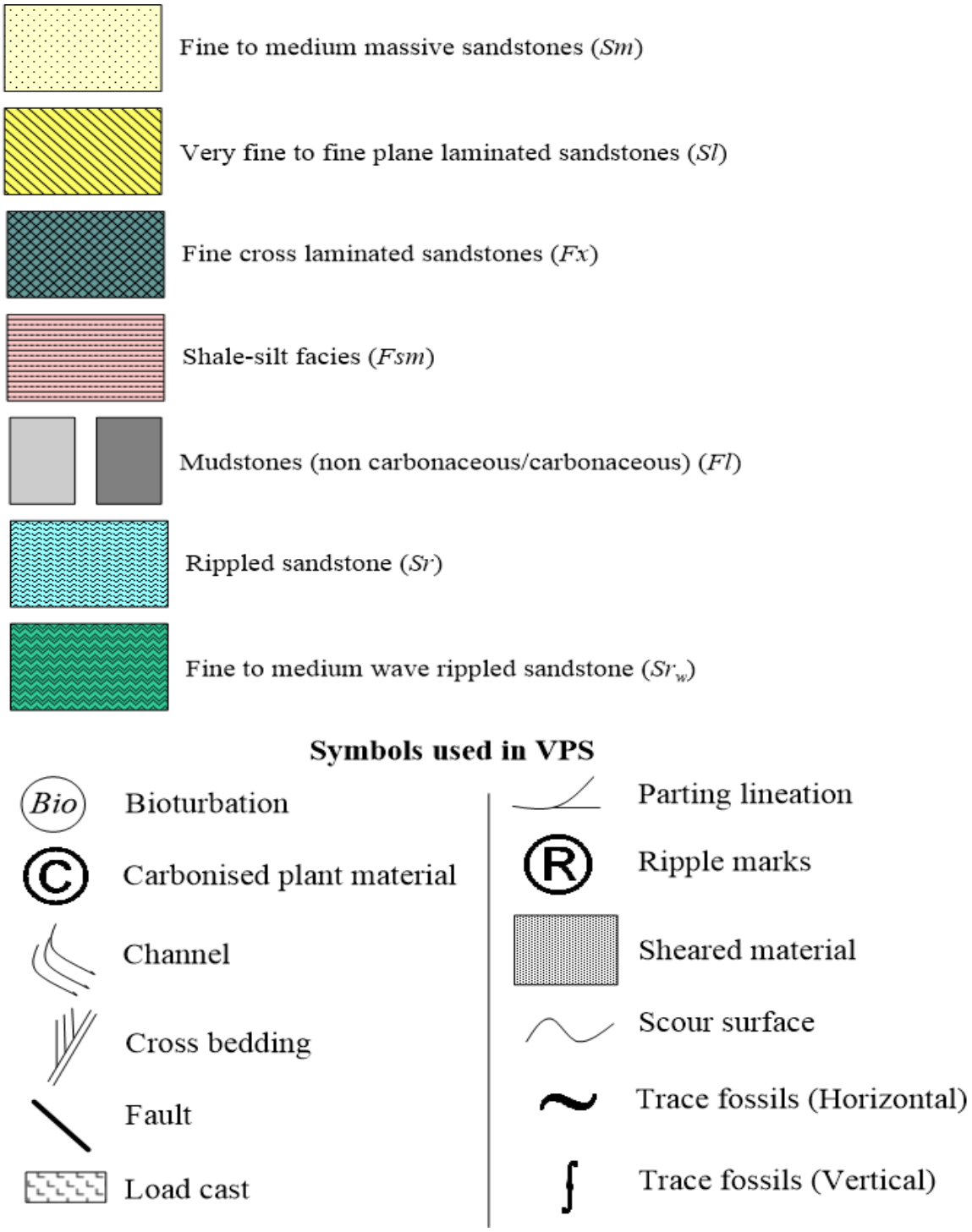

Fig. 5: Reference table for symbols used in vertical profile sections

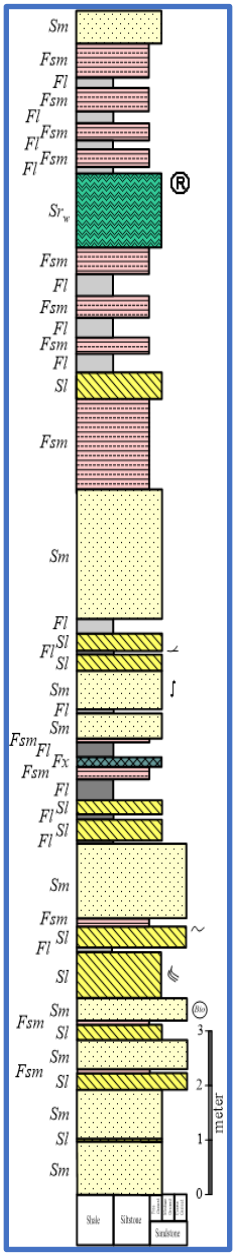

Fig. 6: VPS 1 South West of Jotsoma (25°39'46.04"N 94°03'14.15"E)

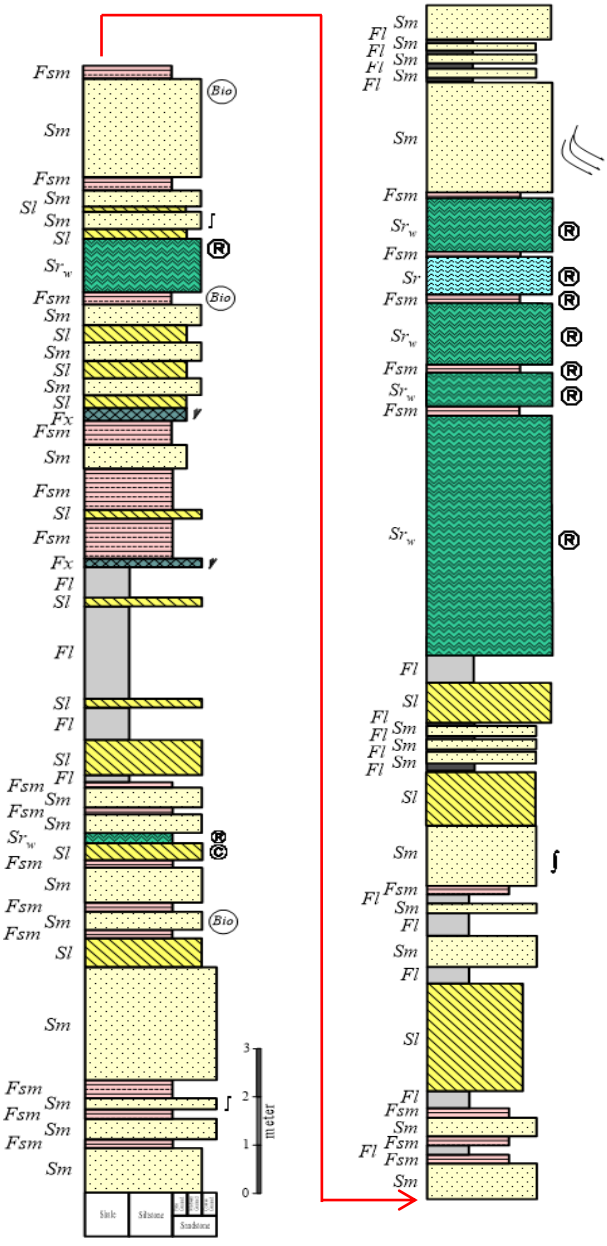

Fig. 7: VPS 2 Near Sazolie College, Jotsoma (25°39'33.48"N 94°04'33.48"E)

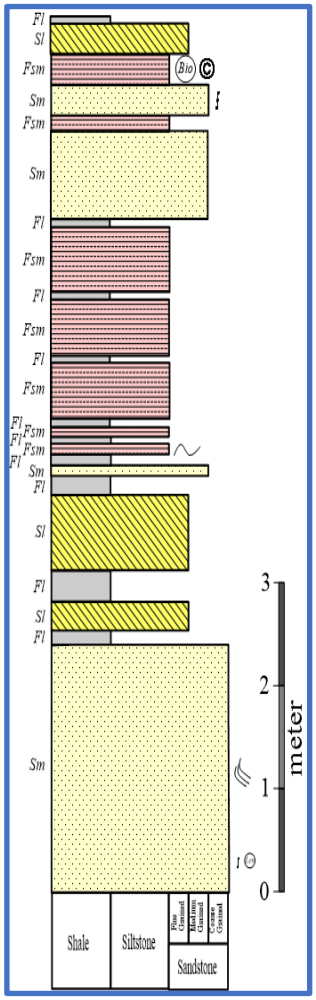

Fig. 8: VPS 3 Jotsoma-Khonoma Road (25°40'10.98"N 94°03'02.48"E)

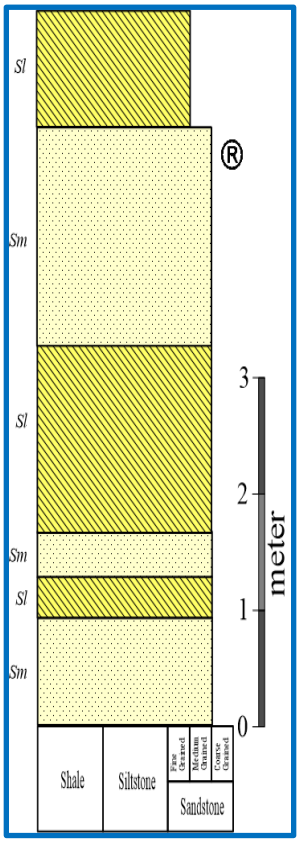

Fig. 9: VPS 4 Jotsoma-Khonoma Road (25°40'14.45"N 94°02'25.66"E)

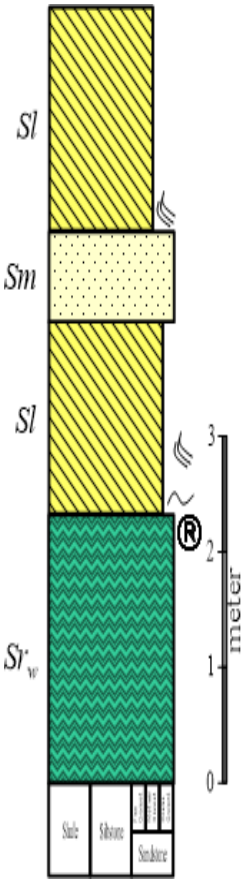

Fig. 10: VPS 5 Opposite *Lovers' Paradise* (25°39'45.08"N 94°03'44.46" E)

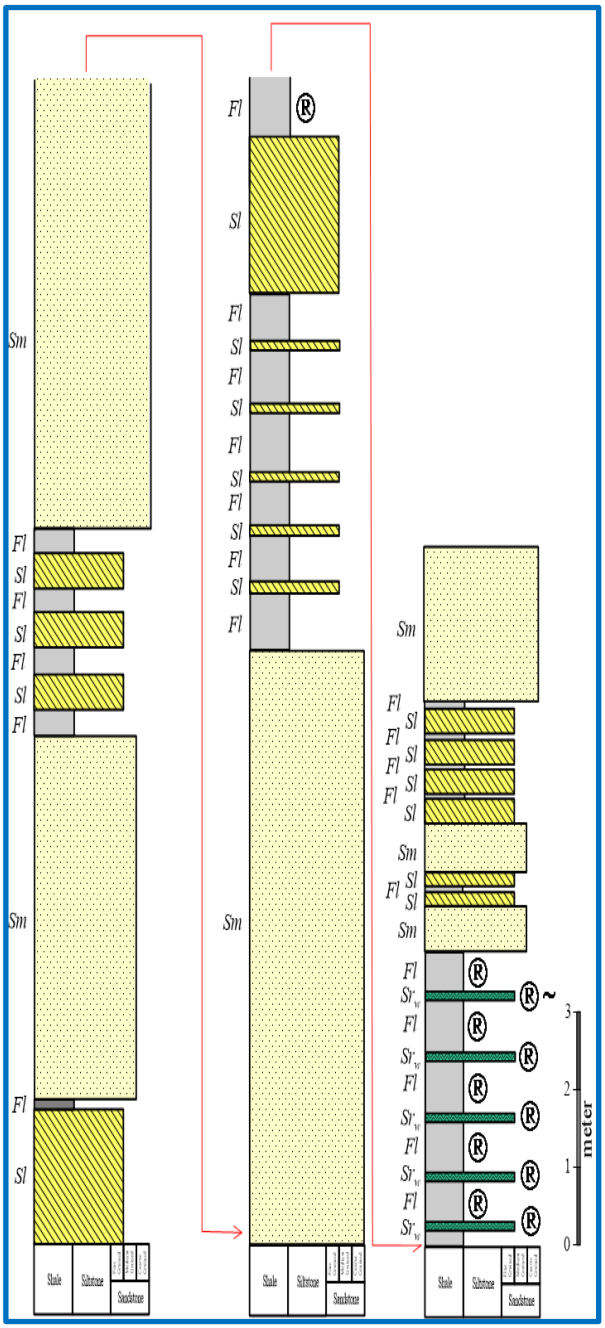

Fig. 11: VPS 6 Near Jotsoma (25°40'09.26"N 94°03'34.47"E)

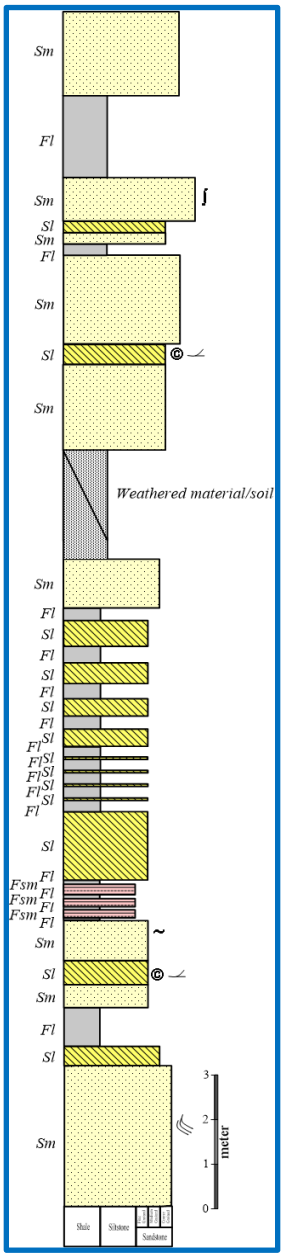

Fig. 12: VPS 7 South of Mezoma (25°39'50.98"N 94°00'42.82"E)

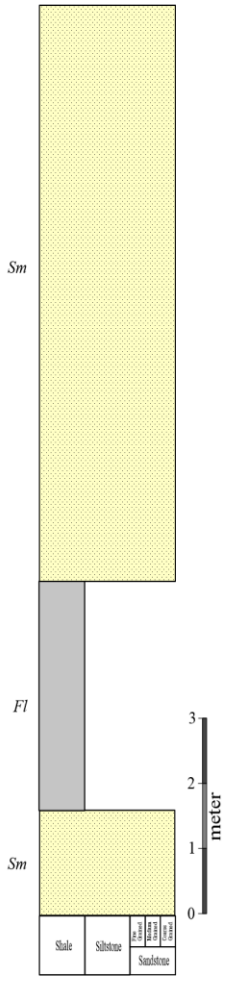

Fig. 13: VPS 8 Khonoma – Mezoma road (25°39'43.63"N 94°00'37.34"E)

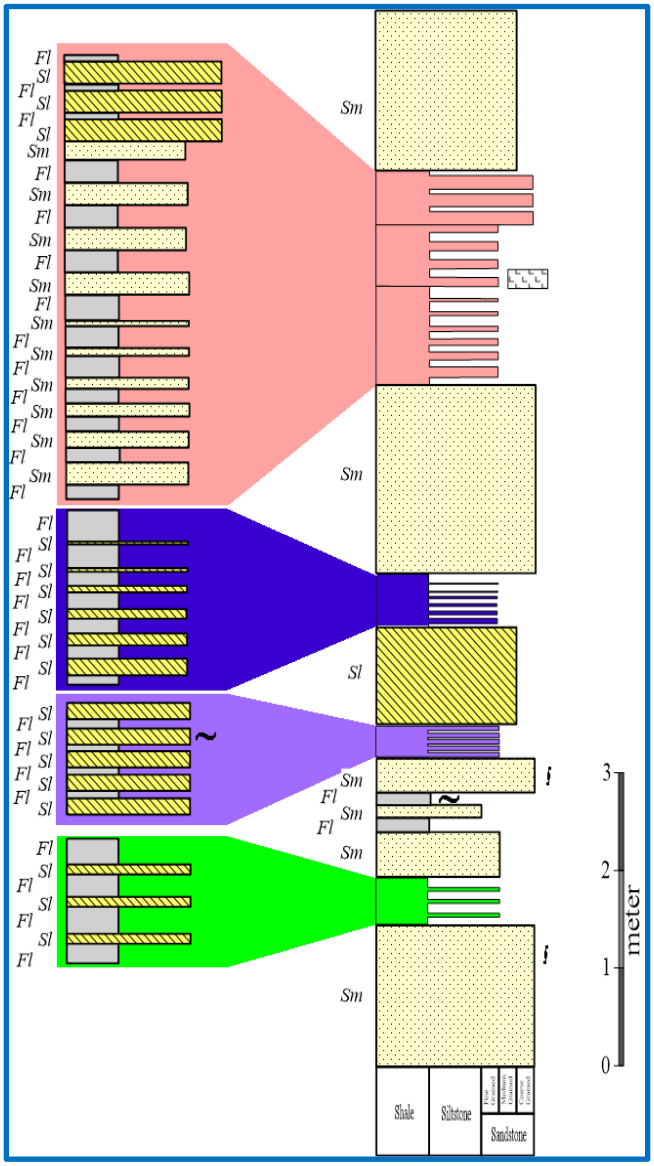

Fig. 14: VPS 9 At Khonoma Village (25°39'06.65"N 94°01'23.99"E)

CHAPTER 4

GRAIN SIZE ANALYSIS

4.1 GENERAL

Relationship between textural properties of clastic sedimentary rocks and the processes operative during sedimentation can be expressed by the equation given by Griffiths (1967), *i.e.*

$$P = f(m, s, sh, o, p)$$

where,

P, an index characterizing the rocks, is a function (*f*) of the proportions and types of mineral species (*m*), their sizes (*s*), shapes (*sh*); orientation (*o*) and packing (*p*).

Hence, the study of these aspects of clastic sediments will throw light not only on the transport mechanism and depositional environments but also on the provenance history.

In this chapter, an attempt has been made to interpret the grain size data in terms of processes responsible for the development of Barail rocks in the study area.

4.2 GRAIN SIZE ANALYSIS

Application of grain size data in environmental interpretation is based on the fact that the grain size of the clastic sediments is a measure of the energy conditions of the depositional environment as well as the depositing medium. In general coarser sediments indicate a higher energy condition where as a low energy condition is reflected by fine sized particles. It has also been shown by many workers that the grain size decreases in the direction of the transport. Grain size attributes in environmental analysis has been attempted by many workers like Wentworth (1922), Krumbein and Pettijohn (1938), Folk (1966), Friedman (1967), Sengupta (1982), McLennan *et al.* (1993) and Visher (1969). However, several limitations must be kept in mind while applying grain size data in palaeo-environment reconstruction. Because the grain size distribution is a function of hydrodynamics and similar hydrodynamics may operate in various environment (Reineck

and Singh, 1980). Controversy still exists among the sedimentologists regarding the effectiveness of various techniques available for classifying and discriminating the sedimentary environment through grain size attributes.

In the present study, however, an attempt has been made to reconstruct the depositional environment of the Barail sediments using the techniques available for the purpose.

4.2.1. METHOD OF STUDY

As the rocks of the study area are hard and compact in nature, thin section technique of grain size analysis has been employed in the present study. This technique of particle size measurement is in practice since mid-20th century and has been improved and justified upon by several workers including Friedman (1962), Stauffer (1966), Conner and Frem (1966), Smith (1966) and Textoris (1971).

The grain size measurement of 30 representative sandstone samples from different lithofacies was carried out with the help of Leica microscope at the Department of Geology, Nagaland University, Kohima Campus, Meriema. More than 200 grains in each of the thin section were measured. Grain size values thus obtained were grouped into half phi (*Ø*) intervals and were used in plotting cumulative curves on arithmetic probability paper.

4.2.2 GRAIN SIZE DISTRIBUTION AND STATISTICAL PARAMETERS

The cumulative curves plotted using measurement data of various samples have been shown in **Fig. 15 - 19**. The data on grain size distribution and descriptive statistical measures have been presented in **Table 4**. Following Visher (1969), analysis and comparative studies of different cumulative curves were carried out in order to understand the transport mechanism and probable depositional environments. The overall characteristics of the cumulative curves point towards a shallow marine to near shore complex at the time of deposition of the Barail sediments in the study area. The statistical measures of grain size distributions were computed using formulae suggested by Folk and Ward (1957) and later modified by Friedman and Sanders (1978). Phi-values (*Ø*) for different percentiles were read from the cumulative curves. Median or *Ø50* represents the

grain size in the exact middle of the population(s) (*i.e.* half the percentiles are finer and half coarser than *Ø50*). The mode corresponds to maximum frequency and can be read directly from size frequency distribution. Other statistical parameters are determined using the following formulae:

i. Graphic mean (M_z):

$$M_Z = \frac{Ø16 + Ø50 + Ø84}{3}$$

ii. Inclusive Graphic Standard Deviation (σ_I):

$$\sigma_I = \frac{Ø84 - Ø16}{4} + \frac{Ø95 - Ø5}{6.6}$$

Verbal Classification:

σ_I under *Ø0.35*	very well sorted
0.35 to *Ø0.50*	well sorted
0.50 to *Ø0.71*	moderately well sorted
0.71 to *Ø1.00*	moderately sorted
2.00 to *Ø4.00*	very poorly sorted
Over *Ø4.00*	extremely poorly sorted

iii. Simple Sorting Measures (SO_S):

$$SO_S = Ø95 - Ø5$$

iv. Simple Skewness Measures (σ_S):

$$\sigma s = (Ø95 + Ø5) - 2\,Ø50$$

v. Inclusive Graphic Skewness (SK_I):

$$SK_I = \frac{(Ø84 + Ø16) - 2\,Ø50}{2(Ø84 - Ø16)} + \frac{(Ø95 + Ø5) - 2\,Ø50}{2(Ø95 - Ø5)}$$

Verbal Classification:

SK_I from +1.00 to + 0.30	strongly define- skewed
+0.30 to +0.10	define- skewed
+0.10 to -0.10	near symmetrical
SK_I = 0.00	symmetrical
SK_I -0.10 to -0.30	coarse- skewed
-0.30 to -1.00	strongly coarse skewed

vi. Graphic Kurtosis (K_G):

$$K_G = \frac{Ø95 - Ø5}{2.44(Ø75 - Ø25)}$$

Verbal Classification:

K_G under 0.67	very platykurtic
0.67 to 0.90	platykurtic
0.90 to 1.11	mesokurtic
1.12 to 1.50	leptokurtic
1.51 to 3.00	very Leptokurtic
Over 3.00	extremely Leptokurtic

The normal Phi-curve has a Kurtosis of 1.00.

4.2.2(A) Mean Grain Size (M_z):

In present study, graphic measures have been preferred as these are simpler to calculate and generally independent of inaccuracies introduced in truncating and grouping of data (Jacquet and Varnet, 1976; Swan *et al.*, 1978). It reflects the average grain size of sediments and thus relates to hydraulic conditions of the depositional environment. In the study area, in general, it shows a decreasing trend towards southeast. M_z values of the studied sediments range between *2-3Ø*.

4.2.2(B) Standard Deviation (σ_I):

Standard deviation reflects the general spread of size distribution and indictes the sorting or current and wave condition of the depositional environment. The values of standard deviation (σ_I) for all the sediments in the study area indicate a gradual improvement in the sorting from northeast to southwest part of the area, the overall sorting being well to moderately sorted.

4.2.2(C) Skewness (SK_I):

It measures the deviation of mean from the median of the grain size distributions. It also gives an idea about the symmetry of the frequency curves. On an average, the size distributions are mostly coarse skewed with some near symmetrical to strongly fine skewed sediments.

4.2.2(D) Kurtosis (K_G):

It measures the degree of peakedness of frequency curves with respect to normal probability curve (K_G =1.00, Mesokurtic). On an average, the value of kurtosis indicates predominance of very platykurtic to platykurtic distribution in the study area. However, some of the samples, especially in the south, show leptokurtic and mesokurtic peakedness.

4.2.3 BIVARIATE STATISTICAL AND TEXTURAL PARAMETERS

Bivariate plots utilizing various statistical parameters have proved to be the convenient means of discriminating various depositional environments i.e. River, Dune, Beach, Shallow marine, etc. In the present investigation, bivariate plots used include Standard deviation versus Skewness, Simple Skewness measures versus Simple Sorting measures, Inclusive graphic Skewness versus Mean size, Inclusive graphic standard deviation versus Inclusive graphic kurtosis. The values used in this exercise correspond to the sieve equivalents.

4.2.3(A) Graphic Skewness (SK_I) Vs Graphic Standard Deviation (σ_I):

For discriminating between beach and river sand, Standard Deviation (sorting) is plotted against Graphic Skewness (SK_I) as suggested by Friedman (1961) and a mostly beach environment has been interpreted for Barail sediments

(**Fig. 20**). Similar trend has also been observed from Moiola and Weiser's (1968) plot (**Fig. 21**).

4.2.3(B) Graphic Mean (M_z) Vs Graphic Skewness (SK_I):

This plot has been effectively used in discriminating river, wave and slack water processes (Stewert, 1958), besides differentiating inland and coastal dune sands (Moiola and Weiser, 1968) and beach and dune sands (Friedman, 1967; Moiola and Weiser, 1968). In the present case, values for the mean size (M_z) and median ($Ø50$) in almost all the samples were found nearly identical and hence, the discriminating boundaries in the Steward's (1958) plot; which are based on median and skewness, may be used appropriately. The scattering of the points for the different samples indicates that the deposition of Barail sediments was influenced mainly by wave processes. On the other hand, the Friedman (1967) and Moiola and Weiser's (1968) plots reflect that almost all the samples have the imprint of a beach complex (**Fig. 22**).

4.2.3(C) Graphic Standard Deviation (σ_I) Vs Graphic Kurtosis (K_G):

The plot of Inclusive Graphic Kurtosis (K_G) versus Inclusive Graphic Standard Deviation (σ_I), which does not provide any environmental interpretation, has been found suitable to understand the degree of sorting. All plot points fall within the range of well sorted to moderately sorted sediments (**Fig. 23**).

4.2.3(D) C-M Diagram:

There have been numerous attempts to relate statistical parameters to different depositional environments (Folk and Ward, 1957; Mason and Folk, 1958; Harris, 1958; Friedman, 1961, 1962, 1967; Sahu, 1964; Chappel, 1967). All such attempts seem to achieve limited success in environmental interpretations. By plotting M (the median or 50th percentile particle diameter in microns) against C (1 percentile, approximate value of maximum grain size in microns) on a log-log paper, Passega (1957, 1964) obtained the C-M diagram to reflect the processes of sediment deposition. Following Passega (1957, 1964, 1977) and also Passega and Benarjee (1969), C-M patterns for Barail sediments were obtained (**Fig. 24**) and compared with their basic C-M patterns. The C-M plot for these sediments

corresponds to generally Class II, III and IV suggesting that Barail sediments have been transported by both graded and uniform suspension with some sediment transported as bed load. The average values for CU (Maximum grain size transported as uniform suspension) and CS (Maximum grain size transported as graded suspension) for Barail sediments correspond to 220 and 430 microns, respectively. The palaeobathymetric estimation using Passega's (1964) Cs-C depth diagram indicates that Barail sediments have been deposited under a shallow marine environment with some influence of fluvia processes. A depth range of very shallow to 60 /70 meters has been estimated for these sediments.

4.2.3(E) Cumulative Curve Analysis:

It has long been established that the shape of the cumulative curve is a function of relative proportion of various log normal distributions of grain size sub-populations (Tanner, 1964; Visher, 1969; Lambiase, 1982). Many workers have also related log normal distributions to specific sediment transport mechanism during the depositional history of the sediments *i.e.* the coarsest sub-population represents the bed load or surface creep mechanism of transportation and the finest represents the suspension, the intermediate size being the saltation sub-population (Visher, 1970; Moss, 1972; Sagoe and Visher, 1977; Middleton, 1976). However, interpretation of cumulative curves must be made with caution with respect to minimum number of grain measure, loss of finer grain size due to diagenetic changes and sampling error (James and Oaks, 1977; Tanner, 1964; Middleton, 1976; Walton *et al.*, 1980).

In the present investigation, cumulative curves for 30 samples from the study area have been plotted for understanding the depositional history of Barail sediments (**Fig. 15 to 19)**. Sediments in the study area appear to have been transported under graded suspension mechanism with little influence of rolling and uniform suspension.

4.2.3(F) Linear Discriminant Functions:

In the present work, linear discriminant function of Sahu (1964) and Sevon (1966), in which all the statistical parameters used in the analysis have been

combined to a linear equation, have also been attempted. Nevertheless, the effectiveness of discriminant functions to decipher various depositional environments has been questioned by Tucker and Vacher, (1980).

Following are the four empirically established discriminant functions of Sahu (1964) employed in the present investigation to differentiate sediments from eolian, beach, shallow agitated marine, fluvial (deltaic) and turbidite environments.

i. Y_1: Differentiates eolian from beach environment.

It is expressed as,

$$Y_1 = -3.5688\, M_Z + 3.7016\, \sigma_I^2 - 2.0766\, SK_I + 3.1135\, K_G$$

If,

Y_1 =< -2.7411, it indicates eolian deposition
Y_1 => -2.7411, it indicates beach deposition

ii. Y_2: Differentiates beach from shallow agitated marine environment.

It is expressed as,

$$Y_2 = 15.6534\, M_Z + 67.7091\, \sigma_I^2 - 18.1071\, SK_I + 18.5043\, K_G$$

If,

Y_2 < 65.3650, it indicates beach deposition
Y_2 > 65.3650, it indicates shallow agitated marine processes

iii. Y_3: Differentiates shallow agitated marine processes from fluvial (deltaic) deposition.

It is expressed as,

$$Y_3 = 0.2852\, M_Z + 8.7604\, \sigma_I^2 - 4.8932\, SK_I + 0.04821\, K_G$$

If,

Y_3 < -7.4190, it indicates fluvial (deltaic) deposition
Y_3 > -7.4190, it indicates shallow agitated marine deposition

iv. Y_4: Differentiates fluvial (deltaic) environment from turbidity current deposition.

It is expressed as,

$$Y_4 = 0.7215\, M_Z + 0.4030\, \sigma_I^2 - 6.7322\, SK_I + 5.2927\, K_G$$

If,

$Y_4 < 9.8433$, it indicates turbidity current deposition
$Y_4 > 9.8433$, it indicates fluvial (deltaic) deposition

In the above discriminant functions, M_z, σ_I^2, SK_I and K_G represent Graphic Mean, the variance, Graphic Skewness and Graphic Kurtosis, respectively. Results obtained through these four discriminant functions have been presented in **Table 5**.

Based on the discriminant functions used, the Barail sediments have been found to be associated dominantly with shallow agitated marine with minor elements of beach, eolian, and to some extent turbidity currents.

The log-log plot of mean phi deviation (σ_I^2) of all samples versus the ratio of standard deviation of kurtosis (SK_G) to standard deviation of mean size (SM_z) times the standard deviation of variance $S(\sigma_I^2)$ of samples belonging to Barail sediments have also been used after Sahu (1964) for further discrimination among environments (**Fig. 25**). Unlike different predictions given in **Table 5**, this plot indicates an overall beach to shallow marine environment associated with palaeobathymetric fluctuation for the deposition of Barail sediments.

4.2.3(G) Multigroup Discriminant Function Analysis:

The linear discriminant function of Sahu (1964) could not yield optimal result for Barail sediments. It may be because of the fact that this hypothesis is restricted to two groups only; whereas sample may not belong to any of the two environments, *i.e.* eolian-beach, beach-shallow agitated marine, shallow agitated marine fluvial (deltaic) and fluvial (deltaic) turbidite. To overcome this problem, the application of multigroup discrimination after Sahu (1983) was tested, as the method ensures:

i) the alternative hypothesis may belong to anyone of the several groups;
ii) ratio of among-group to within group quadratic forms is to be maximized;
iii) only significant number of coordinates are to be retained for the discrimination space; and
iv) a simple euclidean distance for purposes of classification in the discrimination space.

In the present study, Sahu's (1983) empirically retained discriminating Eigen's vectors V_1 and V_2 have been used. These discriminant functions may be expressed as:

$$V_1 = 0.48048\, M_Z + 0.62301\, \sigma_I^2 - 0.40602\, SK_I + 0.44413\, K_G$$
$$V_2 = 0.24523\, M_Z - \ 0.45905\, \sigma_I^2 - 0.15715\, SK_I + 0.83931\, K_G$$

Where,

M_z, σ_I^2, SK_I and K_G represents the mean size, the size variance, graphic skewness and graphic kurtosis, respectively.

Values of V_1 and V_2 for different samples of Barail sediments, SW of Kohima are listed in **Table 6**. The diagram of V_1 and V_2 with $V_1 \Lambda V_2$ = 74.4º, after Sahu (1983) was used suitably for the differentiation of depositional environment of the Barail sediments under study. The plot (**Fig. 26**) indicates on an average, a shallow marine environment for the deposition of Barail sediments.

4.2.4 DISCUSSION AND GEOLOGICAL INTERPRETATION

The discrimination of depositional environments of Barail sediments using bivariate and multivariate analysis reflects somewhat diversified sedimentary environment. For a given sample, such interpretations become apparent by switching to different set of grain size parameters. Nevertheless, such plots are restricted to selective depositional environments only and ignore variations in grain size, sedimentation processes, climate, tectonic and wave energy fluctuations within the depositional environments. It may be emphasized here that the boundaries among different environments in the bivariate plots are purely subjective or empirical lines of approach.

Linear discriminant functions and log-log plot of (σ_I^2) versus (SK_G/SM_z).$S(\sigma_I^2)$ after Sahu (1964), the multigroup discrimination and plot of V_1 and V_2 with $V_1 \Lambda V_2$ = 74.4° after Sahu (1983), the C-M patterns and shapes of cumulative grain size distribution curves are, however, applicable for distinguishing broad aspects of depositional environment of the studied Barail sediments.

On the whole, however, it may be concluded that the Barail sediments in the study area seem to have been deposited in a near shore-shallow marine agitated environment. Skewness being <1 too supports the above view (Reineck and Singh, 1980).Variations observed in textural parameters can be attributed to fluctuating energy regime during the deposition of these sediments (Duane, 1964; Casshyap and Khan, 1982; Mahendar and Banerji, 1989; Chaudhary, 1993; Lakhar and Hazarika, 2000). According to Ghosh and Chaterjee (1994), the stratigraphic changes in the variability of size parameters also probably indicate changes in environmental energy conditions, such as water depth and wave intensity. Positive skewed nature indicates some fluvial influence (Lakhar and Hazarika, 2000). Grain size variation, both laterally and vertically, also indicates a fluctuating energy regime within a shallow marine depositional set up (Srivastava and Pandey, 2008).

4.3 TEXTURAL MATURITY

A semi quantitative approach for estimation of textural maturity has been given by Folk (1951, 1974). He expressed textural maturity in terms of clay matrix percent, sorting and roundness. Considering clay matrix variation from 1.96 to 12.02 percent, an immature to mature character may be assigned to the Barail sediments. From the point of view of sorting, on an average, these are very well sorted to moderately sorted and hence display mature to super mature character. This is further substantiated by the association of sub- rounded grains with both matrix- poor and matrix-rich sediments, and by the presence of well sorted grains in the matrix rich sediments.

Signatures of textural inversion within the Oligocene Barail sediments can be obtained through the mixing of fluvial/beach sediments within upper shore face environment (Pettijohn, Potter and Siever, 1972). However, role of digenetic processes in

generating the matrix and also mixing of contrasting sediments through biogenic activities cannot be ruled out.

4.4 PALAEOCURRENT ANALYSIS

In recent years, increasing attentions have been paid to interpret the dispersal patterns and depositional environments of siliciclastic rocks on the basis of systematic measurement of both, the directional structures as well as the scalar quantities (Potter and Pettijohn, 1977). In the study area, not many directional structures are preserved except at higher stratigraphic levels where current ripples are preserved. Structures like asymmetrical ripples and channel cuts have been observed and measured for the interpretation of palaeocurrents. In order to understand the dispersal patterns in the study area, systematic mapping of scalars like grain-size variations and proportions of sand and mud have been employed, following the methods suggested by Potter and Pettijohn (1977).

Aerial variations of mean grain-size indicates that the competency of transport medium was decreasing gradually from SSE to NNW in the western part, SW to NE in the central part and SE to NW in the eastern part of the study area. This is further substantiated by decreasing sand-mud ratio in the direction inferred from variation in mean grain size. The palaeocurrent directions measured directly at outcrop especially from asymmetrical ripples/channel cuts (N120°), are also in conformity with the direction obtained through scalars. Based on these observations, it may be inferred that the basin was undulatory in nature and sediments supply was made from different directions.

Sample No.	M_Z	σ_I	SK_I	K_G	SO_S	σ_S
M1/17	2.47	0.78 (moderately sorted)	0.78 (Strongly fine skewed)	1.17 (Leptokurtic)	2.85	0.45
M3/17	3.63	0.63 (moderately well sorted)	-0.46 (Strongly coarse skewed)	0.70 (Platykurtic)	2.15	-0.15
M7/17	2.00	0.45 (well sorted)	0.10 (near symmetrical)	0.35 (very platykurtic)	1.55	0.05
Y5	2.10	0.57 (moderately well sorted)	-0.09 (near symmetrical)	0.63 (very platykurtic)	1.80	-0.10
Y4	2.15	0.6l (moderately well sorted)	0.34 (Strongly fine skewed)	0.72 (Platykurtic)	1.95	0.25
Z3	2.50	0.39 (well sorted)	0.07 (near symmetrical)	0.27 (very platykurtic)	1.40	0.10
K4/17	2.69	0.61 (moderately well sorted)	-0.01 (near symmetrical)	0.71 (Platykurtic)	2.00	0.00
K6/17	2.32	0.81 (moderately sorted)	0.64 (Strongly fine skewed)	1.30 (Leptokurtic)	2.65	0.45
K2/17	2.32	0.80 (moderately sorted)	0.46 (Strongly fine skewed)	1.14 (Leptokurtic)	2.53	0.33
K3/17	2.77	0.56 (moderately well sorted)	-0.05 (near symmetrical)	0.70 (Platykurtic)	1.90	0.00
L4-3	2.67	0.64 (moderately well sorted)	0.40 (Strongly fine skewed)	0.80 (Platykurtic)	2.16	0.34

R7/17	3.17	0.70 (moderately well sorted)	0.26 (fine skewed)	0.94 (Mesokurtic)	2.30	0.10
R1/17	2.58	0.67 (moderately well sorted)	0.52 (Strongly fine skewed)	0.87 (Platykurtic)	2.23	0.33
L4-9	2.64	0.63 (moderately well sorted)	0.37 (Strongly fine skewed)	0.82 (Platykurtic)	2.21	0.35
R5/17	2.90	0.56 (moderately well sorted)	0.09 (nearly symmetrical)	0.51 (very platykurtic)	1.70	0.10
L4-6	2.26	0.49 (well sorted)	0.21 (fine skewed)	0.46 (very platykurtic)	1.60	0.16
R6/17	3.08	0.47 (well sorted)	-0.14 (coarse skewed)	0.37 (very platykurtic)	1.55	-0.15
L4-7	2.45	0.47 (well sorted)	-0.27 (coarse skewed)	0.43 (very platykurtic)	1.55	-0.25
L4-5	2.43	0.41 (well sorted)	-0.22 (coarse skewed)	0.32 (very platykurtic)	1.40	-0.20
R25/14	2.58	0.42 (well sorted)	-0.06 (near symmetrical)	0.34 (very platykurtic)	1.34	-0.06
R26/14	2.63	0.43 (well sorted)	-0.16 (coarse skewed)	0.29 (very platykurtic)	1.41	-0.19
R17/13	2.44	0.39 (well sorted)	-0.21 (coarse skewed)	0.31 (very platykurtic)	1.32	-0.22
R9/14	2.75	0.41 (well sorted)	-0.01 (near symmetrical)	0.28 (very platykurtic)	1.25	-0.03

R10/14	2.84	0.43 (well sorted)	0.16 (fine skewed)	0.34 (very platykurtic)	1.45	0.15
R60/15	2.54	0.68 (moderately well sorted)	0.66 (strongly fine skewed)	0.80 (Platykurtic)	2.30	0.50
R16/15	2.50	0.38 (well sorted)	0 (symmetrical)	0.27 (very platykurtic)	1.20	0.00
R48/15	2.79	0.53 (moderately well sorted)	0.50 (strongly fine skewed)	0.54 (very platykurtic)	1.88	0.52
R56/15	2.18	0.42 (well sorted)	-0.13 (strongly coarse skewed)	0.22 (very platykurtic)	1.35	-0.15
R35/15	2.61	0.41 (well sorted)	-0.24 (strongly coarse skewed)	0.29 (very platykurtic)	1.43	-0.27
R38/15	2.06	0.38 (well sorted)	-0.08 (nearly symmetrical)	0.28 (very platykurtic)	1.37	-0.09

Table 4: Grain size data and statistical measures of selected samples

Sample	**Y1**		**Y2**		**Y3**		**Y4**	
M1/17	-4.52615	eolian	114.5311	Shallow	-0.77209	Shallow	12.97495	fluvial
M3/17	-8.3646	eolian	87.29319	Shallow	-4.61711	Shallow	3.089339	turbidity
M7/17	-5.52187	eolian	52.77622	Beach	-0.66434	Shallow	3.901593	turbidity
Y5	-4.14108	eolian	64.39692	Beach	-2.68479	Shallow	4.095845	turbidity
Y4	-4.76621	eolian	77.3594	Shallow	-0.93861	Shallow	7.48123	turbidity
Z3	-7.67301	eolian	55.23736	Beach	-0.24433	Shallow	3.641903	turbidity
K4/17	-5.99787	eolian	79.42465	Shallow	-2.49591	Shallow	5.48642	turbidity
K6/17	-3.08104	eolian	115.4587	Shallow	-1.96186	Shallow	12.59408	fluvial
K2/17	-3.32467	eolian	107.2873	Shallow	-2.58819	Shallow	10.54101	fluvial
K3/17	-6.40468	eolian	76.09653	Shallow	-2.22187	Shallow	5.207424	turbidity
L4/3	-6.34853	eolian	90.59233	Shallow	-0.83707	Shallow	8.6583	turbidity

R7/17	-7.08994	eolian	103.6837	Shallow	-2.07769	Shallow	8.793865	turbidity
R1/17	-5.91052	eolian	95.35865	Shallow	-0.6114	Shallow	9.780078	turbidity
L4/9	-6.20568	eolian	89.31499	Shallow	-0.84745	Shallow	8.585948	turbidity
R5/17	-7.79169	eolian	76.77148	Shallow	-1.45601	Shallow	5.2312	turbidity
L4/6	-6.21829	eolian	63.77695	Beach	-0.43597	Shallow	5.372224	turbidity
R6/17	-8.74005	eolian	67.20638	Shallow	-1.74248	Shallow	3.142259	turbidity
L4/7	-6.02246	eolian	56.20465	Beach	-2.53169	Shallow	2.18	turbidity
L4/5	-6.61599	eolian	51.10492	Beach	-1.8552	Shallow	1.876356	turbidity
R25/14	-7.39253	eolian	56.97028	Beach	-1.06012	Shallow	3.182718	turbidity
R26/14	-7.50377	eolian	55.68788	Beach	-1.58529	Shallow	2.311174	turbidity
R17/13	-6.74689	eolian	50.29033	Beach	-1.66856	Shallow	1.923379	turbidity
R9/14	-8.26914	eolian	59.31443	Beach	-0.75513	Shallow	3.33816	turbidity
R10/14	-8.75498	eolian	65.71223	Shallow	0.024624	Shallow	4.866041	turbidity
R60/15	-6.23599	eolian	97.05731	Shallow	-0.06905	Shallow	10.33205	fluvial
R16/15	-7.54019	eolian	53.71712	Beach	-0.5511	Shallow	3.176631	turbidity
R48/15	-8.27457	eolian	81.3924	Shallow	0.803517	Shallow	8.144037	turbidity
R56/15	-6.14621	eolian	47.48572	Beach	-1.5734	Shallow	1.783386	turbidity
R35/15	-7.27683	eolian	53.06922	Beach	-1.89976	Shallow	1.751035	turbidity
R38/15	-5.78172	eolian	45.45682	Beach	-1.08586	Shallow	2.327032	turbidity

Table 5: The four discriminant functions of Barail sediments (after Sahu, 1964)

Sample	V1	V2	Sample	V1	V2
M1/17	2.40	1.43	L4/6	1.53	0.86
M3/17	2.12	1.23	R6/17	1.73	0.94
M7/17	1.28	0.71	L4/7	1.40	0.82
Y5	1.46	0.88	L4/5	1.33	0.75
Y4	1.72	1.01	R25/14	1.48	0.83
Z3	1.44	0.78	R26/14	1.44	0.78
K4/17	1.84	1.09	R17/13	1.32	0.76
K6/17	2.36	1.46	R9/14	1.55	0.83
K2/17	2.20	1.31	R10/14	1.70	0.92
K3/17	1.82	1.11	R60/15	2.13	1.19
L4/3	2.05	1.20	R16/15	1.41	0.77
R7/17	2.35	1.38	R48/15	1.96	1.09
R1/17	2.12	1.24	R56/15	1.20	0.62
L4/9	2.03	1.21	R35/15	1.39	0.77
R5/17	1.85	1.01	R38/15	1.17	0.66

Table 6: Values of V_1 and V_2 for different samples of Barail sediments

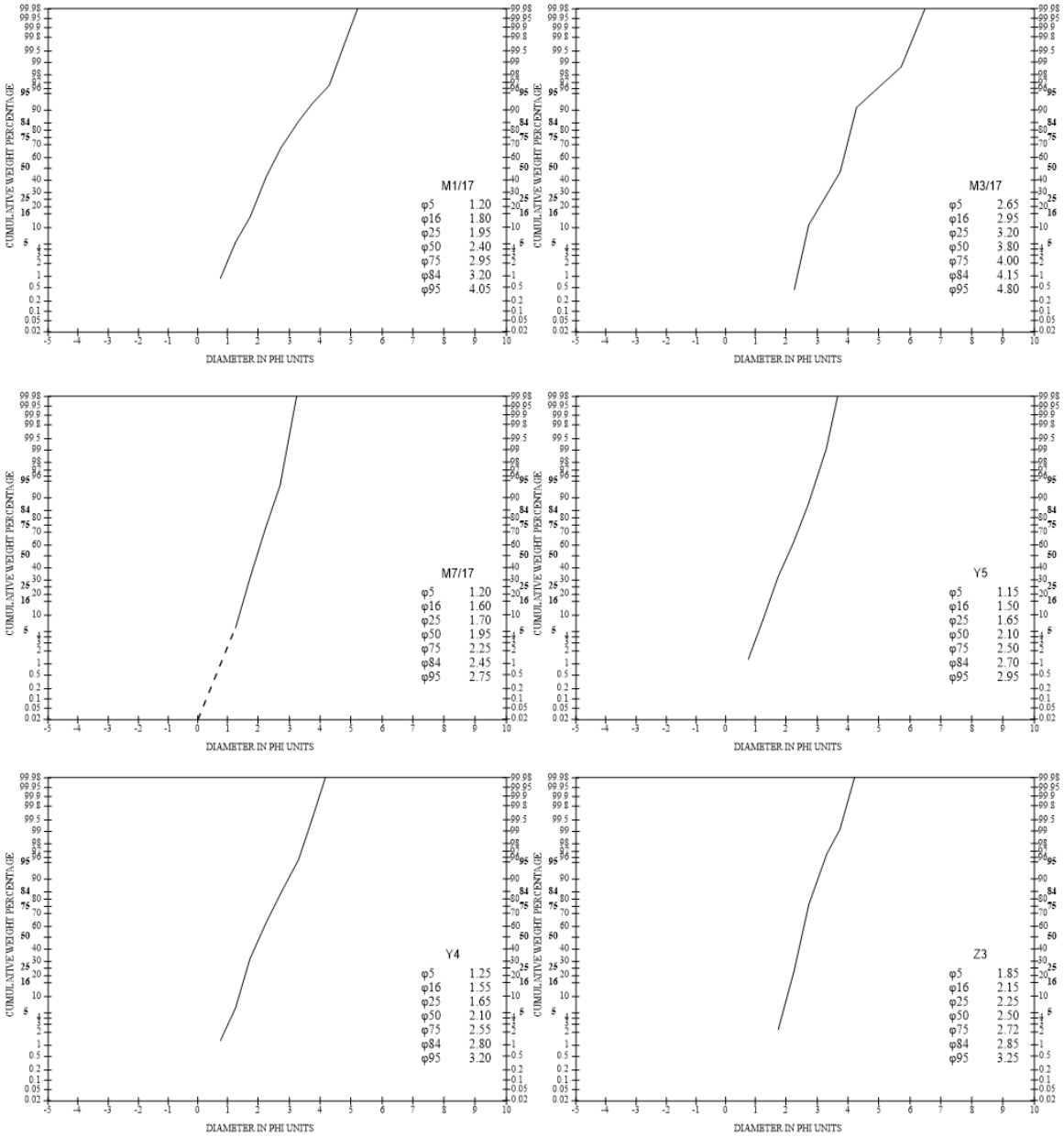

Fig. 15: Grain size distribution curves of samples from Mezoma (25°39'50.98"N, 94°00'42.82"E)

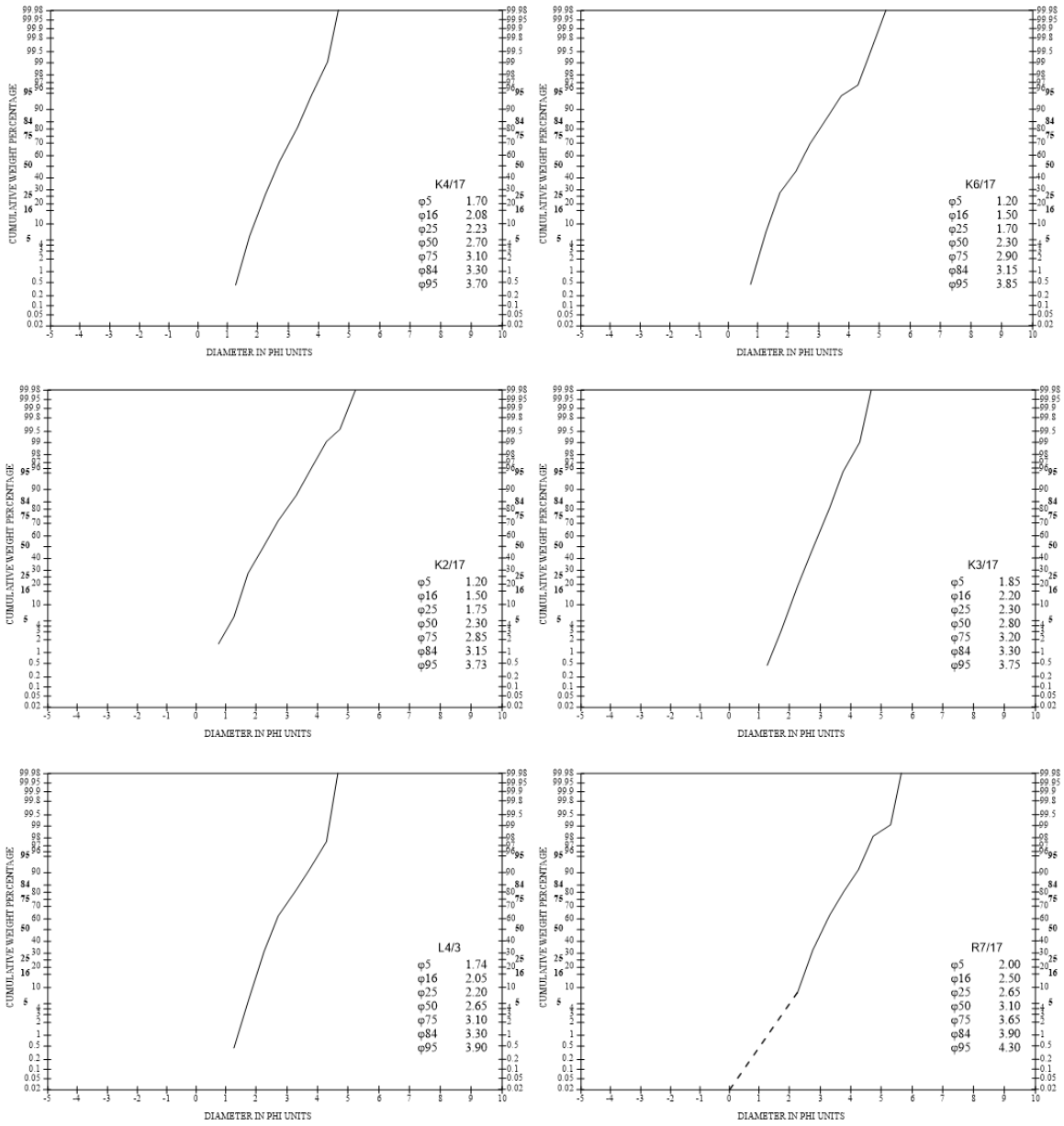

Fig. 16: Grain size distribution curves of samples from Khonoma (25°39'06.65"N, 94°01'23.99"E) and Jotsoma-Khonoma road section (25°40'09.26"N, 94°03'34.47"E, L4/3 & R7/17)

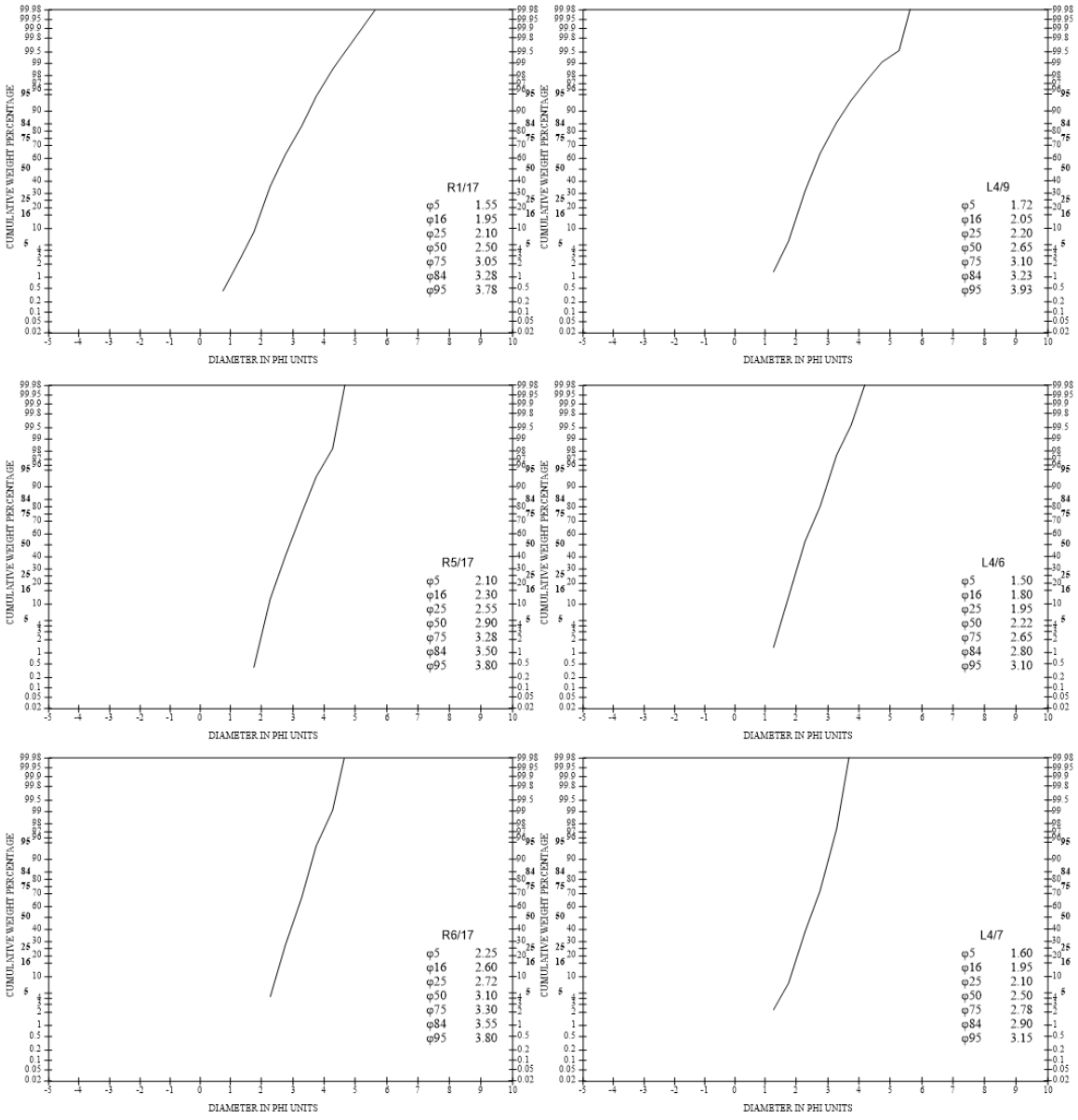

Fig. 17: Grain size distribution curves of samples from Jotsoma-Khonoma road (25°40'14.45"N, 94°02'25.66"E)

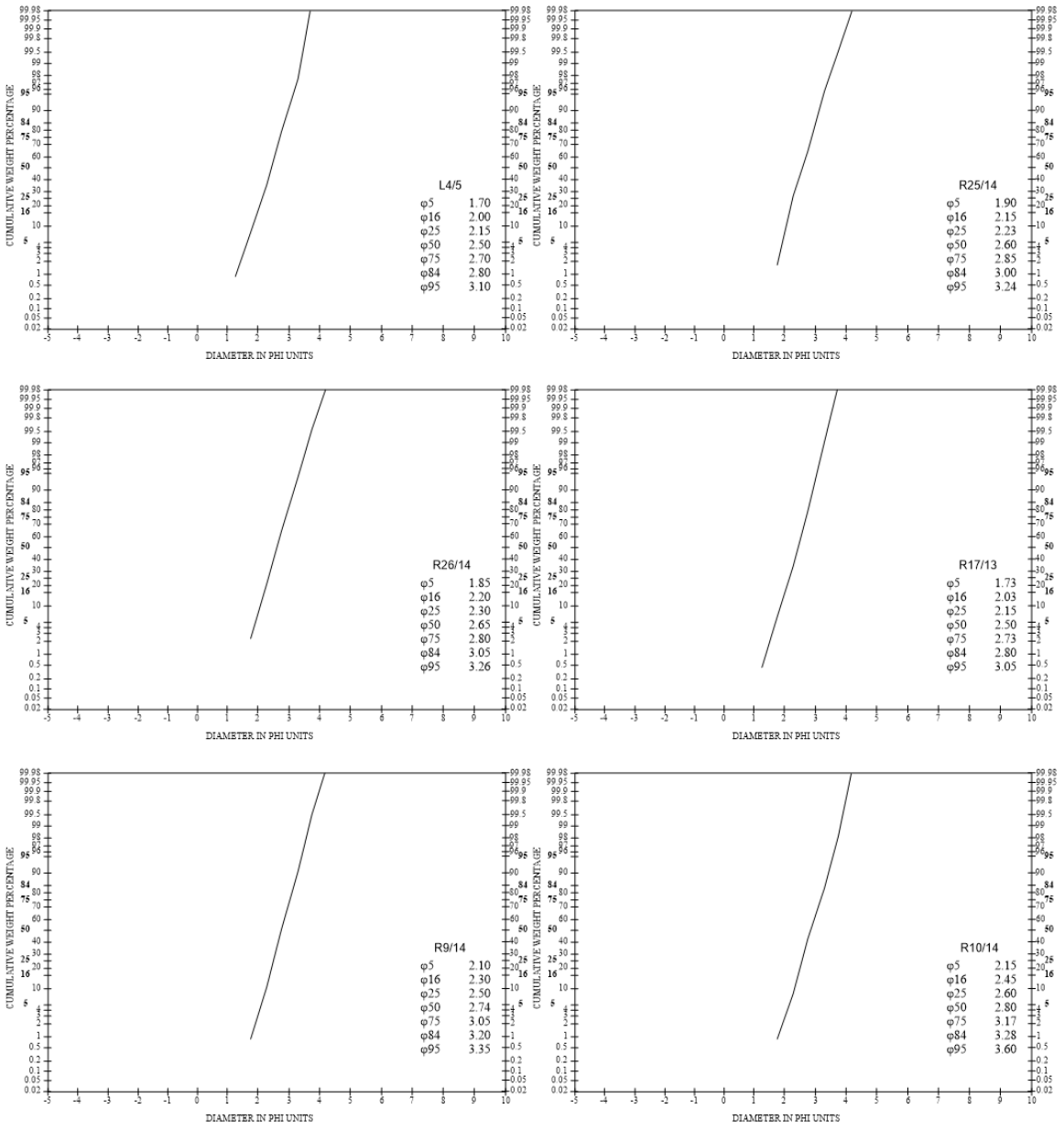

Fig. 18: Grain size distribution curves of samples from Jotsoma-Khonoma road (25°39'46.04"N, 94°03'14.15"E)

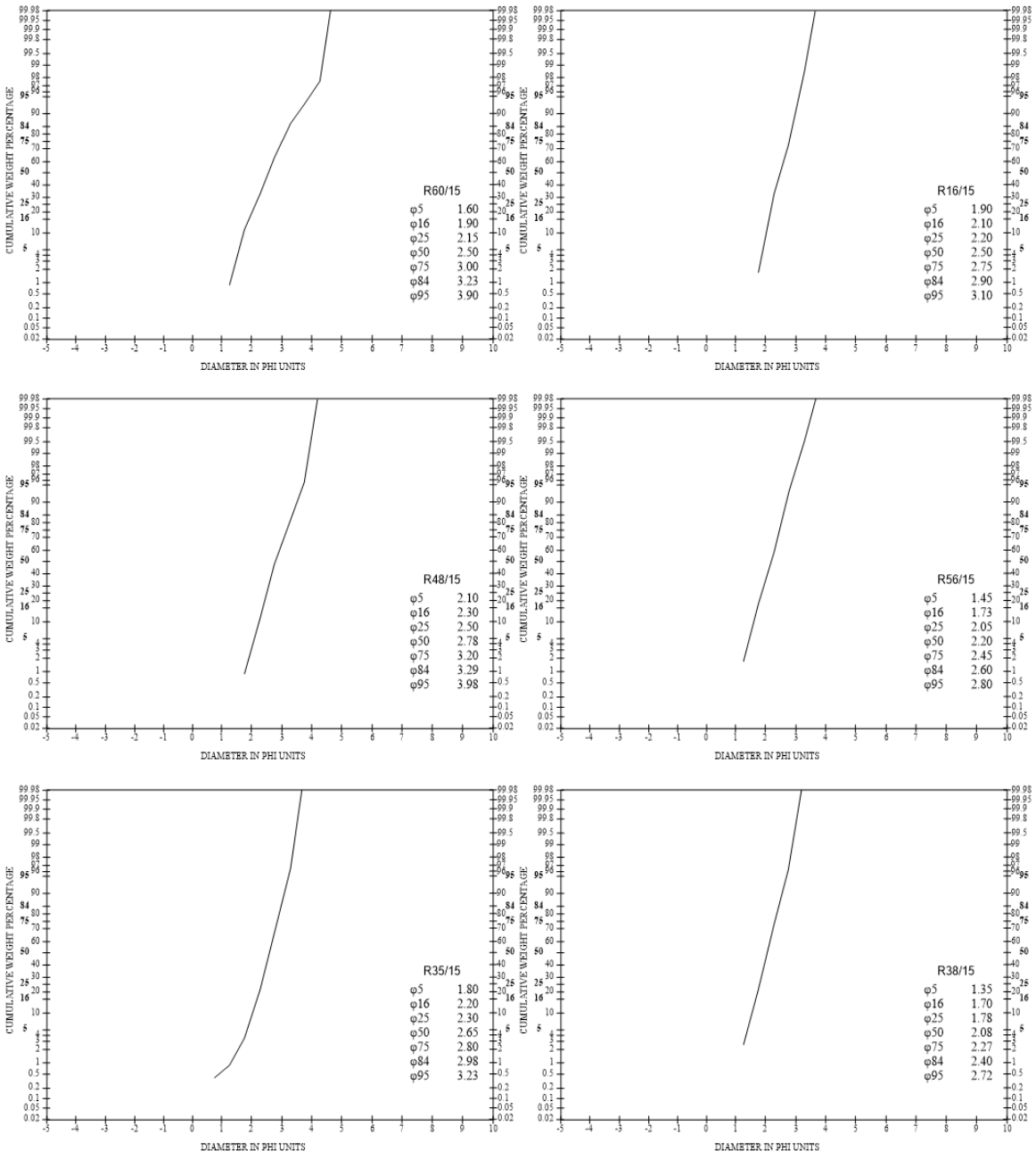

Fig. 19: Grain size distribution curves of samples from Jotsoma (25°39'33.48"N, 94°04'33.48"E)

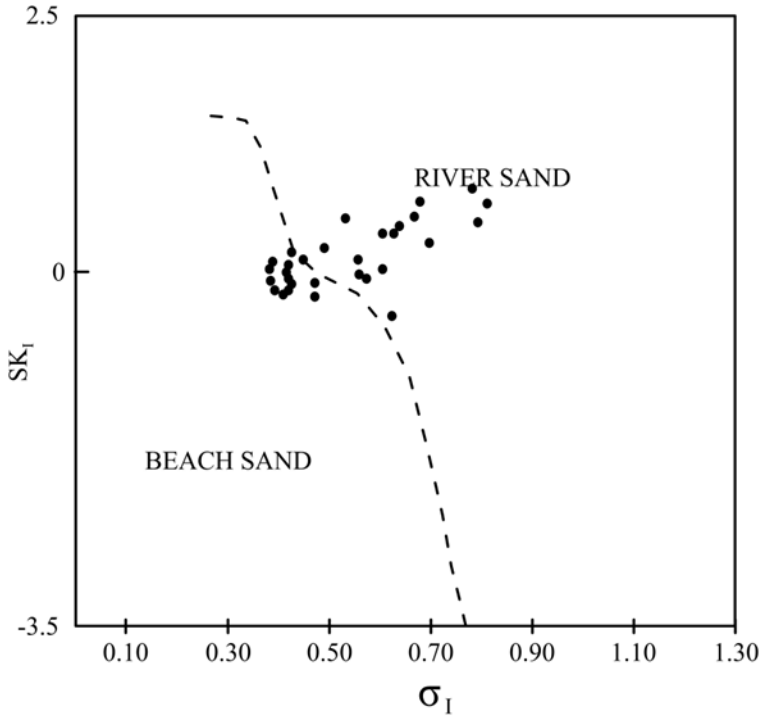

Fig. 20: Inclusive Graphic Skewness plotted against Inclusive Graphic Standard Deviation (after Friedman, 1961)

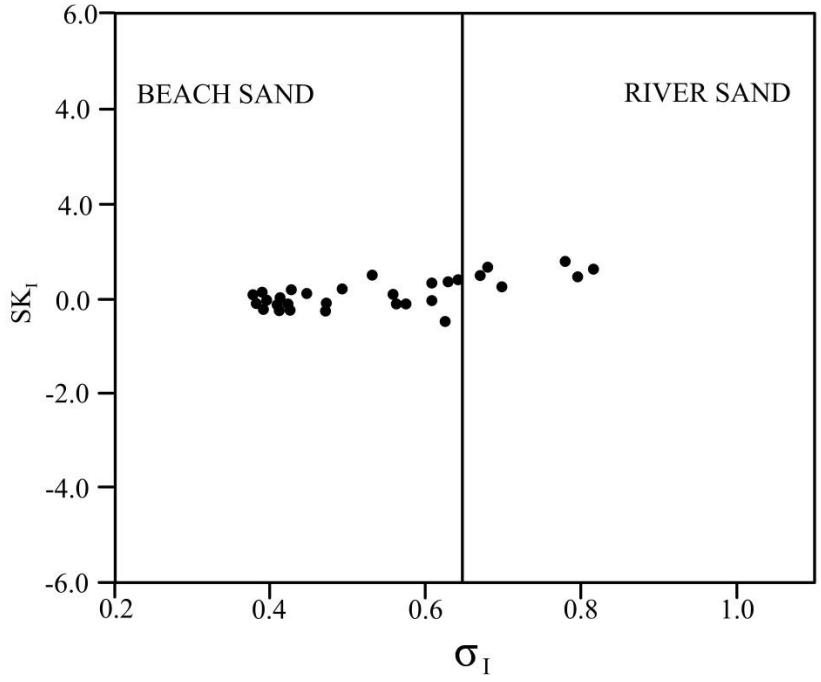

Fig. 21: Graphic Skewness plotted against Graphic Standard Deviation (after Moiola and Weiser, 1968)

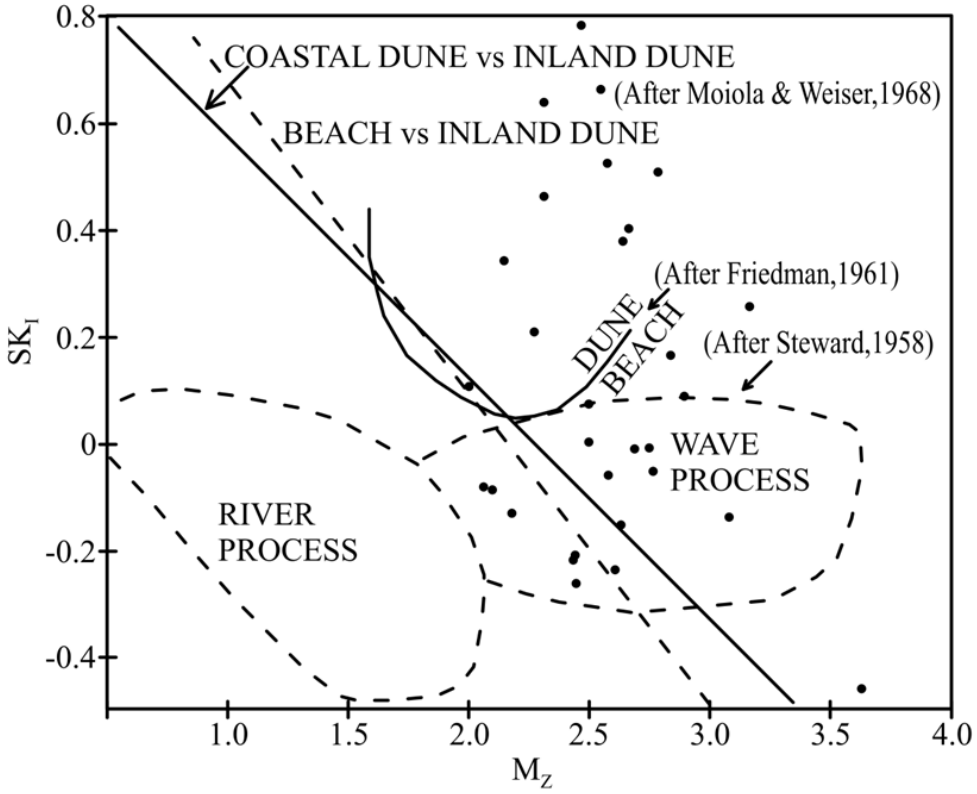

Fig. 22: Plot of Graphical Mean against Inclusive Graphic Skewness

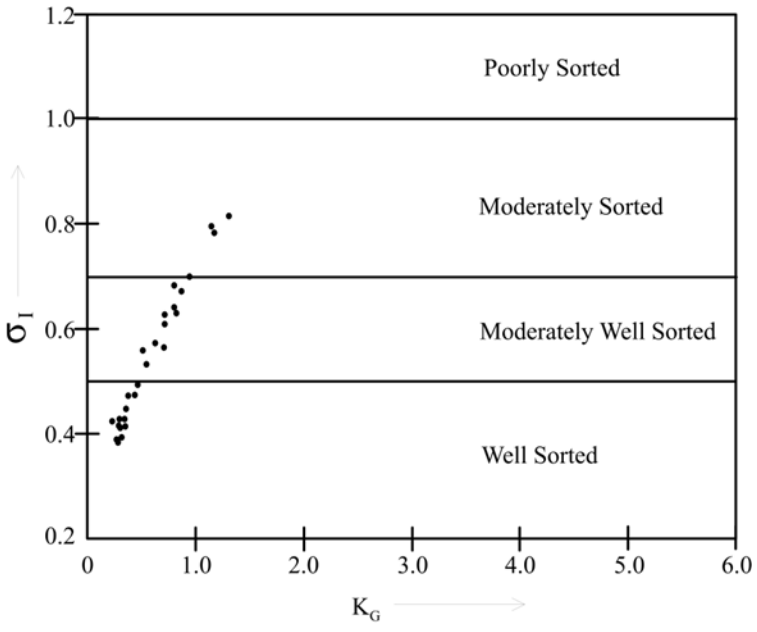

Fig. 23: Plot of Inclusive Graphic Kurtosis versus Inclusive Graphic Standard Deviation

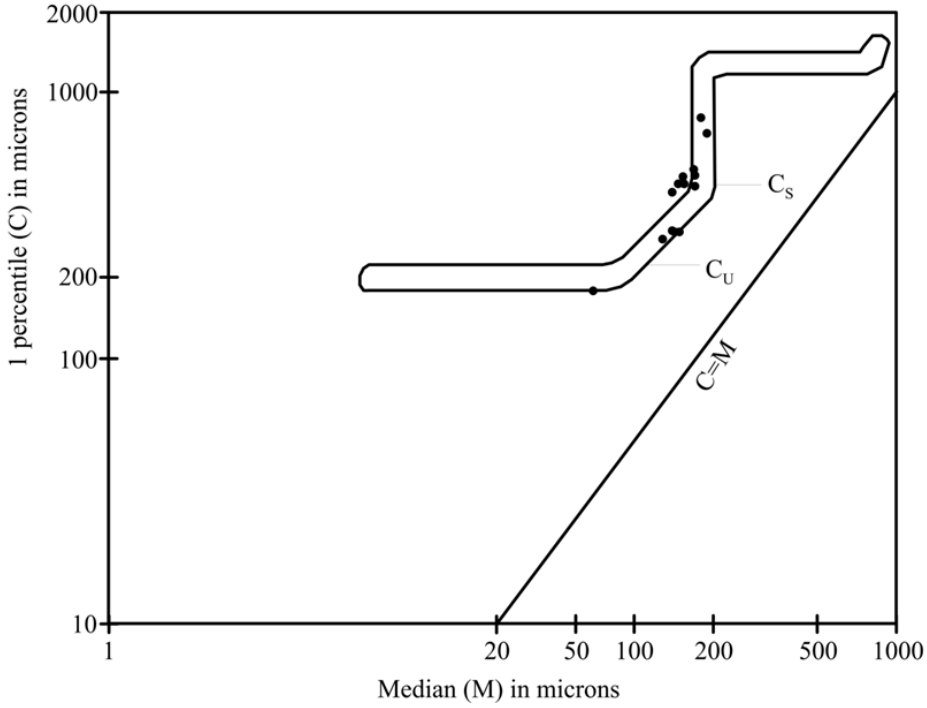

Fig. 24: C-M diagram plot of Barail sediments (after Passega, 1957)

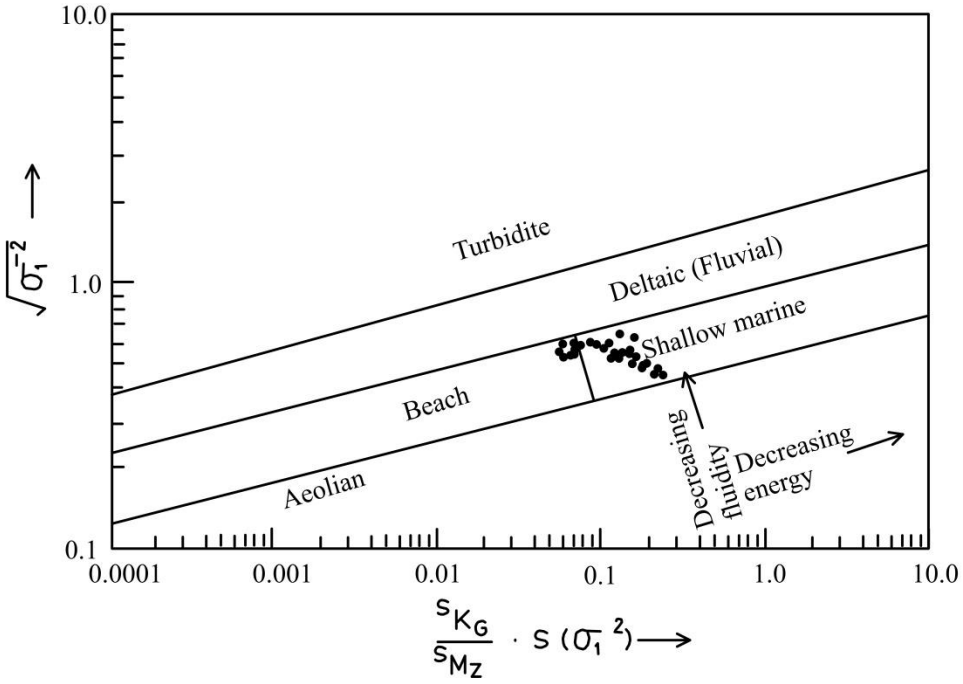

Fig. 25: The log-log plot of mean phi deviation versus the ratio of standard deviation of kurtosis to standard deviation of mean size times the standard deviation of variance (after Sahu, 1964)

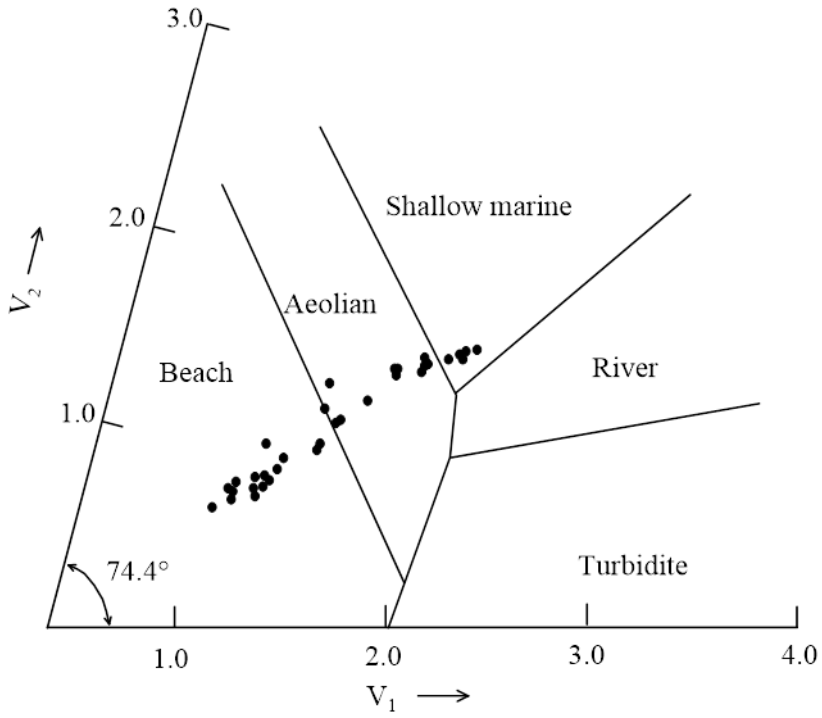

Fig. 26: Plot of V_1 against V_2 of Barail sediments (after Sahu, 1964)

CHAPTER 5

PETROGRAPHY AND MAJOR OXIDE GEOCHEMISTRY

5.1 GENERAL

Detrital composition of clastic rocks has been correlated with the rate of source area uplift and basin subsidence by many workers (Dickinson and Rich, 1972; Dickinson and Suczek, 1979; Dickinson *et al*., 1983; Miall, 1990). Appearance of a particular mineral assemblage has been successfully used in assessing tectonic events responsible for specific petrographic character of the rock unit in a stratigraphic succession. Following this, 41 thin sections were examined under the microscope and substantial data on the modal composition as well as digenetic aspects were generated. Scanning Electron Microscopic examination of 8 freshly fractured sandstone sample surfaces have also been carried out to substantiate the petrographic observations. Further to support the observations made on modal composition, 20 samples were also analysed through XRF for their major oxides composition.

5.2 PETROGRAPHY

The Oligocene Barail sandstones of the study area are hard and compact in nature and comprise of fine to medium sand fractions and typically display steel gray and light yellow colour. More than 250 grains in each of the thin sections were counted for estimation of framework grains. A brief description of framework grains has been presented in subsection 5.2.1. The overall detrital composition of Barail sandstones in the study area can be expressed as Q 66.42%, F 3.73%, RF 8.92%, Mi 6.60%, 3.14% heavies, including both opaques and non opaques; and CT 3.41%, M 7.78% by volume (**Table 7**).

5.2.1 FRAMEWORK GRAINS

Quartz: There are three basic quartz types namely, non-undulatory quartz, undulatory quartz and polycrystalline quartz, which comprises the total quartz population in a clastic rock (Conolly, 1965). Monocrystalline non-undulatory quartz grains (QNU)

are generally identified by their complete extinction upon a slight (less than 1°) rotation of microscopic stage (Blatt and Christie, 1963), while the monocrytalline undulatory quartz grains (QU) can be distinguished by their wavy extinction. Polycrystalline quartz grains, consisting of 2 to 3 units as well as > 3 units, are generally distinguished from metaquartzite rock fragments by the presence of smooth, non-sutured boundaries between separate units.

Quartz is the dominant framework grain in Barail sandstones. Out of the total quartz content (66.26%, **Table 7**), nearly 79.63% are non-undulatory, 17.85% fall under undulose category and 2.52% are polycrystalline grains (**Table 8**). Some of the quartz grains were seen to contain inclusions (**Plate 8c** & **8d**). They are sub-angular to sub-round in shape (**Plates 8**, **9**, **10**, **11**, **12** & **13**). However, few well rounded grains are also seen.

Feldspar: The feldspar content ranges between nil to 18.52%, (average 3.73%, **Table 7**). Among the feldspar varieties (**Table 8**), the plagioclase feldspar (89.95%) is most common and represented by sodic end member showing characteristic albite twinning (**Plates 8e**, **8f**, **9a**, **9b**, **9c**, **9d**, **10a**, **11b**, **12d**, **12e** & **13f**). K-feldspar (10.05%) is represented by both orthoclase and microcline but is observed mainly in the sandstones of the upper stratigraphic levels. Microcline (**Plates 9e**, **9f**, **10a**, **10b** & **10c**) and orthoclase (**Plate 10d**, **10e** & **10f**), both altered as well as fresh feldspar grains, were observed; the former being associated with the matrix (**Plate 9c** & **9d**). At places, precipitations of silica on feldspar grains have also been observed.

Mica: The mica content ranges from 0.44% to 16.13% (**Table 7**). Observed flakey minerals include biotite, muscovite and chlorite. These occur in the form of shreds and flakes, many of which have been bent and warped around quartz grains. Reconstituted mica is not uncommon (**Plates 11b**, **11c**, **11d**, **12e**, **13c** & **13e**).

Rock Fragments: Rock fragments constitute a significant portion of the detrital composition next to quartz and are identified by their compositional and textural criteria (Dickinson, 1970). On an average, these constitute nearly 8.92% of the total detrital composition, the range being 0% to 15.63% (**Table 7**). All the three major types, viz.

sedimentary, metamorphic and igneous rock fragments were observed in order of decreasing abundance. Sandstone/silt stones and cherts represent the sedimentary rock fragments (**Plates 9b**, **11a**, **11b**, **11f**, **13a**, **13b**, **13c**, **13d** & **13e**) whereas schist and phyllites characterize the metamorphics (**Plates 10b**, **11e**, **13b** & **13c**). Volcanic glasses, though very few, are also seen (**Plates 8e** & **12a**).

5.2.2 MATRIX AND CEMENT

Cements are authigenic minerals that fill interstitial areas that were originally open pore spaces. Several minerals may act as cements in sandstones; however clay minerals, carbonates, quartz and iron cement are particularly common cements. In the present study, both silica as well as iron cements are present (**Plates 8d**, **9e**, **9f** & **10a**). Silica cements occur both in syntaxial and epitaxial fashion. Yellowish/red coloured iron oxides form the other cement and occur around the grains or as over-coating. Total cement ranges from 0.83% to 6.83% by volume.

Matrix is finer-grained material that fills interstitial spaces among framework grains. The upper size limit of material in sandstones considered to be matrix is arbitrary and debatable; however, a maximum size of 0.03 mm appears to be favored by many workers (Boggs, Jr., 2012). Identification of type of matrix under microscope is a rather difficult task. Quartz, mica and some feldspar enmeshed in clay have also been considered as matrix. At places, grain boundaries have been digested by the matrix.

5.2.3 CLAY MINERALS

Both whole rock and clay fractions were analyzed for their clay and other mineral contents at Gauhati University, Assam using XRD technique. Altogether 12 sandstone samples were analysed. The machine was set between 4° to 30° for the oriented samples while glycolated samples were run between 4° to 10°. Almost all the analysed samples record the presence of kaolinite and montmorillonite (**Fig. 28a**). Illite was also recorded in few samples (**Fig. 28b**). In addition to these, other clay minerals observed includes nimite (chlorite group), dickite (kaoline group) and gibbsite (kaolinite byproduct). Also, in SEM images (**Plates 18** & **19**), presence of illite was noticed.

Illite: This clay mineral has registered its presence in some of the samples. Illite is produced in the sediments by decomposition of feldspar as well as degradation of mica; at least in the initial stages of weathering under alkaline conditions enriched with Ca2+ ions. However, transformation of kaolinite into illite is not very uncommon. The quick mixing of fresh water sediments with those of marine also favours the formation of illite as the later contains high concentration of K and Mg (Grim, 1968).

Kaolinite: Kaolinite is the most abundant among the clay minerals analysed. It is the common alteration product of K-feldspar under acidic condition favoured by a good drainage system. Formation of kaolinite has also been recorded in soils under a warm humid climate, where extensive leaching and acidic conditions predominate.

Montmorillonite: Montmorillonite, a member of smectite group, has been recorded in almost all the glycolated samples. Chemically, it is hydrated sodium calcium aluminum magnesium silicate and is commonly found as weathering products of ferromagnesium rocks such as basalts and gabbros. However, they can be formed under a variety of conditions.

Chlorite: It has magnesium and iron in its structures and is produced by the weathering of ferromagnisium minerals in such rocks as basalts and gabbros. Chlorites are found in low and medium rank metamorphic rocks and also in deeply buried sediments.

5.2.4 HEAVY MINERALS

To infer the provenance and also the mineralogical maturity of the Barail sandstones of the study area, 25 indurated samples were analyzed for their heavy mineral contents. Using heavy liquids (Bromoform, Sp. Gravity - 2.89), heavy minerals were separated following the method suggested by Folk (1980). Grain mounts were prepared and examined under the microscope for identification of both opaque as well as non-opaque heavy minerals.

Heavy minerals recorded in Barail sandstones include anhedral, euhedral, subhedral and recycled zircon with and without inclusions (**Plate 14**); euhedral, subhedral and

rounded tourmaline (**Plate 15**); anhedral to subhedral rutile (**Plate 16**); and kyanite (**Plate 17a**), staurolite (**Plate 17b**) and silliminate (**Plate 17c**). The iron oxide grains comprise the opaque varieties (**Plate 17d**). The heavy minerals identified show a specific trend of their abundance i.e. Zircon > Tourmaline > Rutile > Opaques > Kyanite > Staurolite > Silliminate. Relative abundance of heavy minerals according to type and shape are represented by Pie diagrams (**Fig. 27**). The heavy minerals assemblage is dominated by well-rounded to sub rounded/sub angular varieties suggesting either long transport or a recycled origin (Srivastava and Pandey, 2011; Srivastava and Kebenle, 2018). However, contribution from a crystalline source cannot be ruled out as suggested by the presence of angular and euhedral varieties. High ZTR index suggests that the studied sandstones are mineralogically highly matured. Nevertheless, the assemblage, as a whole, points towards mixed source for the Barail sandstones, the substantial contribution coming from the igneous source. A few well rounded zircon grains have also been noticed in photomicrographs (**Plate 12f**).

5.3 NOMENCLATURE, CLASSIFICATION AND MODAL ANALYSIS

A number of schemes and systems of sandstone classifications have been proposed by many workers including Okada (1971), Pettijohn *et al.*, (1972), Pettijohn (1975), Folk (1980) and Zuffa (1980). However, there is no single scheme which could satisfy all the parameters of sandstone classification. In this study, Folk's (1980) scheme has been adopted for nomenclature and classification of the sandstones present in the area.

In this scheme, the three end members, *i.e.* detrital quartz, feldspar and rock fragments have been considered to represent the three corners of the triangle. Following Folk (1980), sandstones of the study area have been classified into two main categories *viz* litharenite and sublith-arenite sandstones. However, some studied samples fall under the quartzarenite, sub-feldsarenite and feldspathic litharenite categories also (**Fig. 29**).

Discriminatory diagrams suggested by Dickenson and Suczek (1979), were used for understanding the probable provenance and tectonic settings of the Barail sandstones. The *poly quartz-lithic volcanic-lithic sedimentary* (**Fig. 30**) and the *mono quartz-plagioclase-potash feldspar* (**Fig. 31**) plot suggest that these sediments were derived from

a collision suture, fold thrust belt in a continental block provenance. Both the *total quartz-feldspar-lithic* (**Fig. 32**) and *mono quartz-feldspar-lithic fragment* (**Fig. 33**) plots indicate that almost all the samples are from recycled orogen provenances. The *mono quartz-feldspar-lithic fragment* **(Fig. 34)** and *quartz-feldspar-lithic fragment* (**Fig. 35**) plots (after Dickenson *et al.*, 1983) also shows a mostly recycled orogeny provenance with some contribution from craton interior.

Diamond diagrams (after Basu *et al.*, 1975 and Tortosa *et al.*, 1991), based on quartz types (mono crystalline undulatory, non undulatory, polycrystalline 2-3and >3 units), show middle and upper rank metamorphic and plutonic rocks as the source rocks (**Fig. 37a** & **37b**).

5.4 DIAGENESIS

According to Blatt *et al.*, (1980), diagenetic changes begin near the surface and continue up to deeper levels before metamorphism sets in. Burial time, temperature and subsurface water chemistry generally control the rate and type of diagenetic changes. Microscope is still the main instrument for identification of diagenetic modifications. However, Scanning Electron Microscopic (SEM) technique has greatly enhanced our understanding of diagenetic process and it has also helped in understanding the phisico-chemical conditions which sediments had undergone. Many workers (Pitman, 1972; Krinsley and Doornkamp, 1973; Ingersoll, 1974; Marzolf, 1976) have suggested that the appearance of diagenetic signatures within sediments is co-relatable with increasing depth. Eight (8) freshly broken Barail sandstone samples have been examined under SEM at the IIT, Gauhati, Assam. The diagenetic features identified in the studied sandstones include neomorphic growth, silica rims, solution cavities and dissolution pits besides well-developed kaolinite, illite-smectite layered clay and degradation of feldspar (**Plates 18** & **19**).

5.4.1 EFFECTS OF DIAGENESIS

Silica overgrowth is one of the most common features of early diagenesis. However, presence of matrix does not allow the overgrowth as it acts as barrier against the silica solution (Carozzi, 1960; Heald and Lorese, 1974). The deep burial diagenesis is

represented by fracturing, crushing, bending and warping of micaceous minerals around detrital quartz. Various diagenetic features observed in Barail sandstones include compaction, authigenesis and cementation (**Plates 8**, **9**, **10**, **11**, **12** & **13**).

5.4.2 DIAGENETIC STAGE

Various diagenetic stages observed in Barail sandstones are locomorphic, redoxmorphic and phyllomorphic. Progressive appearance of certain features characterizes these stages. According to Bjorkum and Gjelsvik (1988), iron oxide precipitation signifies the redoxomorphic stage, whereas modified grain to grain contacts, corrosion of detrital grains, alteration of feldspar and silica over growth represent the locomorphic stage (Borak and Friedman, 1981). Phyllomorphic stage is represented by authigenic mica.

5.4.3 DIAGENETIC ENVIRONMENT

Two categories of diagenetic modifications are preserved in these sediments: early and late diagenesis. Early diagenesis includes silica overgrowth and precipitation of calcitic and iron cements (Carozzi, 1960; Heald and Lorese, 1974). According to Sengupta (1994), late diagenetic phase is represented by fracturing, crushing, bending and warping of micaceous material under increasing pressure and temperature conditions *i.e.* late diagenesis.

5.4.4 CEMENTS

Dominant cementing material in these siliciclastics is silica. Epitaxial and syntaxial overgrowths and neomorphic quartz have been observed. Other diagenetic features observed are enlargement of quartz grains and thick rims of silica cement around detrital quartz grains. Kichu and Srivastava (2018) have suggested that underlying thick shale/mudstones column of Disang Group experiencing continuous and uninterrupted loading could have supplied silica for cementation in Barail sandstones. In addition to that, diagenetic transformation of silicates including clay minerals (Towe, 1962) and devitrification of volcanic glasses (Surdam and Boles, 1979), and pressure solution effects (Dapples, 1979) might have been other sources for the supply of silica for

cementation. The overgrowths might have also occurred above 80°C at a depth of 1.5 to 2 km (Surdam *et al.*, 1989; Dutton and Diggs, 1990).

In the present study, ferruginous (iron oxide) cement has been noticed. Iron bearing accessory minerals of metamorphic/igneous rock fragments as well as phyllosilicates could have also supplied iron cement. A major source of iron cement may be the weathering of iron rich mineral as suggested by Walker (1974). Presence of ferruginous cement in the studied sandstones suggests an enhanced oxidation of meteoric water.

5.4.5 QUARTZ OVERGROWTH

Possibilities of quartz overgrowths are more where the grains are uncoated. Presence of clay matrix around quartz grain does not facilitate the overgrowth (Heald and Lorese, 1974). Presence of authigenic quartz in these sediments indicate the early diagenetic modification under eogenetic marine conditions (Burley *et al.*, 1985). Neo-quartz crystals also suggest early diagenetic conditions and are developed at the stress points (Blatt *et al.*, 1980).

5.4.6 ALBITIZATION

Presence of small blebs and indistinct and diffused twinnings is an important feature of albitized feldspar where twin lamella has a vague and irregular twinning which do not pass through the whole crystal. Fractures and cleavage traces are the plane of weakness along which albitization generally progresses. Some of them show chess board like fabric (**Plate 12b**). Albitization occurs at temperatures of the order of 100-150°C (Boles, 1982; Surdam *et al.*, 1989) and also at temperatures as low as 70-100°C (Morad *et al.*, 1990). Presence of authigenic feldspar in the studied samples suggests increasing pressure and temperature (>100°C) in response to burial and thermal history.

5.4.7 GRAIN CONTACTS

All possible types of grain contacts (floating, straight, concavo-convex and sutured) have been noticed. Reactions between matrix and cements could impart floating characters to the grains. Corroded grain boundaries are the product of such reactions. These corroded boundaries are filled by iron oxide and thus show a floating character. In the studied samples, penetrative contacts (concavo-convex and sutured) are dominant

over other types (long and floating). A deep burial condition of diagenesis has been interpreted on the basis of dominance of concavo-convex and sutured contacts and low proportion of long and floating contacts suggest.

5.5 GEOCHEMICAL ANALYSIS

For better understanding of the provenance and palaeoclimate and also to compliment the data generated through petrographic studies, geochemical aspects of sedimentary rock, are also being used. Geochemical attributes and framework composition of sandstones, their provenance type and the tectonic environment have provided considerable impetus to the subject (Kakul ,1968; Crook,1974; Schwab,1975; Bhatia ,1983; Suttner and Dutta ,1986; and McLennan ,1989).

For the purpose, 20 Barail sandstone samples have been analysed for their major element composition and data have been presented in **Table 9**. The samples were analysed using an automatic X-ray Fluorescence Spectrometer at Wadia Institute of Himalayan Geology, Dehradun. In order to determine the types of sandstones according to their chemical compositions, the plot of log (Fe_2O_3/K_2O) versus log (SiO_2/Al_2O_3) (**Fig. 38**), after Herron (1988), has been used. The clustering of data points clearly indicates the dominance of litharenite sandstones in the area with a few samples falling in the wacke field.

The bivariate plots of Fe_2O_3 (Total) + MgO vs K_2O/ Na_2O (**Fig. 39**), Fe_2O_3 (Total) + MgO vs Al_2O_3/SiO_2 (**Fig. 40**) and Fe_2O_3 (Total) + MgO vs TiO_2 (**Fig. 41**), after Bhatia (1983), have been utilized, for understanding the tectonic settings. A dominantly passive margin setting for the Barail sandstones has been indicated. This is further substantiated by the plot of K_2O/Na_2O vs SiO_2 (after Roser and Korsch, 1986, **Fig. 42**).

It is well known that passive margin settings are the primary sites of major river systems (Potter, 1978a) and typically have provenance consisting of recycled sedimentary debris and/or older plutonic metamorphic material, with a relatively small volcanic component (Potter, 1978b). The triangular plots CaO-NaO_2-K_2O and Fe_2O_3-MgO-TiO_2 (**Fig. 44 & 45**), after LeMaitre (1976) and Condie (1967), further substantiate derivation of detritus from passive margin type of tectonic settings. The clustering of data points in these plots further indicates granodioritic and granitic source for the Barail

sediments under study. As passive margins comprise rifted margin along the edges of the continents, remnant ocean basin adjacent to collision orogen, and inactive or extinct convergent margins, the signature of granodioritic and granitic provenance appears to have been existed along rifted basin receiving sediments for the area under study.

The palaeoclimate, as inferred from the bivariate plot of $Al_2O_3+K_2O+Na_2O$ *vs* SiO_2, after Suttner and Dutta (1986), appears to have been largely humid (**Fig. 43**). This is also supported by the plot of QFL, after Suttner *et al.*, 1981 (**Fig. 36**).

Sm No.	***T. Qtz%***	***T. Feld%***	***T. RF%***	***Mica%***	***HM%***	**Cement (Vol. %)**	**Matrix (Vol. %)**
R 08/14	*84.28*	*0.87*	*3.93*	*0.44*	*1.31*	*2.62*	*6.55*
R 09/14	*78.04*	*4.21*	*1.87*	*0.93*	*1.87*	*4.67*	*8.41*
R 10/14	*62.59*	*2.88*	*6.47*	*7.55*	*6.12*	*5.04*	*9.35*
R 16/15	*73.15*	*0.67*	*2.68*	*2.01*	*0.00*	*5.37*	*16.11*
R 19/14	*71.61*	*3.39*	*0.00*	*6.78*	*2.12*	*6.78*	*9.32*
R 25/14	*67.66*	*0.85*	*5.11*	*9.79*	*4.68*	*4.26*	*7.66*
R 26/14	*73.45*	*2.91*	*2.55*	*7.64*	*6.18*	*1.45*	*5.82*
R 29/15	*80.69*	*0.43*	*3.00*	*2.58*	*2.15*	*5.15*	*6.01*
R 35/15	*74.89*	*2.16*	*6.06*	*2.16*	*4.33*	*1.73*	*8.66*
R 38/15	*83.04*	*0.00*	*3.57*	*0.45*	*0.45*	*0.89*	*11.61*
R 48/15	*71.49*	*0.41*	*5.79*	*6.20*	*3.72*	*2.48*	*9.92*
R 56/15	*80.17*	*0.83*	*5.79*	*2.89*	*2.07*	*0.83*	*7.44*
R 58/15	*83.25*	*0.96*	*1.44*	*1.91*	*3.83*	*0.96*	*7.66*
R 60/15	*79.29*	*1.18*	*6.51*	*0.59*	*1.78*	*2.37*	*8.28*
R 1/17	*57.14*	*3.78*	*14.71*	*10.50*	*2.94*	*2.52*	*8.40*
R 5/17	*58.13*	*4.47*	*10.16*	*12.20*	*2.03*	*3.25*	*9.76*
R 6/17	*59.68*	*2.02*	*6.05*	*16.13*	*0.40*	*6.05*	*9.68*
R 7/17	*53.79*	*7.24*	*8.28*	*13.79*	*3.79*	*6.21*	*6.90*
L4-3	*68.51*	*0.85*	*8.94*	*2.98*	*7.66*	*3.40*	*7.66*
L4-5	*55.75*	*3.54*	*15.49*	*13.72*	*3.54*	*1.77*	*6.19*

L4-6	*66.53*	*7.76*	*12.24*	*1.63*	*2.86*	*2.45*	*6.53*
L4-7	*62.39*	*5.56*	*14.96*	*2.14*	*2.99*	*4.27*	*7.69*
L4-9	*59.65*	*7.46*	*10.96*	*6.58*	*4.82*	*3.51*	*7.02*
K 2/17	*58.33*	*6.06*	*13.26*	*7.58*	*7.20*	*3.79*	*3.79*
K 3/17	*54.27*	*4.78*	*11.95*	*10.24*	*3.07*	*6.83*	*8.87*
K 4/17	*65.11*	*2.55*	*7.66*	*4.68*	*6.38*	*4.26*	*9.36*
K 6/17	*66.39*	*8.40*	*9.66*	*5.46*	*0.00*	*1.68*	*8.40*
M 1/17	*58.87*	*6.45*	*14.11*	*2.82*	*4.84*	*3.23*	*9.68*
M 3/17	*61.79*	*2.03*	*8.94*	*12.20*	*2.03*	*4.88*	*8.13*
M 4/17	*69.57*	*3.04*	*5.65*	*8.26*	*4.78*	*1.74*	*6.96*
M 7/17	*68.38*	*5.93*	*11.86*	*3.16*	*1.98*	*3.16*	*5.53*
Y1	*64.09*	*0.91*	*11.36*	*15.91*	*0.45*	*2.73*	*4.55*
Y2	*62.93*	*2.16*	*12.93*	*12.93*	*0.43*	*1.72*	*6.90*
Y3	*52.96*	*18.52*	*11.11*	*2.22*	*1.11*	*6.67*	*7.41*
Y4	*62.98*	*2.55*	*12.77*	*6.81*	*3.83*	*5.11*	*5.96*
Y5	*66.12*	*0.83*	*12.40*	*7.44*	*2.48*	*2.48*	*8.26*
Z1	*58.37*	*3.86*	*10.73*	*10.73*	*6.01*	*3.43*	*6.87*
Z2	*58.78*	*2.86*	*12.24*	*12.24*	*5.71*	*4.08*	*4.08*
Z3	*60.46*	*6.84*	*13.31*	*6.84*	*1.90*	*1.52*	*9.13*
Z4	*60.71*	*6.25*	*15.63*	*4.91*	*2.68*	*2.68*	*7.14*
Z5	*67.87*	*4.52*	*13.57*	*4.52*	*2.26*	*1.81*	*5.43*

Table 7: Detritus composition of Barail sediments in the study area

	Poly Qtz		**Mono Qtz**		**Percentage**			**Feldspar**		**Percentage**	
Slide No.	**2-3**	**>3**	**Und**	**Non Und**	**Poly**	**Und**	**Non Und**	**Potash**	**Plag.**	**Potash**	**Plag**
R 08/14	7	6	60	120	*6.74*	*31.09*	*62.18*	0	2	*0.00*	*100*
R 09/14	5	0	15	147	*2.99*	*8.98*	*88.02*	1	8	*11.11*	*88.89*
R	0	0	24	150	*0.00*	*13.79*	*86.21*	0	8	*0.00*	*100.00*

10/14											
R 16/15	0	1	29	79	*0.92*	*26.61*	*72.48*	0	1	*0.00*	*100.00*
R 19/14	0	0	9	160	*0.00*	*5.33*	*94.67*	0	8	*0.00*	*100.00*
R 25/14	0	0	19	140	*0.00*	*11.95*	*88.05*	0	2	*0.00*	*100.00*
R 26/14	1	0	31	170	*0.50*	*15.35*	*84.16*	0	8	*0.00*	*100.00*
R 29/15	2	0	44	142	*1.06*	*23.40*	*75.53*	0	1	*0.00*	*100.00*
R 35/15	0	0	23	150	*0.00*	*13.29*	*86.71*	0	5	*0.00*	*100.00*
R 38/15	1	0	45	140	*0.54*	*24.19*	*75.27*	0	0	*0.00*	*0.00*
R 48/15	0	0	15	158	*0.00*	*8.67*	*91.33*	0	1	*0.00*	*100.00*
R 56/15	2	0	17	175	*1.03*	*8.76*	*90.21*	0	2	*0.00*	*100.00*
R 58/15	0	0	15	159	*0.00*	*8.62*	*91.38*	0	2	*0.00*	*100.00*
R 60/15	5	13	32	84	*13.43*	*23.88*	*62.69*	0	2	*0.00*	*100.00*
R 01/17	0	0	35	101	*0.00*	*25.74*	*74.26*	0	9	*0.00*	*100.00*
R 05/17	0	0	8	135	*0.00*	*5.59*	*94.41*	0	11	*0.00*	*100.00*
R 06/17	1	2	45	100	*2.03*	*30.41*	*67.57*	0	5	*0.00*	*100.00*
R 07/17	0	9	9	138	*5.77*	*5.77*	*88.46*	1	20	*4.76*	*95.24*
L4-3	5	0	27	129	*3.11*	*16.77*	*80.12*	0	2	*0.00*	*100.00*
L4-5	0	0	23	103	*0.00*	*18.25*	*81.75*	1	7	*12.50*	*87.50*
L4-6	4	3	19	137	*4.29*	*11.66*	*84.05*	0	19	*0.00*	*100.00*
L4-7	0	3	45	98	*2.05*	*30.82*	*67.12*	1	12	*7.69*	*92.31*
L4-9	0	1	0	135	*0.74*	*0.00*	*99.26*	3	14	*17.65*	*82.35*
K 2/17	3	4	12	135	*4.55*	*7.79*	*87.66*	2	14	*12.50*	*87.50*

K 3/17	3	8	23	125	*6.92*	*14.47*	*78.62*	0	14	*0.00*	*100.00*
K 4/17	2	2	11	138	*2.61*	*7.19*	*90.20*	0	6	*0.00*	*100.00*
K 6/17	3	3	50	102	*3.80*	*31.65*	*64.56*	1	19	*5.00*	*95.00*
M 1/17	5	0	24	117	*3.42*	*16.44*	*80.14*	0	16	*0.00*	*100.00*
M 3/17	0	0	10	142	*0.00*	*6.58*	*93.42*	0	5	*0.00*	*100.00*
M 4/17	0	0	50	110	*0.00*	*31.25*	*68.75*	2	5	*28.57*	*71.43*
M 7/17	5	0	57	111	*2.89*	*32.95*	*64.16*	2	13	*13.33*	*86.67*
Y1	0	4	38	99	*2.84*	*26.95*	*70.21*	0	2	*0.00*	*100.00*
Y2	0	2	21	123	*1.37*	*14.38*	*84.25*	3	2	*60.00*	*40.00*
Y3	6	5	32	100	*7.69*	*22.38*	*69.93*	8	42	*16.00*	*84.00*
Y4	0	12	38	98	*8.11*	*25.68*	*66.22*	3	3	*50.00*	*50.00*
Y5	0	8	32	120	*5.00*	*20.00*	*75.00*	2	0	*100.00*	*0.00*
Z1	0	5	48	83	*3.68*	*35.29*	*61.03*	0	9	*0.00*	*100.00*
Z2	0	0	24	120	*0.00*	*16.67*	*83.33*	2	5	*28.57*	*71.43*
Z3	0	4	25	130	*2.52*	*15.72*	*81.76*	1	17	*5.56*	*94.44*
Z4	0	3	33	100	*2.21*	*24.26*	*73.53*	5	9	*35.71*	*64.29*
Z5	1	0	20	129	*0.67*	*13.33*	*86.00*	0	10	*0.00*	*100.00*

Table 8: Percentages of different types of Quartz and Feldspar in Barail sandstones

Sample	Na_2O%	MgO%	Al_2O_3%	SiO_2%	P_2O_5%	K_2O%	CaO%	TiO_2%	MnO%	Fe_2O_3%	SUM
K1/17	0.55	0.36	6.16	87.31	0.06	0.70	0.03	0.30	0.02	2.83	98.32
K5/17	0.70	0.54	6.98	85.47	0.06	0.87	0.08	0.55	0.02	2.66	97.93
L4-1	0.58	0.20	5.91	89.18	0.05	0.77	0.03	0.40	0.00	1.66	98.78
L4-4	0.50	0.21	5.31	90.69	0.05	0.69	0.02	0.42	0.01	1.67	99.57
L4-9	0.58	0.23	6.17	89.28	0.04	0.82	0.02	0.37	0.01	1.63	99.15
M3/17	0.67	0.44	7.82	84.47	0.07	0.99	0.03	0.59	0.02	2.72	97.82
M6/17	0.85	0.43	8.48	84.43	0.08	1.24	0.07	0.54	0.01	2.20	98.33
M8/17	0.65	0.28	5.65	89.23	0.07	0.77	0.07	0.95	0.01	1.56	99.24
R1/17	0.61	0.20	4.24	90.77	0.05	0.58	0.10	0.29	0.01	1.51	98.36
R3/17	0.92	0.63	8.33	83.79	0.06	1.05	0.06	0.53	0.01	3.12	98.50
R4/14	0.81	0.40	6.13	87.50	0.06	0.87	0.20	0.60	0.02	2.14	98.73
R4/17	0.78	0.35	5.84	88.40	0.07	0.82	0.10	0.39	0.02	1.87	98.64
R6/17	0.93	0.84	11.64	76.80	0.10	1.90	0.23	0.62	0.03	3.38	96.47
R33/16	0.61	0.30	5.79	89.16	0.04	0.75	0.06	0.44	0.01	1.57	98.73
R36/15	0.77	0.44	8.49	85.03	0.08	1.12	0.06	0.48	0.01	2.31	98.79
R37/16	0.84	0.54	9.73	81.42	0.07	1.33	0.09	0.64	0.05	2.68	97.39
R40/16	0.73	0.57	9.02	82.53	0.09	1.23	0.10	0.56	0.01	2.74	97.58
R57/16	0.59	0.38	6.04	88.21	0.06	0.74	0.08	0.41	0.01	2.15	98.67
R59/15	0.57	0.41	6.26	87.44	0.08	0.73	0.12	0.64	0.02	2.60	98.87
R63/15	0.55	0.40	6.07	87.88	0.06	0.68	0.09	0.45	0.01	2.33	98.52

Table 9: Percentage of major oxides in sandstone samples

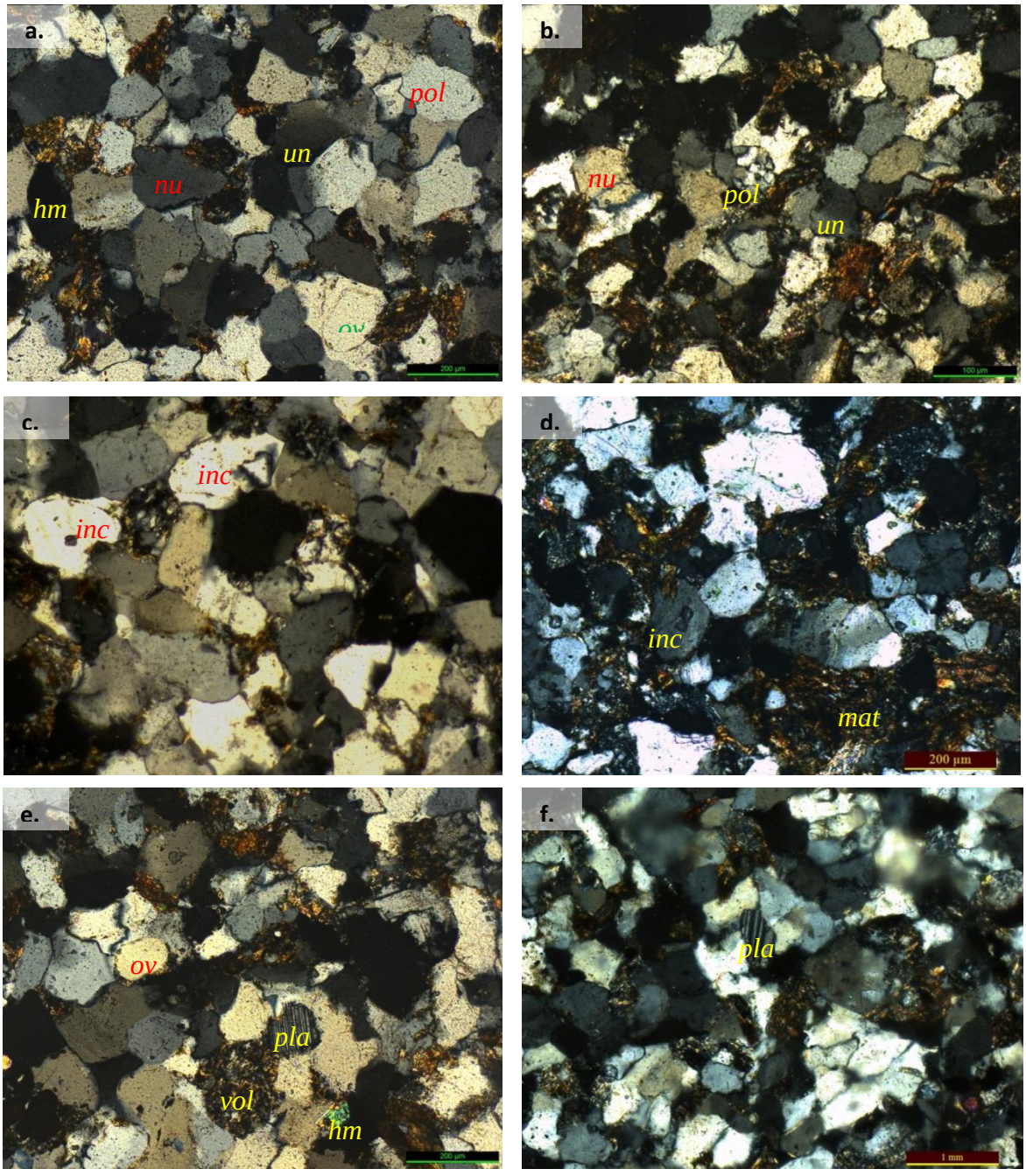

Plate 8: Photomicrographs showing **a**) polycrystalline (*pol*), undulatory (*un*) and non-undulatory (*nu*) quartz; heavy mineral (*hm*); quartz overgrowth (*ov*) **b**) polycrystalline quartz (*pol*); non-undulatory quartz with straight contact (*nu*); undulatory quartz (*un*) **c)** quartz inclusions (*inc*); overgrowths (*ov*) **d**) quartz inclusions (*inc*), ferruginous matrix (*mat*) **e**) quartz overgrowth (*ov*); plagioclase (*pla*); heavy mineral (*hm*); volcanics (*vol*) **f**) plagioclase feldspar (*pla*)

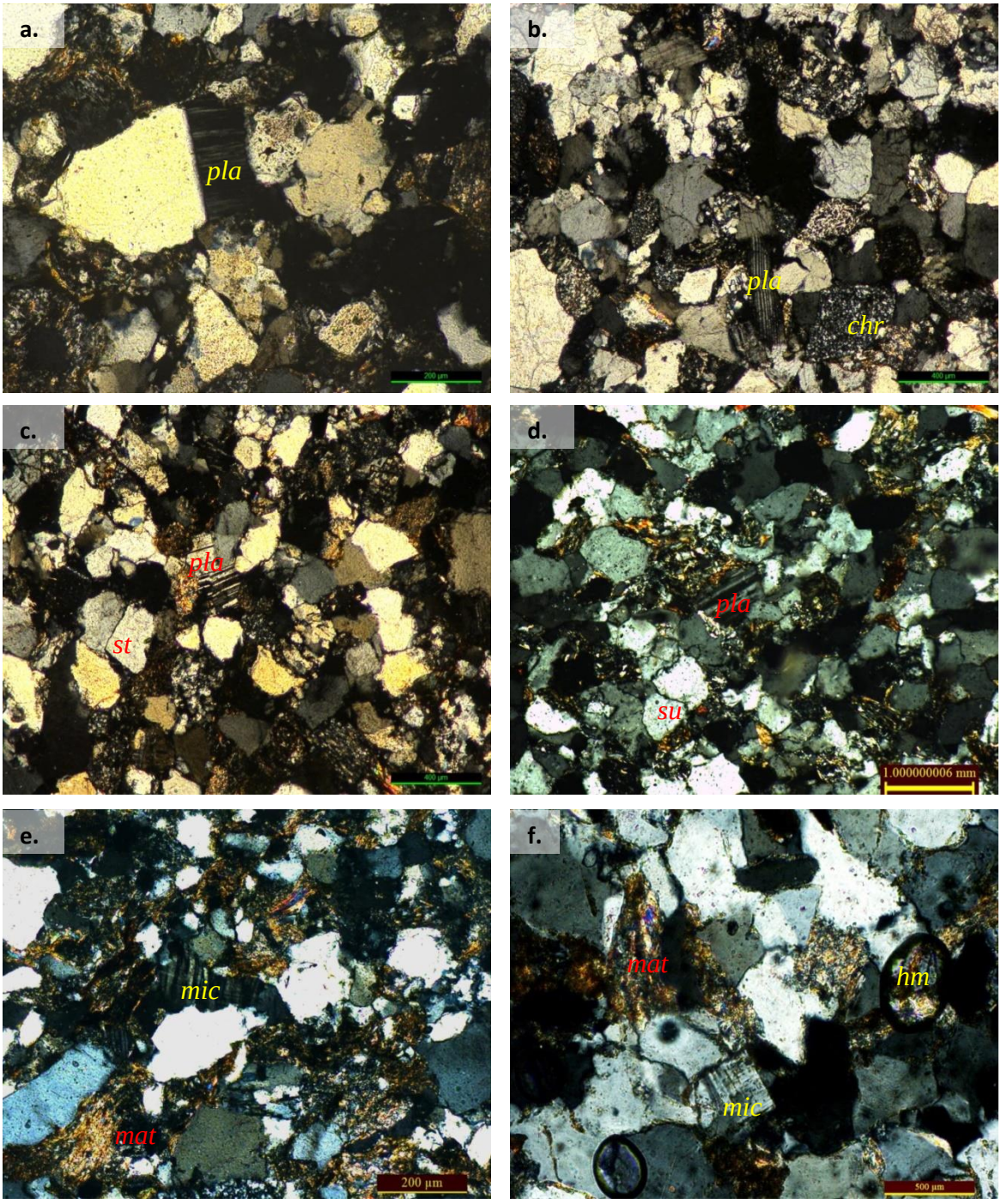

Plate 9: Photomicrographs showing **a**) plagioclase in straight contact with quartz grain (*pla*) **b**) plagioclase (*pla*); chert (*chr*) **c)** plagioclase (*pla*); straight contact between quartz grains (*st*) **d**) plagioclase (*pla*); sutured contacts (*su*) **e**) microcline (*mic*); matrix (*mat*) **f**) microcline (*mic*); heavy mineral (*hm*); matrix (*mat*)

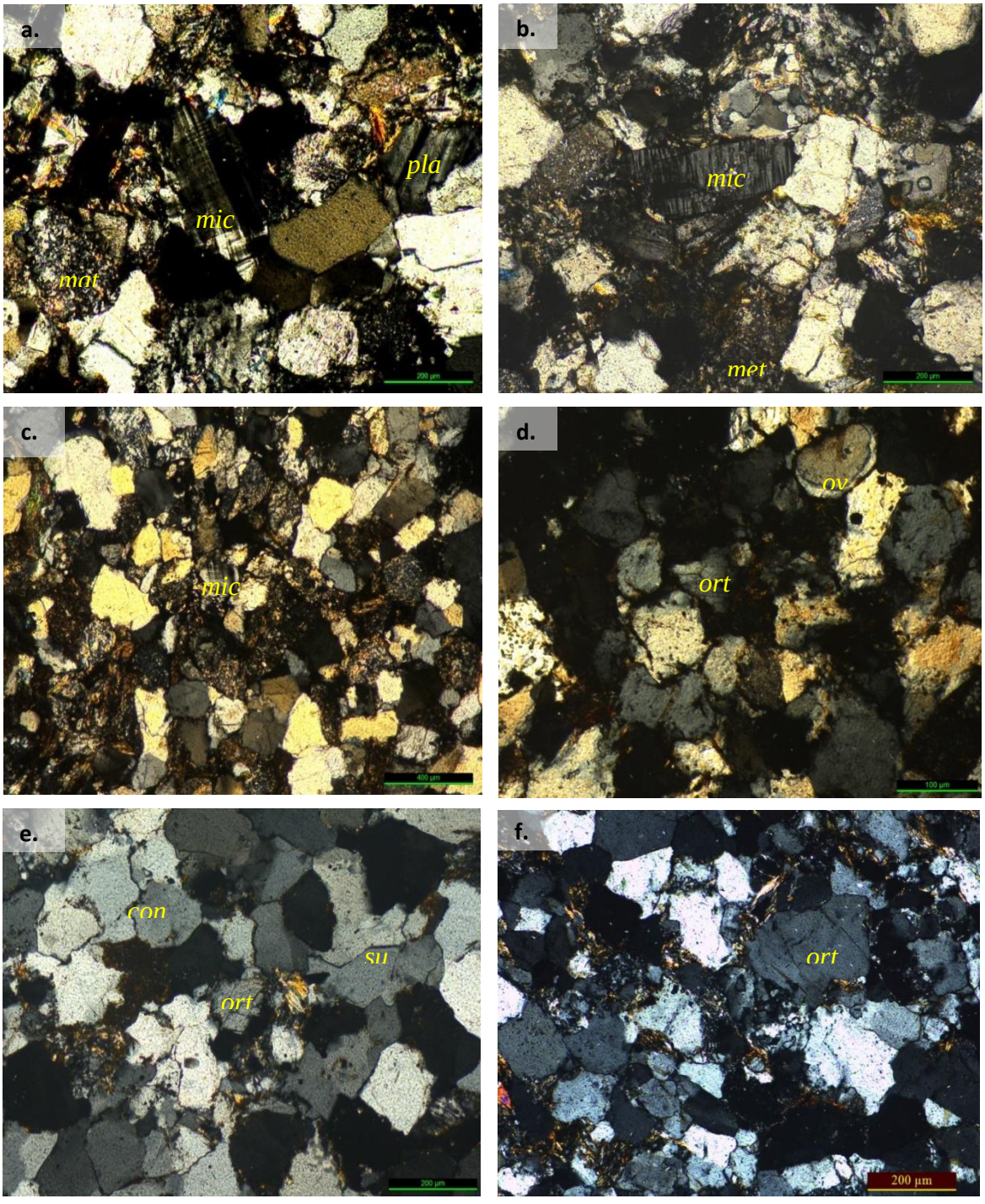

Plate 10: Photomicrographs showing **a**) euhedral microcline (*mic*); plagioclase (*pla*); matrix (*mat*) **b**) microcline (*mic*); metamorphic rock fragment (*met*) **c)** microcline (*mic*) **d**) orthoclase (*ort*); silica overgrowth on quartz grain (*ov*) **e**) orthoclase (*ort*); sutured contact (*su*); concavo-convex contact (*con*) **f**) orthoclase (*ort*)

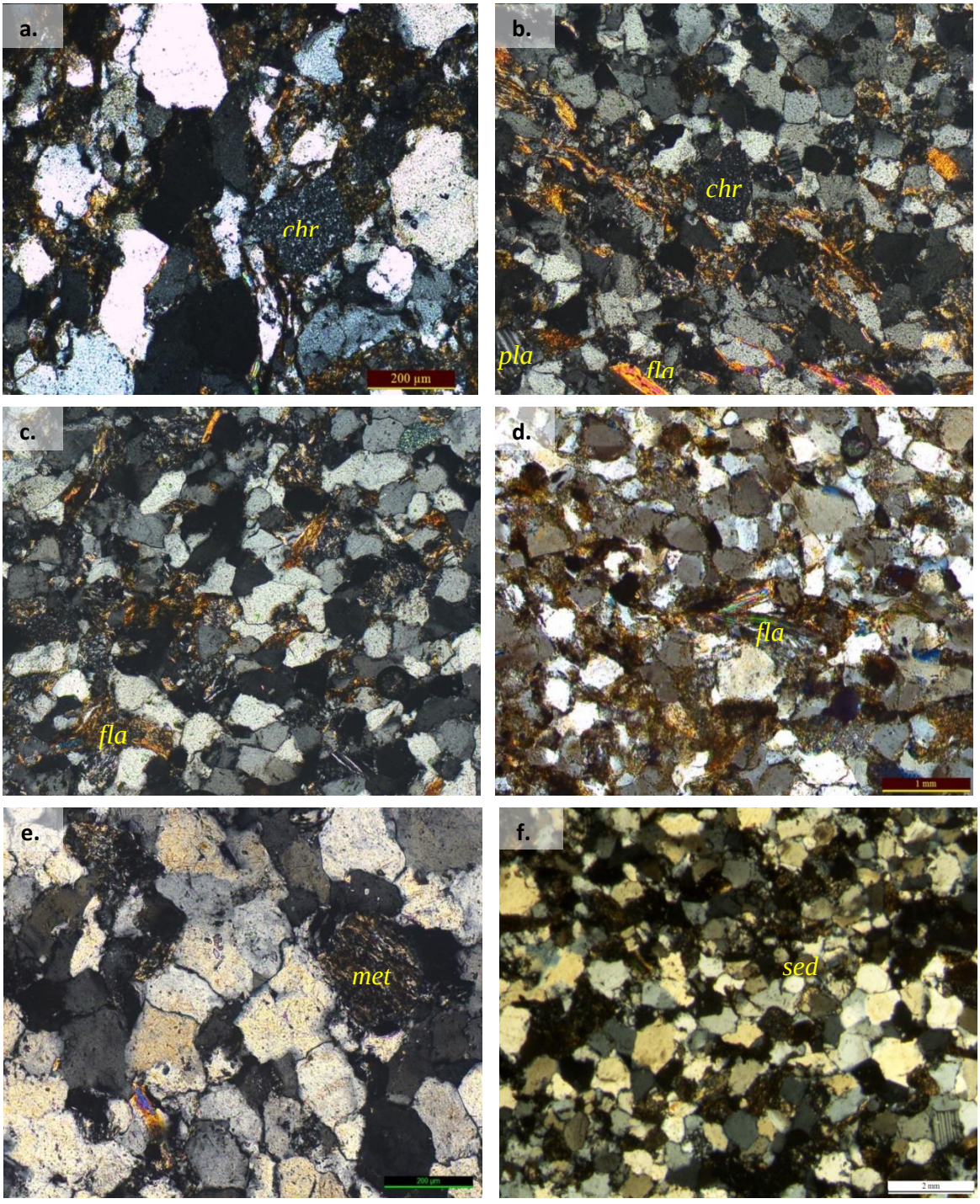

Plate 11: Photomicrographs showing **a**) chert (*chr*) **b**) chert (*chr*); mica (*fla*); plagioclase (*pla*) **c)** reconstituted mica (*fla*) **d**) bending of mica (*fla*) **e**) metamorphic rock fragment (*met*) **f**) sedimentary rock fragment (*sed*)

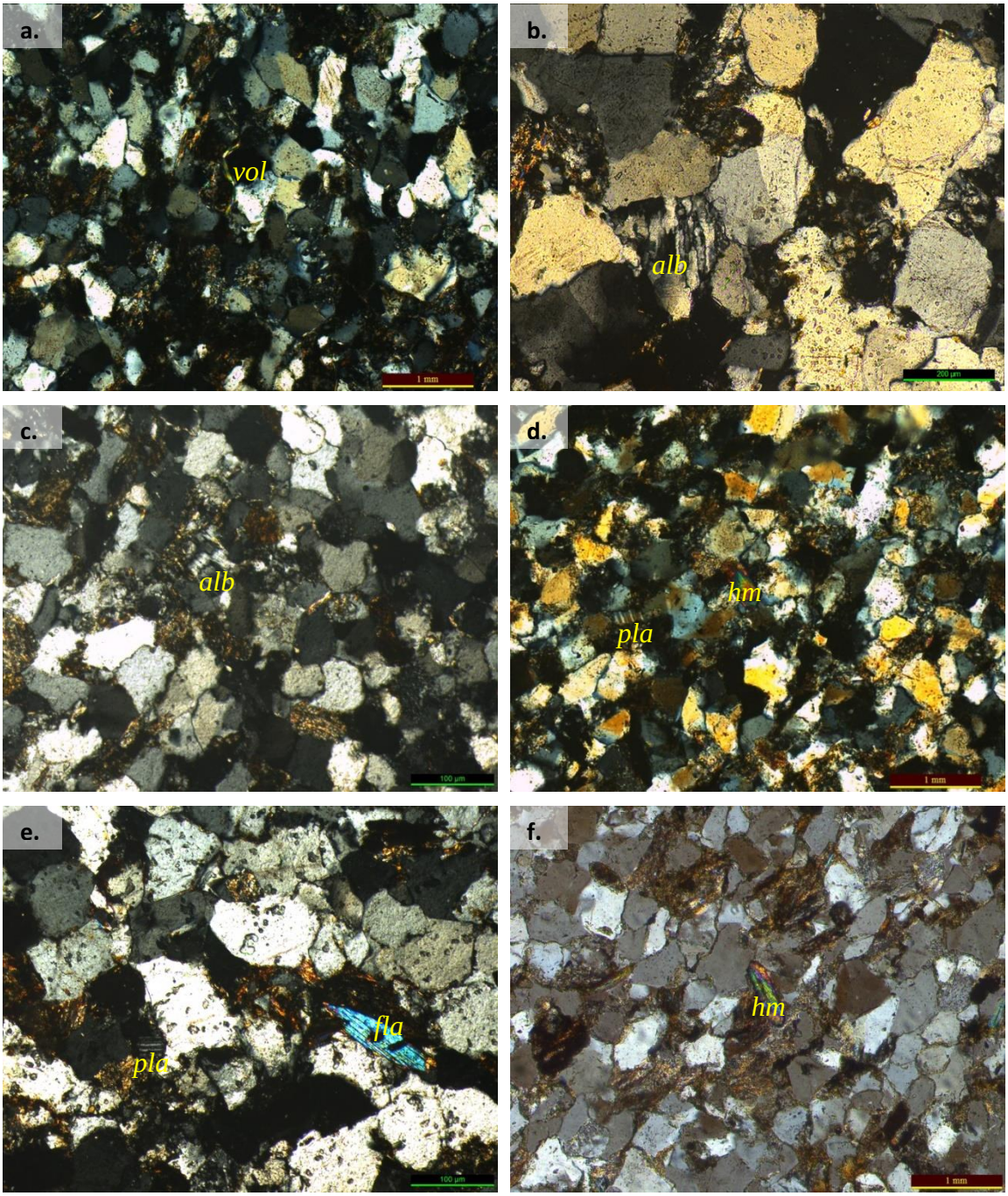

Plate 12: Photomicrographs showing **a**) volcanic fragment (*vol*) **b**) chessboard-like albitized feldspar (*alb*) **c)** albitized feldspar (*alb*) **d**) overgrowth on heavy mineral (*hm*); plagioclase (*pla*) **e**) biotite (*fla*); plagioclase (*pla*) **f**) well rounded zircon (*hm*)

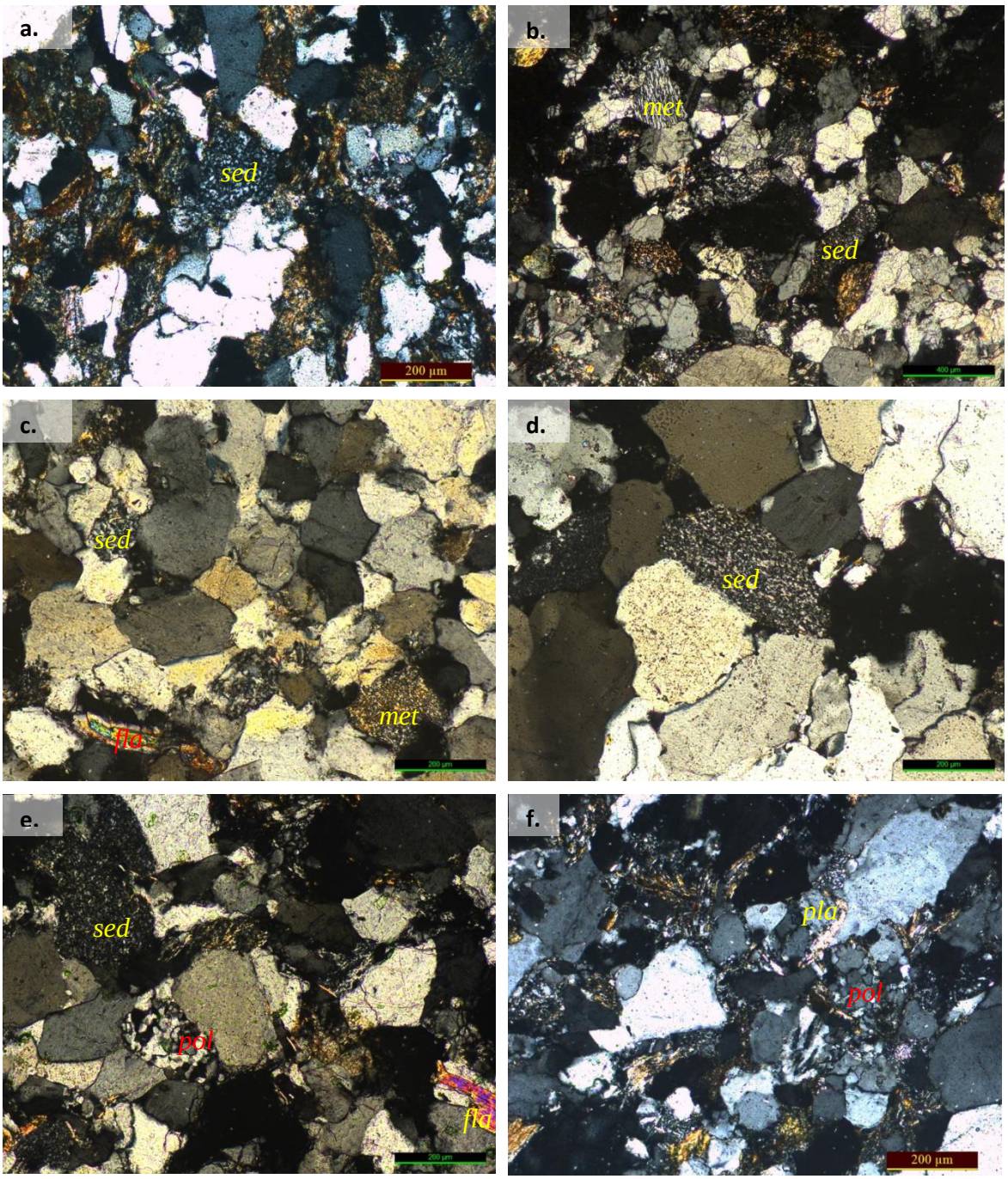

Plate 13: Photomicrographs showing **a**) siltstone fragment (*sed*) **b**) schist (*met*); siltstone (*sed*) **c)** siltstone (*sed*); schist (*met*); mica (*fla*) **d**) sitlstone (*sed*) **e**) mica (*fla*); polycrystalline quartz (*pol*); siltstone (*sed*) **f**) polycrystalline quartz (*pol*); plagioclase (*pla*)

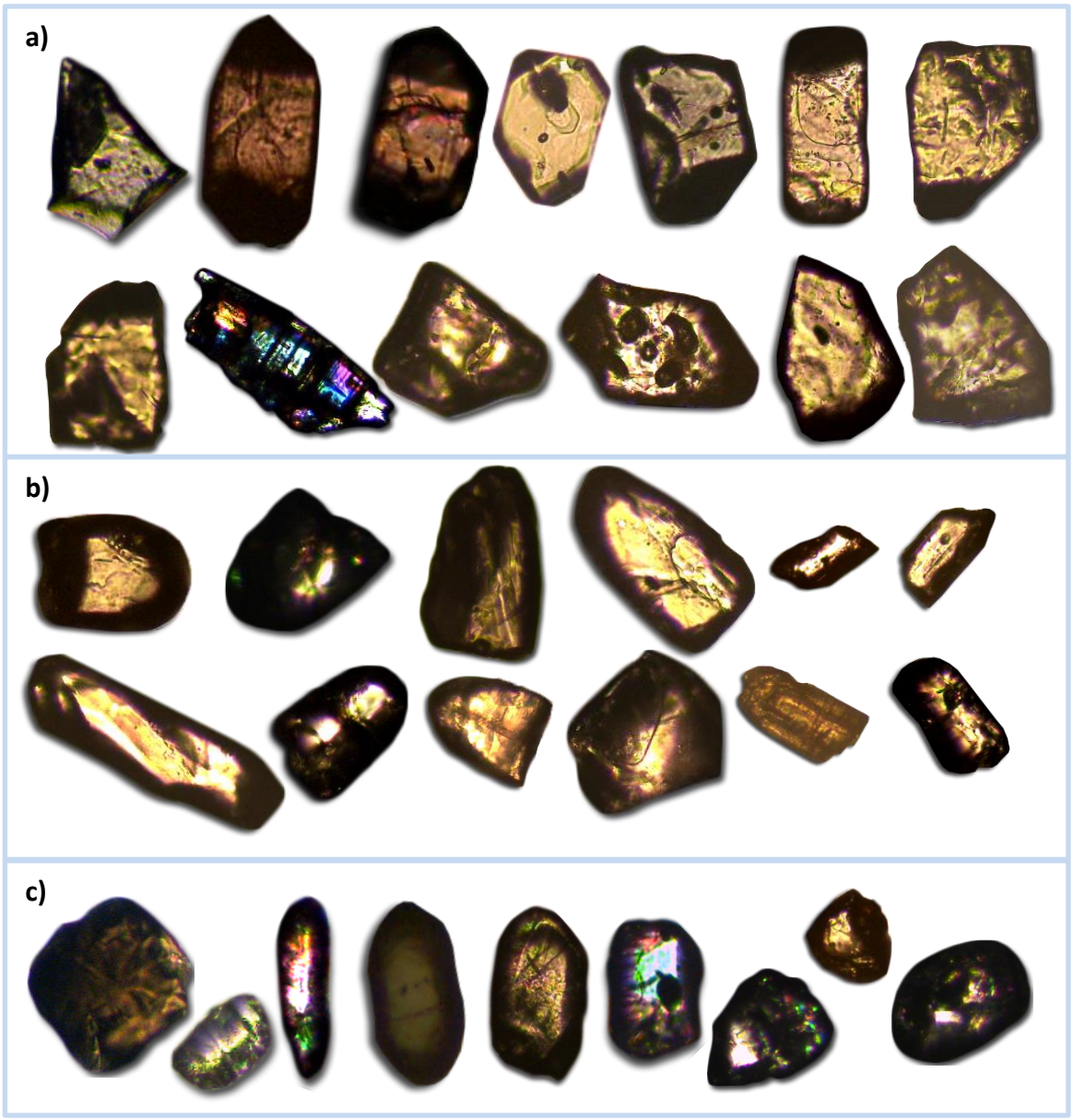

Plate 14: a) euhedral to subhedral zircon **b)** anhedral zircon **c)** recycled zircon

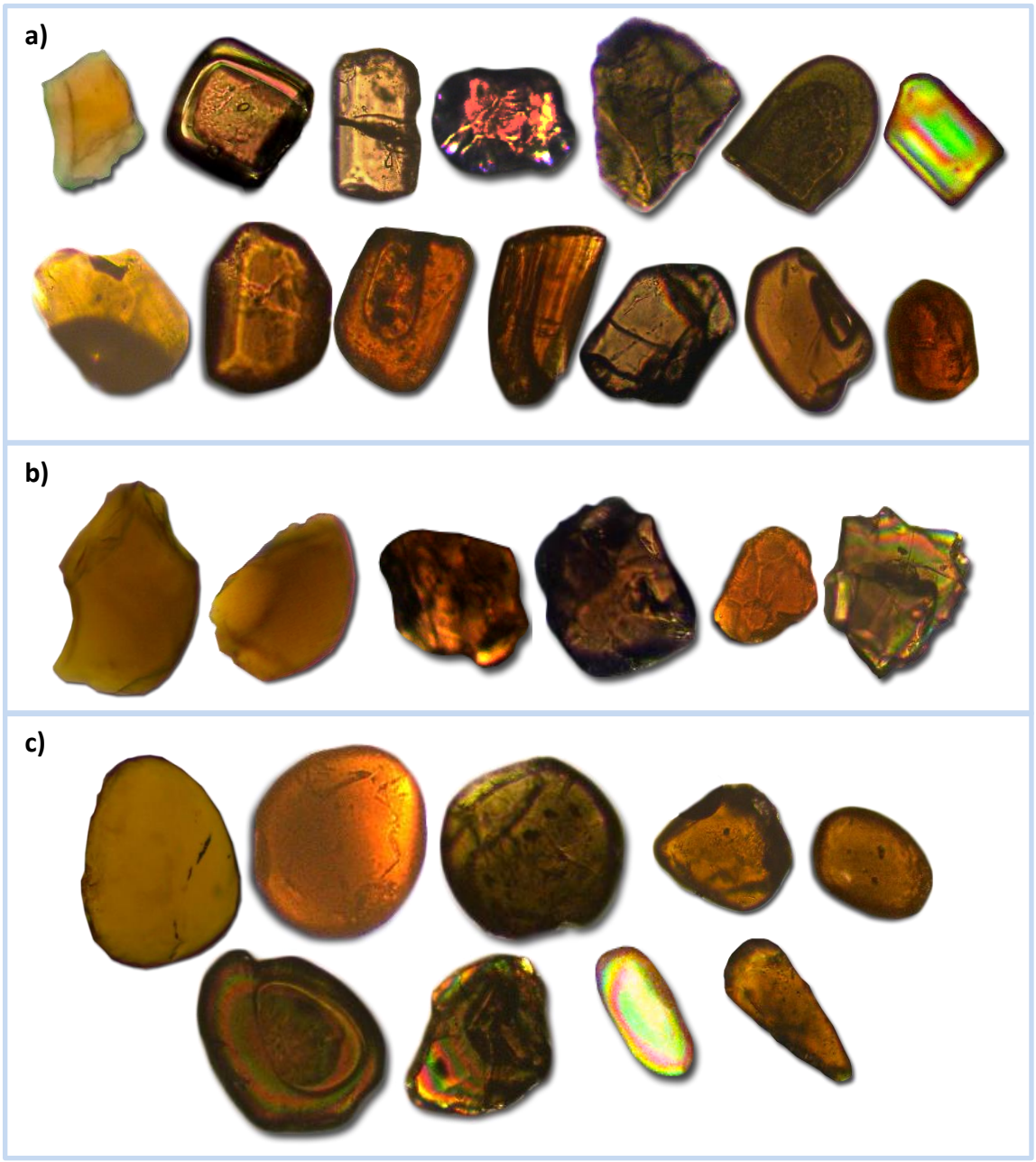

Plate 15: a) euhedral to subhedral tourmaline **b)** anhedral tourmaline **c)** rounded tourmaline

Plate 16: a) euhedral to subhedral rutile **b)** anhedral to sub-rounded rutile

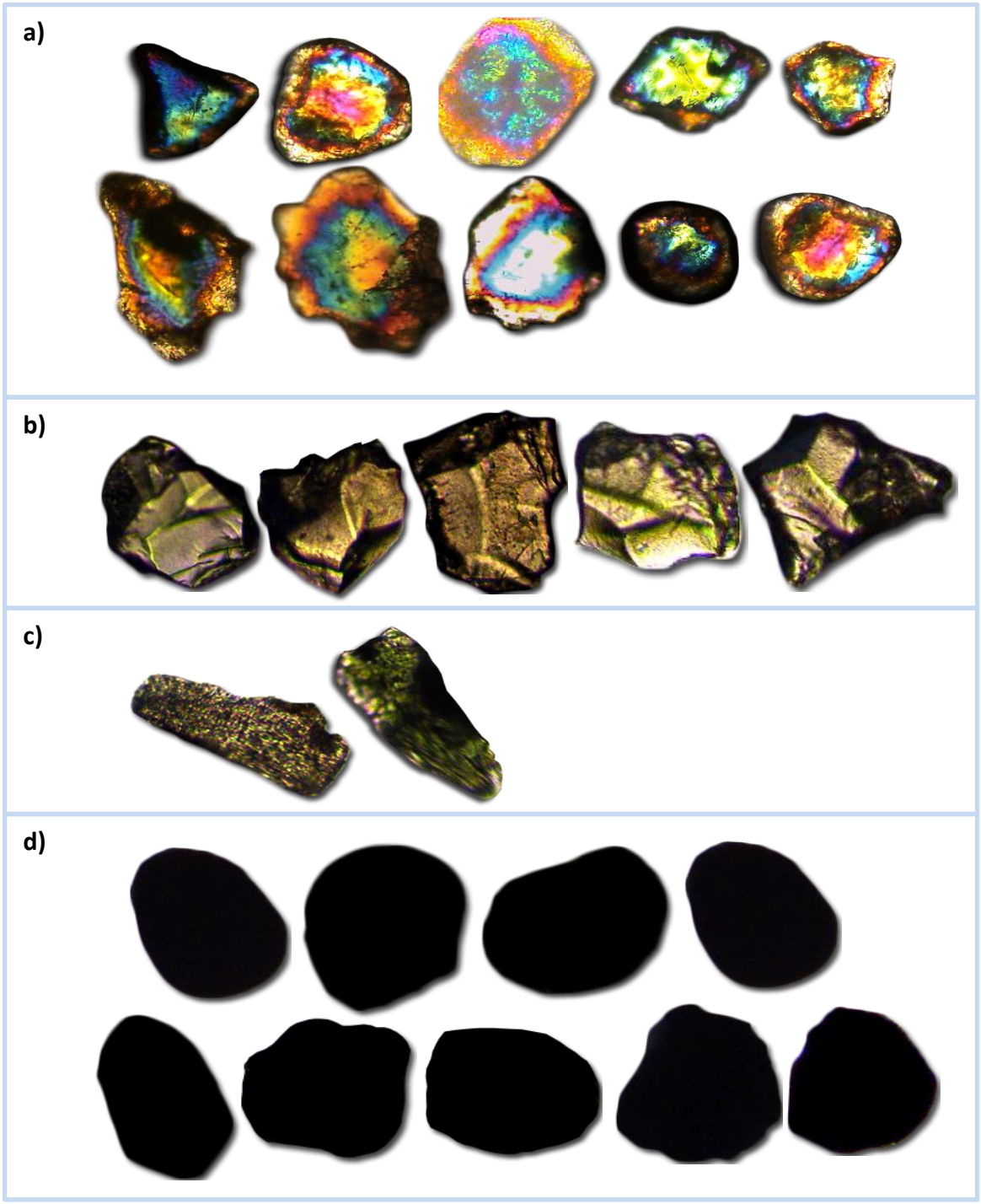

Plate 17: a) kyanite **b)** staurolite **c)** silliminate **d)** opaques (iron oxide)

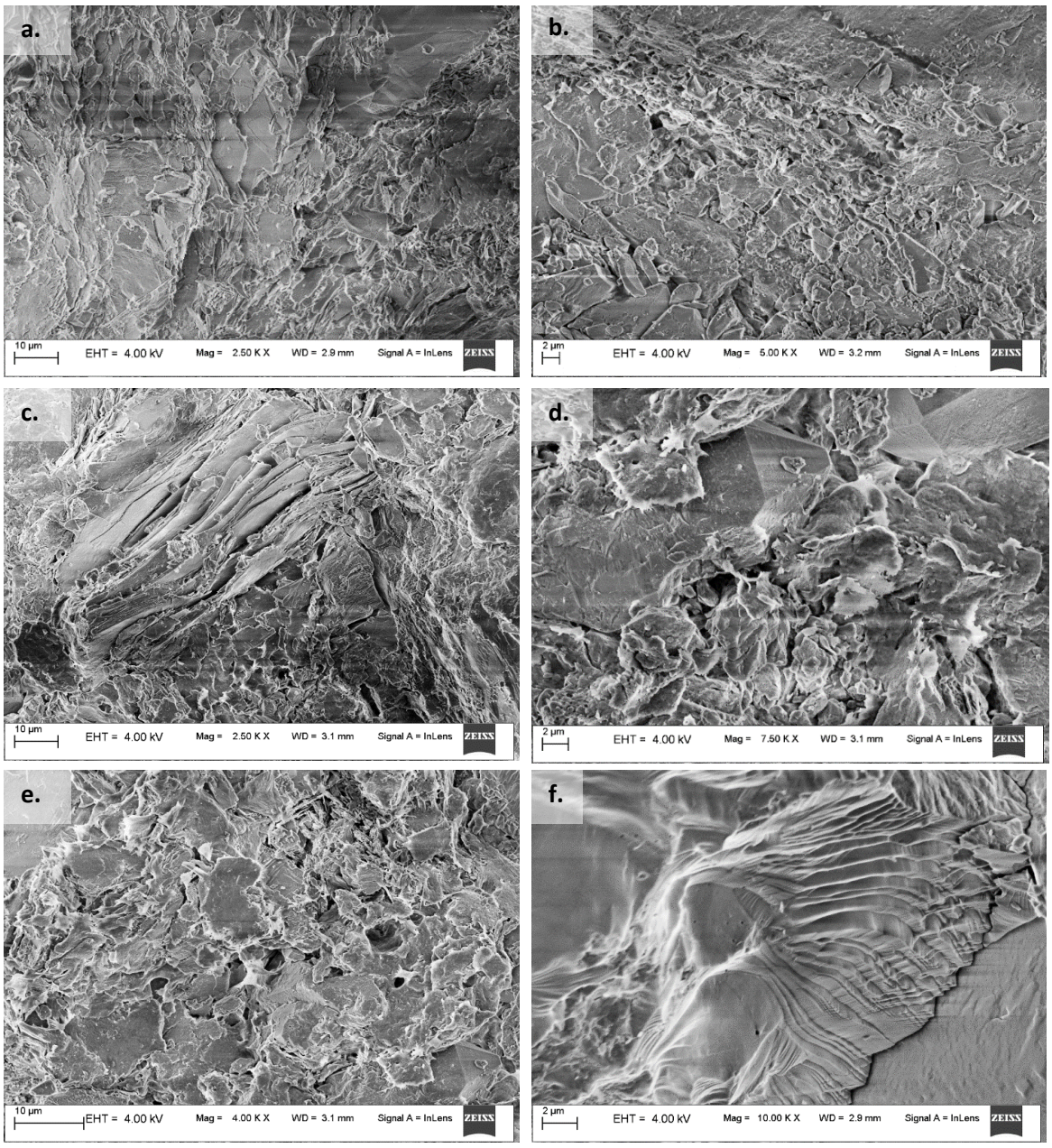

Plate 18: SEM photographs showing **a)** neo-quartz with dissolution pits **b)** illite-smectite layers **c)** kaolinite books **d)** neomorphic growth **e)** dissolution pits **f)** kaolinite layers

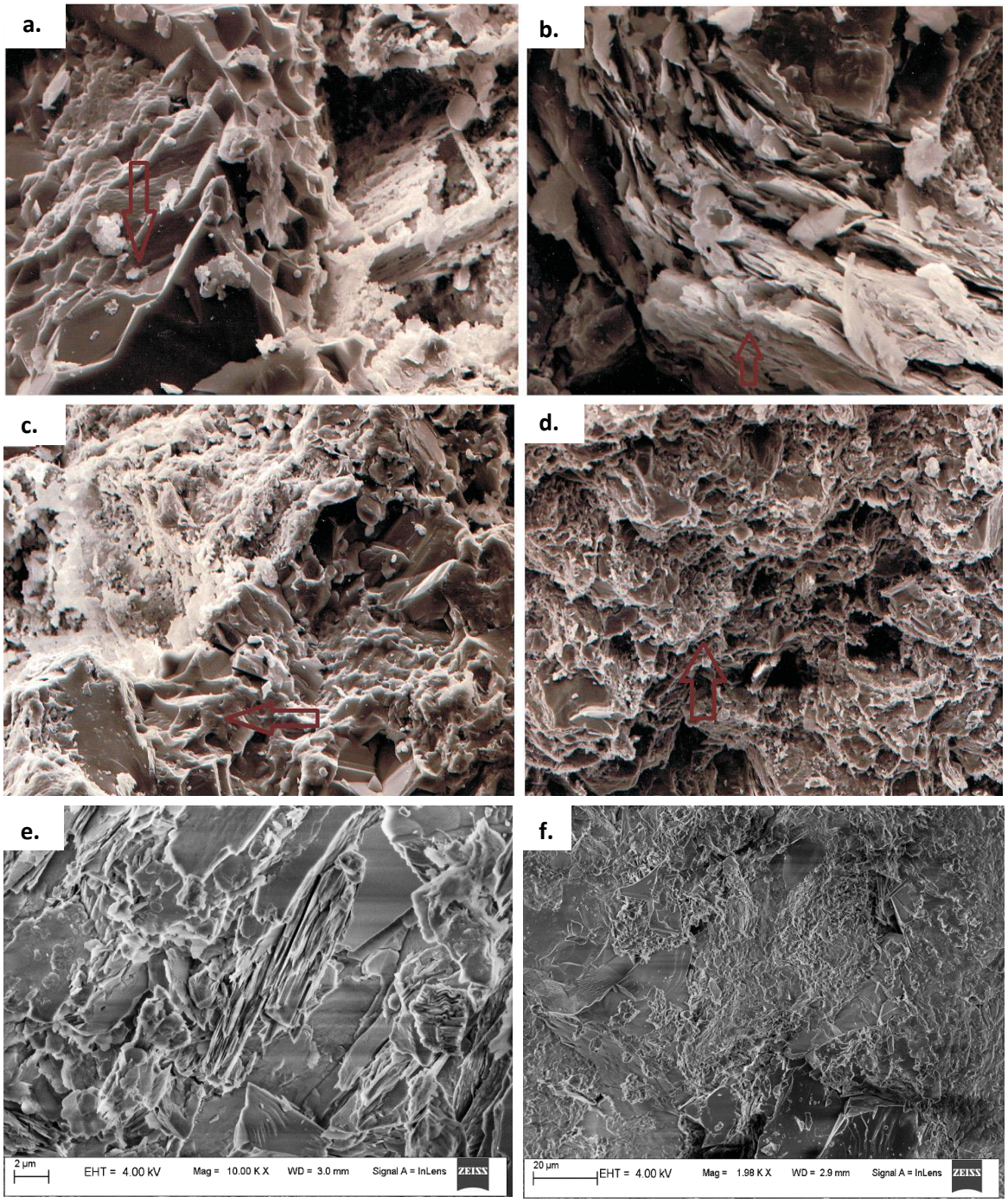

Plate 19: SEM photographs showing **a)** silica rims **b)** layered clay **c)** silicious growth **d)** illite **e)** kaolinite book **f)** Illite

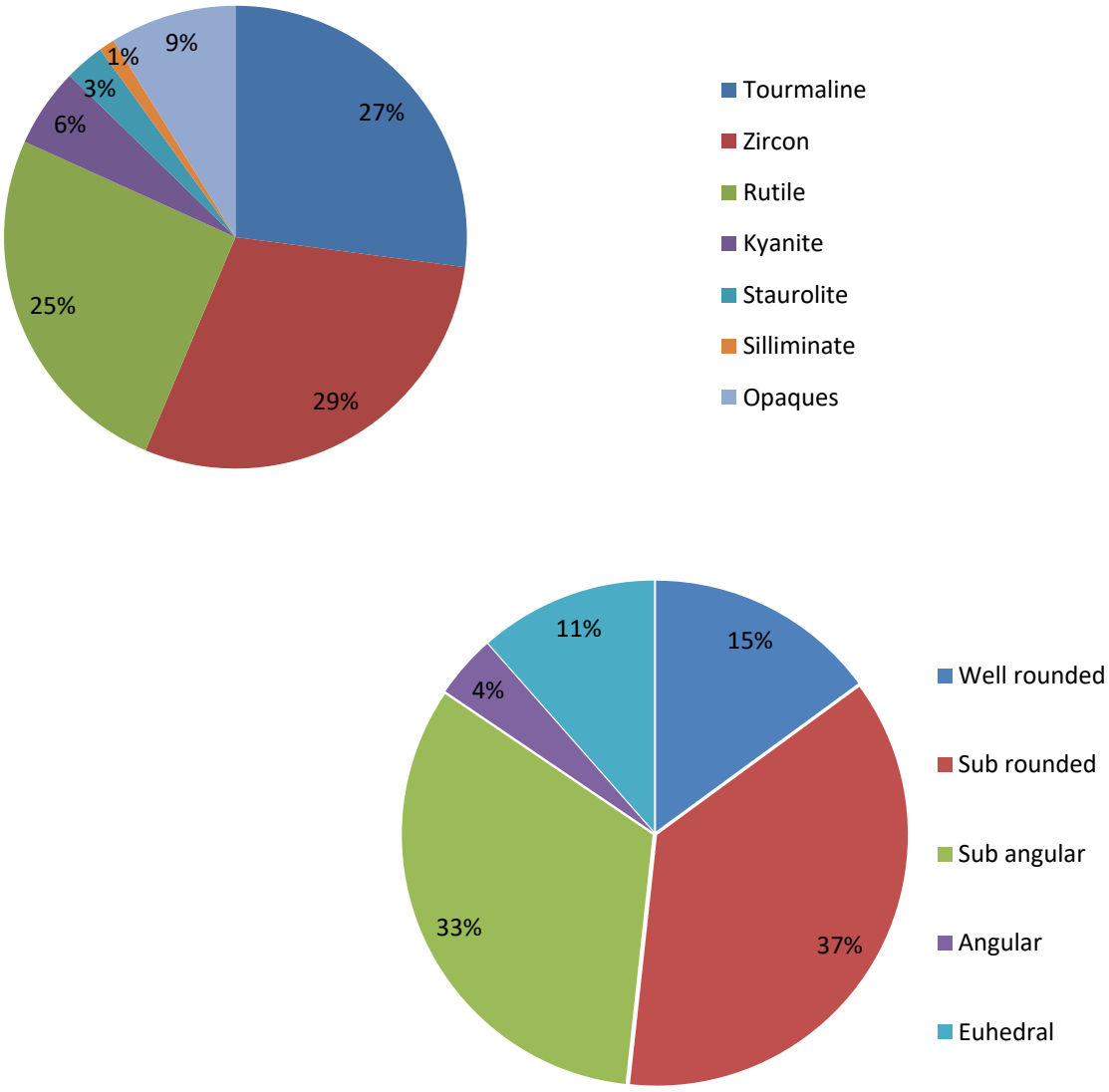

Fig. 27: Distribution of heavy minerals according to variety and shape in Barail sandstones

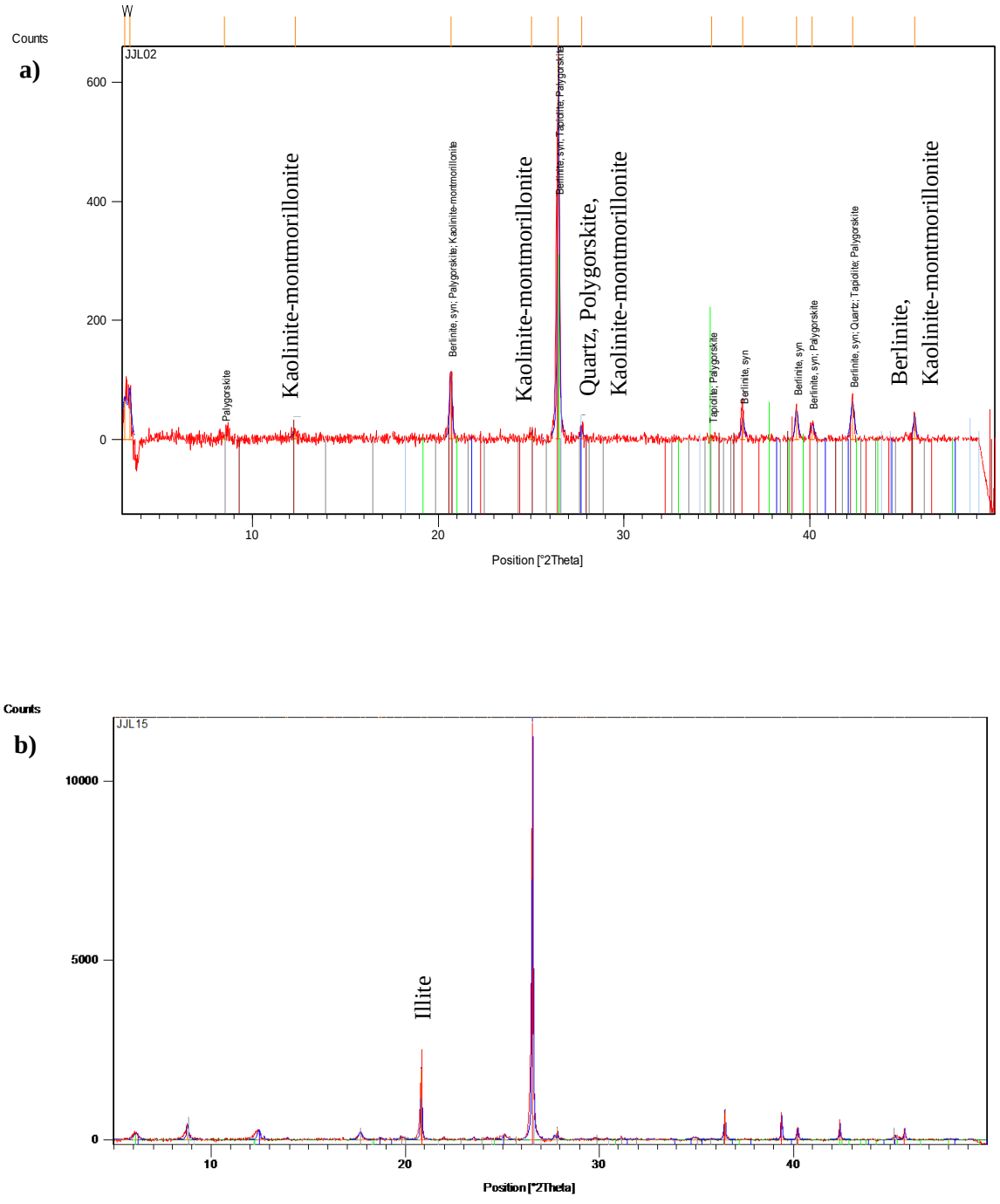

Fig 28: XRD curves for samples **a)** R36/15 and **b)** JJL15

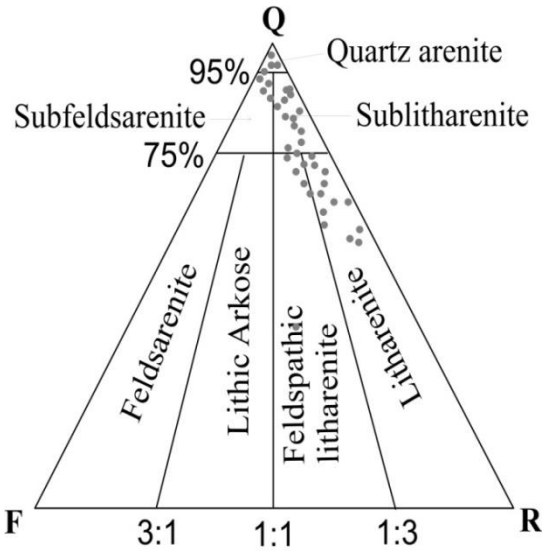

Fig. 29: Ternary plot of total quartz, feldspar and rock fragments (after Folk, 1980)

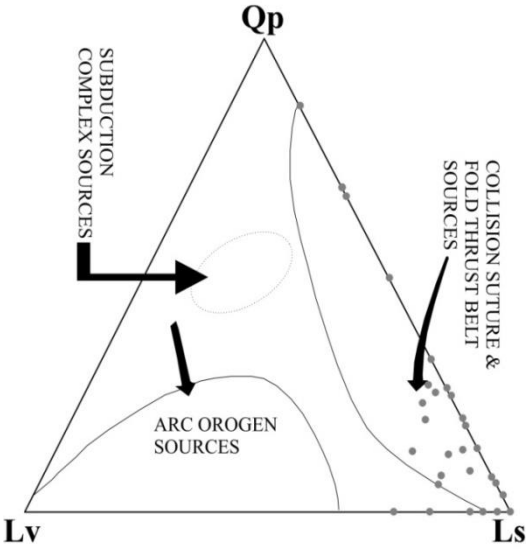

Fig. 30: Ternary plot of quartz (poly), lithic (volcanic) and lithic (sedimentary) (after Dickenson & Suczek, 1979)

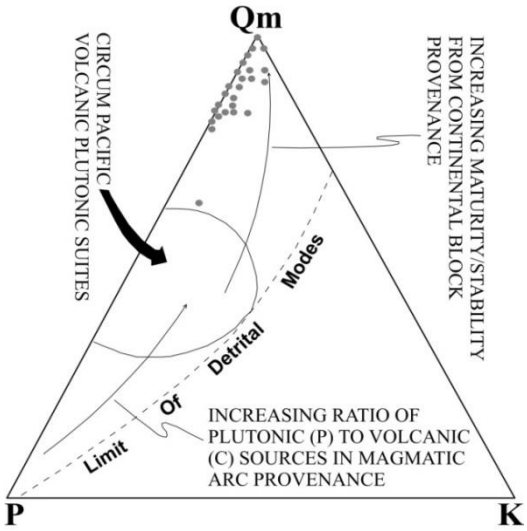

Fig. 31: Ternary plot of quartz (mono), feldspar (sodic) and feldspar (potash) (after Dickenson & Suczek, 1979)

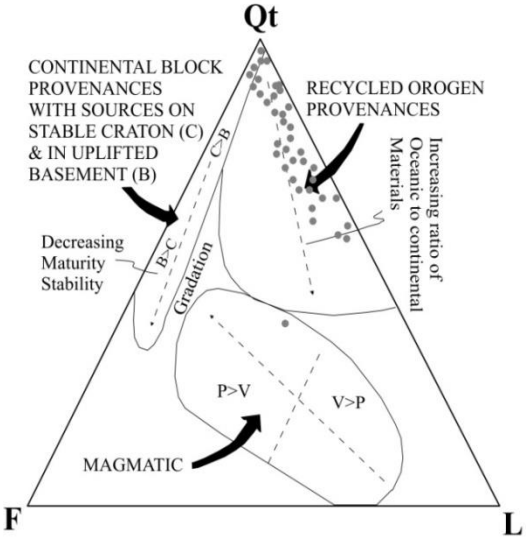

Fig. 32: Ternary plot of total quartz, feldspar and lithic fragments (after Dickenson & Suczek, 1979)

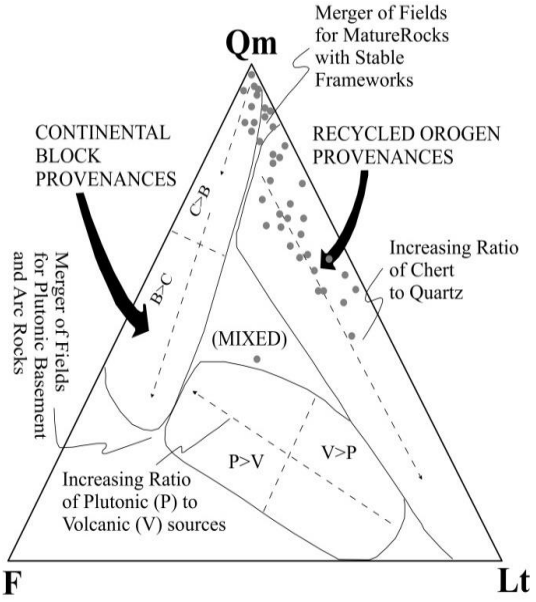

Fig. 33: Ternary plot of quartz (mono), feldspar and lithic fragments (after Dickenson & Suczek, 1979)

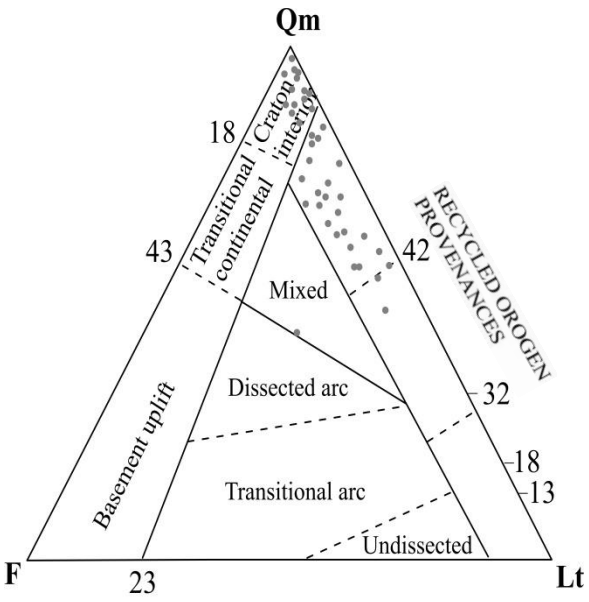

Fig. 34: Ternary plot of quartz (mono), feldspar and lithic fragments (after Dickenson *et al.*, 1983)

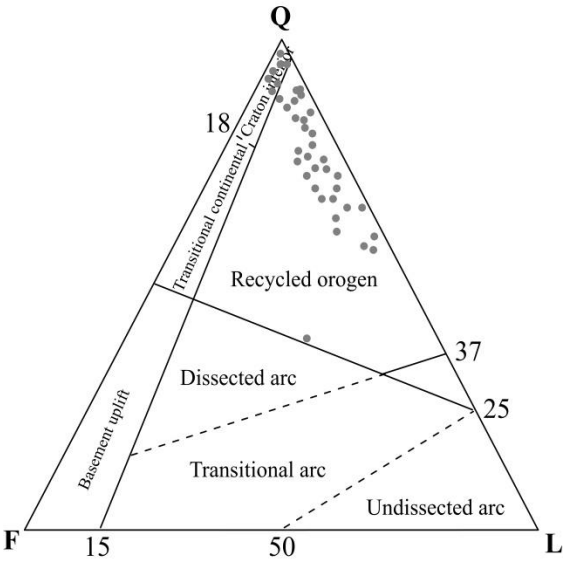

Fig. 35: Ternary plot of total quartz, feldspar and lithic fragments (after Dickenson *et al.*, 1983)

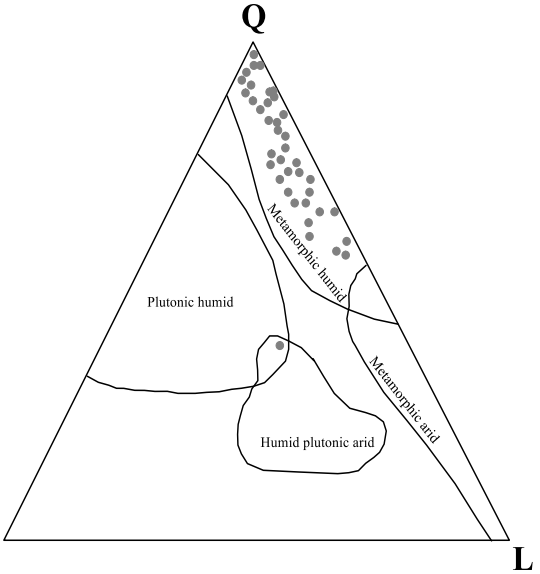

Fig. 36: Ternary plot of total quartz, feldspar and lithic fragments (after Suttner *et al.*, 1981)

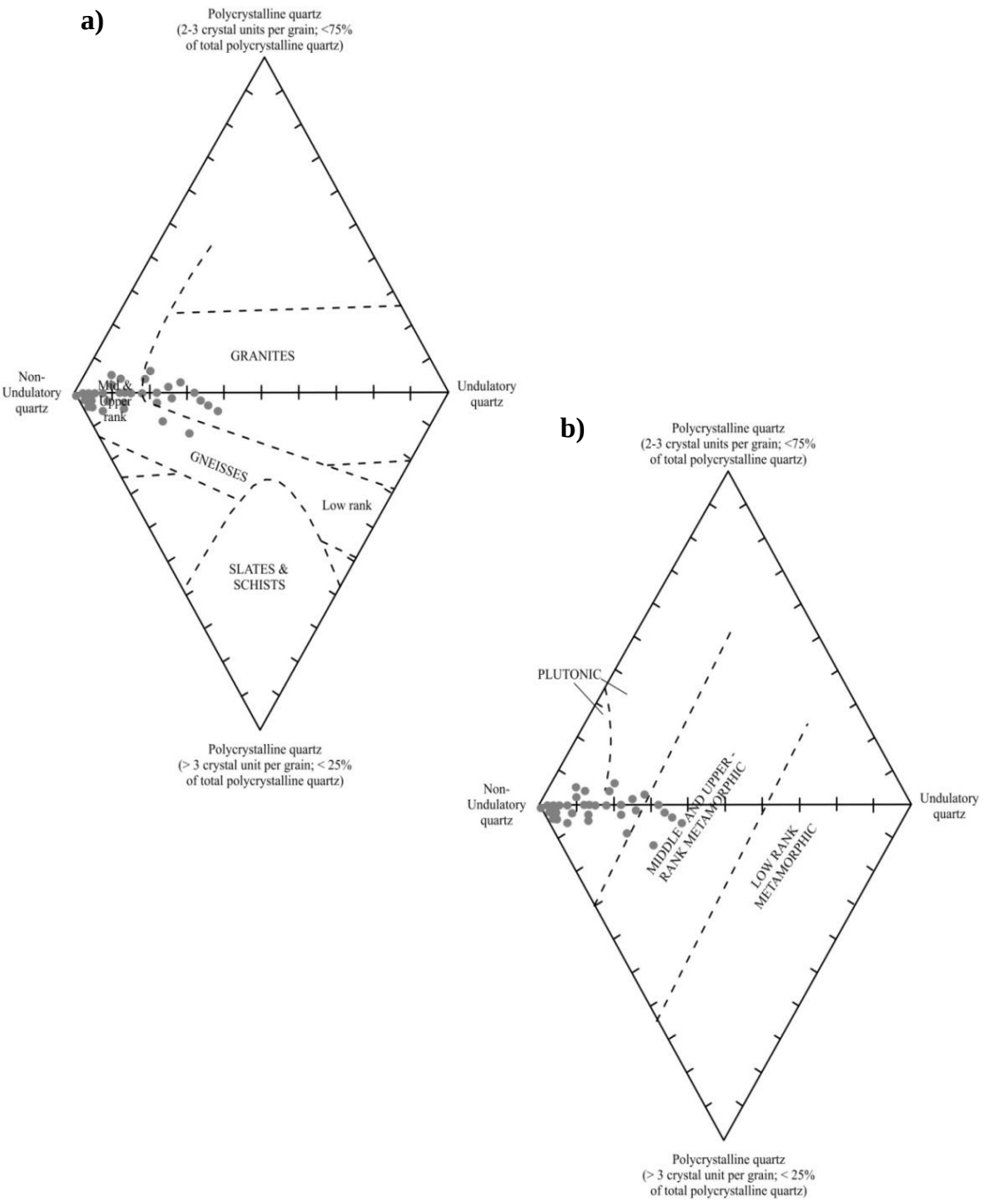

Fig. 37: Diamond plot of non-undulatory quartz, undulatory quartz, polycrystalline quartz (2-3 units) and polycrystalline quartz (>3 units) after **a)** Tortosa *et al.* (1991) and **b)** Basu *et al.* (1975)

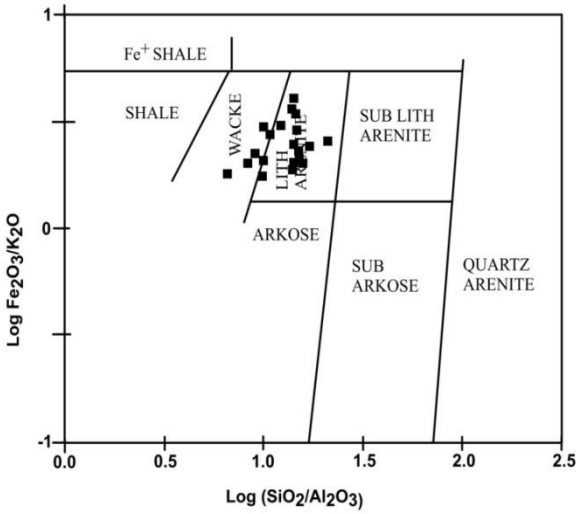

Fig. 38: Bivariate plot of log (Fe_2O_3/K_2O) vs log (SiO_2/Al_2O_3) (after Herron, 1988)

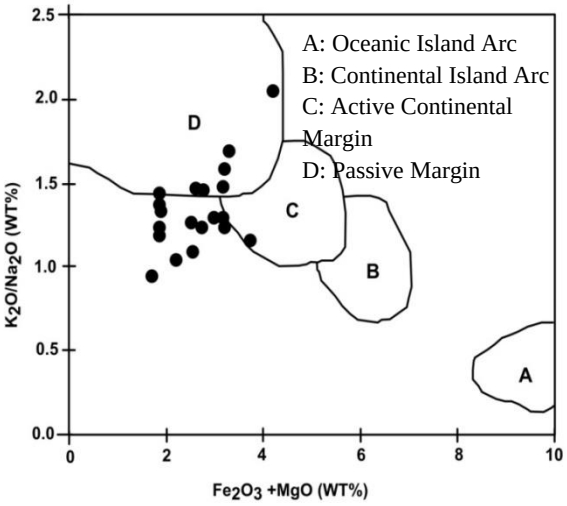

Fig. 39: Bivariate plot of K_2O/Na_2O vs Fe_2O_3/MgO (after Bhatia, 1983)

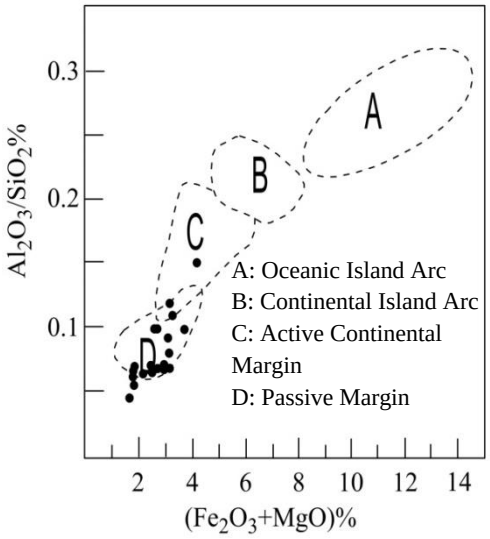

Fig. 40: Bivariate plot of Al_2O_3/SiO_2 vs Fe_2O_3/MgO (after Bhatia, 1983)

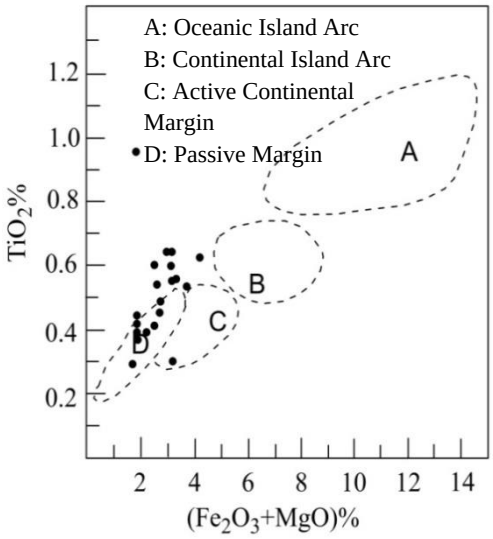

Fig. 41: Bivariate plot of TiO_2/SiO_2 vs Fe_2O_3/MgO (after Bhatia, 1983)

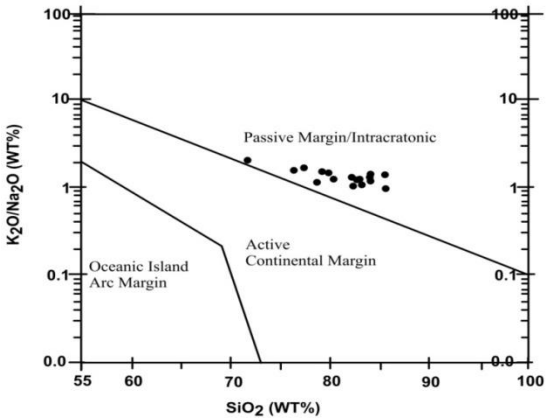

Fig. 42: Bivariate plot of K_2O/Na_2O_3 vs SiO_2 (after Roser & Korsch, 1986)

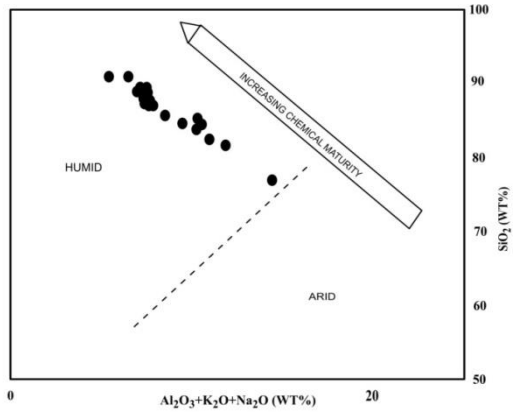

Fig. 43: Bivariate plot of SiO_2 vs $Al_2O_3+K_2O+Na_2O_3$ (after Suttner & Dutta, 1986)

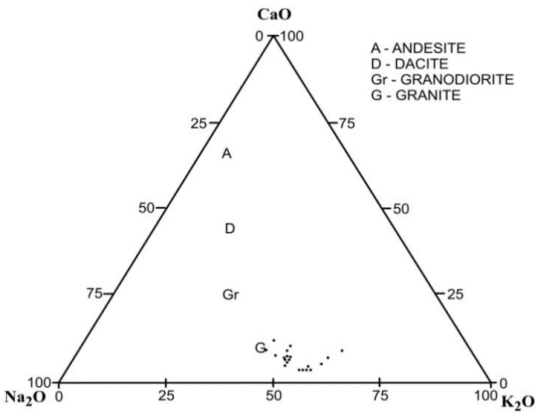

Fig. 44: Ternary plot of CaO-Na_2O-K_2O (after LeMaitre, 1976)

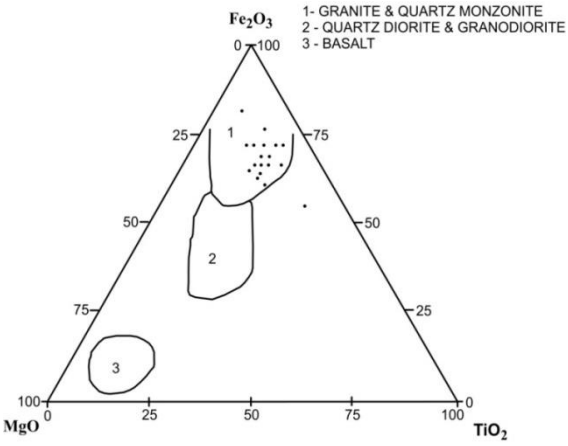

Fig. 45: Ternary plot of Fe_2O_3-MgO-TiO_2 (after Condie, 1967)

CHAPTER 6

DEPOSITIONAL ENVIRONMENT AND TECTONIC PROVENANCE

6.1 RECONSTRUCTION OF PALAEOENVIRONMENTS

Interpretation of ancient products in terms of normal as well as catastrophic processes and their resultant facies mosaic in space and time has always been aided by the study of modern sedimentary processes (Johnson and Stride, 1969; Swift, 1969; Swift *et al*., 1971; Hubert and Hyde, 1982; Reading, 1986). Climatic changes, pelagic sedimentation, organic growth, diagenetic modifications, tidal and fluvial currents are the normal sedimentary processes which persist for longer period of time. The catastrophic processes, such as storm surges, flood, earthquakes, volcanism and tectonic impulses, on the other hand, occur instantaneously. However, the distinction between these processes in the depositional facies depends upon the preservation potential of the environment (Goldring, 1965). Nevertheless, study of modern sedimentary processes provides an effective tool in understanding the depositional environments of ancient sedimentary deposits. In general, the methodology involves the development of regional framework of sedimentary deposits on the basis of lithology, geometry, sedimentary structures, palaeocurrents and facies associations for interpretation of facies sequences of ancient sediments. This is usually succeeded by reconstructions of depositional environment and sub-environments and development of suitable conceptual model.

The present study demonstrates that the Barail sediments were deposited in a coastal complex with fluctuating energy regime. The study area is dominated by coarsening upward sequences with a few sequences showing fining upward trends. This may be explained as progradation of shoreface towards offshore, which have been traversed by fining upward tidal-inlet channel deposits (Leeder, 1982). The description of different depositional environments responsible for generation of different lithofacies in the Barail sediments as given below:

6.1.1 MESOTIDAL SHOREFACE ENVIRONMENT

According to Hayes (1975), mesotidal coast are characterized by barrier-island with many tidal inlets and spits, well developed ebb as well as flood tidal deltas, salt marshes,

tidal mud flats and channels. Short barrier islands, broken by numerous tidal channels, are found on mesotidal coasts where tide range is between 2 to 4 meters (Prothero, 2004). Barrier islands migrate landward and seaward with changes in sea level and often constitute a significant portion of transgressive or regressive shoreline deposits. The barrier island complex is subdivided into several distinct sub-environments (Prothero, 2004). In the upper shoreface, sandstones develop plane lamination, ripple marks and gently dipping plane laminations with low concentration of trace fossils dominated by vertical traces. On the lower shoreface, offshore shelf processes are important as wave effects are very weak. The lower shoreface is dominated by intensely bioturbated sandy mud. Most of the sedimentary structures are generally obliterated. In this region, horizontal traces dominate. A transition exists between lower shoreface sandstones and offshore mud towards the offshore. This transition is characterized by moderately bioturbated fine sand-mud lithologies.

In the present investigation, the lithofacies Sm/*Fx/Sr/Sr*$_w$ are considered to represent the upper shoreface, while *Sl* and *Fsm* characterize the lower shoreface, as evidenced by the following features:

i. Presence of fine to medium sand, low angle and cross lamination with ocassional pebble lags and burrows in the *Fx* facies, the overall bed geometry being linear or shoe string type.
ii. Occurrence of wedge shaped medium grade channeled sandstones in *Fx* facies.
iii. Presence of asymmetrical ripples with mud drapes and interference ripples in sand lithologies also represent the upper shoreface environment (*Sr*).
iv. Presence of wave formed ripples in fine to medium sandstones with occasional bifurcations representing upper shoreface environment (*Sr*$_w$).
v. Presence of coal streaks, very fine to fine sand and carbonaceous mud intercalations within *Sl* facies. Among the sedimentary structures, plane lamination, well developed horizontal bedding/parallel laminations are very common. Horizontal traces are common.

vi. Presence of shale/siltstone with lamination and bioturbation and horizontal traces in *Fsm* facies represent the low energy lower shoreface environment.

vii. Coarsening and thickening-upward trends with decrease in the shale contents and trace fossils.

viii. Within the overall coarsening upward cycles with occasional preservation of fining upward sequence.

ix. Dominance of moderately well sorted mature to super mature quartzose sandstones showing characteristics of tidal channels, channel margin bars and levees.

x. Laterally extensive sheet/ and or elongate sand body geometry paralleling the palaeoshore.

xi. Occurrence of heterolithic facies in conjugation with current and wave formed sedimentary structures is a typical characteristic of mesotidal shoreface deposits.

6.1.2 OFFSHORE TRANSITION ENVIRONMENT

In this region of a shallow siliciclastic shelf seas tidal range is not appreciable and sediments in the shoreface are influenced by meteorologically induced wave and related currents. Many sedimentologists, including Heward (1981), Einsele and Seilacher (1982), have provided excellent reviews and models for deposits formed in both modern and ancient shallow offshore environments. In offshore transition environment, deposits exhibits wave produced mud stone-silt stone linsen facies. They are represented by thin, impersistent laminae and symmetrical ripples in well sorted medium to coarse silt stones. Deposition of finer sediments from suspension and reworking of coarser silt by oscillatory wave motions is the characteristic feature of the offshore transition environment of low energy. In the present case, lithofacies *Fl* is considered to represent the offshore-transition, owing to the following characteristics:

i. Finely laminated silt-mud facies comprising plane laminations and burrows.

ii. Presence of moderate bioturbation, the burrows being dominantly of *Thalassinoides* and *Chondrites* isp.

iii. Presence of fining and thinning upward sequences in an overall coarsening and thickening upward sequences.

6.2 DEPOSITIONAL HISTORY

Lithofacies analysis, textural, mineralogical and provenance studies of Barail sediments indicate that their deposition was mainly controlled by tectonic impulses during late Eocene-Oligocene period. This tectonic phase in the history of Indo-Burman Ranges (IBR) has been characterized by the presence of a transgressive epiric sea located along passive margin. According to Acharyya (1990, 2007), during early middle Eocene period, there occurred a collision of Naga-Chin-Arakan island arc, located towards east within the oceanic domain of India and Myanmar, with the central Myanmar continental block. The subduction of the Indian plate below the Burmese plate had reorganized the drainage and had also shifted the depocenter with fluctuation in the sea level. Eocene-Oligocene sedimentation continued uninterrupted, where sedimentation kept pace with tectonism. Naik (1998) has visualized this tectonic phase in the region as retrogradation phase leading to the soft collision of northeastern edge of the Indian plate with the Sinian plate, thereby changing the eastern passive margin of India into a collisional belt. Kumar and Naik (2006) have also opined the same and have suggested that this is a classic example of transformation of a passive margin set up into an active margin setting through time in response to the changing plate interaction and evolution of north-east south-west trending foreland basin. It appears that the change from argillaceous phase (Disang Group, Eocene; Krishnan, 1982) to the heterolithic phase (Disang-Barail Transition, Upper Eocene; Srivastava, 2002) occurred due to a change in the plate tectonic regime during early to middle Eocene and passed through progradation phase into fluvio-marine (Barail Group, Oligocene; Krishnan, 1982) set up.

Processes that have been inferred from the various characteristics of the sediments of the study area basically relate to shoreface-offshore sedimentation. In such regions, both tidal (upper shoreface) as well as wave processes play important role. Nevertheless, gently dipping parallel laminations in the sandstone layers suggests low preservation potential in the upper and lower shoreface regions. Intermittent fining upward sequence

within a broad coarsening and thickening sequence in the study area reflect the effect of tidal ebb current.

A conceptual model for the deposition of various lithofacies of the Barail sediments has been envisaged on the basis of the distribution of various lithofacies in the study area (**Fig. 46**). The depositional model depicts the distribution of various lithofacies for a near shore-shallow marine prograding beach face in a wave dominated ebb tidal delta. Generation of northwesterly/northerly wave accompanied by coast parallel (NW-SE) residual currents in the basin was caused by the westerly wind. Lithofacies distributions in the study area also suggests a progressive decrease in the energy of the medium across the shelf in response to decreasing intensity of wave disturbances and increasing water depth. The transgression and regression is the result of thrust sheet loading which is responsible for repetition of shoaling upward cycle in the study area.

6.3 EVIDENCES FROM TRACE FOSSILS

Occurrence and distribution of trace fossils are controlled by environmental parameters such as energy and oxygen levels, salinity and substrate. Seilacher (1967) has also suggested that there exists a clear relationship between distribution pattern, bathymetry and hydrodynamic condition. In the study area, traces are relatively abundant and moderately diverse and belong to either *Skolithos* or *Cruziana* ichnofacies.

The *Skolithos* ichnofacies develops in clean, well sorted, shifting particulate substrates and is related to relatively high level of wave or current energy. Such conditions occur in wide range of high energy shallow water environment but are common in the shoreface and sheltered foreshore (MacEachern *et al.*, 2007). While working with idealized shoreface models for trace fossils, Frey *et al.* (1990) and MacEachern *et al.* (2007) have suggested that *Skolithos* ichnofacies generally grades seaward into *Cruziana* ichnofacies. Both *Ophiomorpha* and *Skolithos* are reported from the environment characterized by changes in sedimentation rate and frequent high energy events (Walker and James, 1992; Singh *et al.*, 2008). *Planolites* occur few centimeters below the sediment-water interface and indicates unconsolidated substrate with relatively moderate to low energy shoreface/offshore conditions (Tiwari *et al.*, 2011).

Cruziana ichnofacies occurs where current action is less intense and food settles at the bottom. Such conditions are generally met at comparatively deeper water. Tracks, trails as well as tunnels dominate in this zone. This assemblage is characteristic of unconsolidated muddy substrate in shallow marine settings with uniform salinity and moderate energy conditions. According to Gilbert and Benner (2002), presence of *Gyrochorte comosa* also suggest low sedimentation rate and fluctuating energy condition in a shallow marine environment with abundant surface food sources. The most common settings correspond to the offshore extending to the very distal fringe of the lower shore face (MacEachern *et al.*, 2007).

Presence of *Skolithos, Planolites, Ophiomorpha, Thalassinoides, Gyrochorte* and *Chondrites* in Barail sediments indicates a shallow marine environment with occasional deep water conditions within shoreface setup. Dominance of *Skolithos* ichnofacies at higher stratigraphic level suggests nearness to the palaeoshore and upper shoreface environment.

Distribution pattern of the ichnofacies suggests that Barail sediments were deposited under fluctuating energy conditions with moderate to strong energy levels, within shoreface environment. It also indicates a tectonically controlled fluctuating environmental regime under dominantly regressive phase with occasional transgression.

6.4 TECTONIC PROVENANCE

Many attempts have been made to interpret the detrital composition of sandstones in terms of tectonic provenance and basin settings (Dickinson and Suczek, 1979; Ingersoll and Suczek, 1979; Dickinson and Valloni, 1980; Dickinson, 1982; Suczek and Ingersoll, 1985 and Korsch (1984). They have attempted to correlate the proportion of detrital framework grains to the various plate tectonic settings and also the plate interaction in the geologic past. Similar attempts have also been made by later workers (Uddin and Lundberg, 1998; Singh *et al.*, 2004; Srivastava *et al.*, 2004; Allen *et al.*, 2008; Srivastava and Pandey, 2011 and many more). Mack (1984) recognized 4 categories of error populations in sandstones where the interpreted tectonic settings and their locations on triangular provenance diagrams do not match.

The different categories of error populations are:

i. Sandstones formed under transitional plate tectonic settings.
ii. Modified sandstone compositions by weathering and/or depositional environment.
iii. Sandstones deposited under tectonic regime not represented in various models of above workers.
iv. Sandstones containing detrital carbonate.

Mack (1984) further suggests that the above sandstone categories are anomalous and considered them as exceptions to the relationship between plate tectonic and sandstones compositions. He also suggested that while using sandstone petrography as an indicator of plate tectonic settings, one should take note of the processes and conditions under which the sandstones were deposited.

The modal composition of various samples has been presented in **Table 7** and **Table 8** respectively. Based on clustering of data points in ternary plots, it may be assumed that the Barail sandstones had derived its detritus largely from a recycled orogen comprising all the three kinds of provenance *viz.* subduction complex province, collision orogenic province and foreland uplift province. Subduction of Indian plate beneath Myanmar plate must have brought the Indian craton lying immediately west close to the depositional site. Presence of angular grains of orthoclase and microcline at higher stratigraphic levels also suggests the same. Presence of these minerals in the studied sandstones further suggests either short transportation and/or high rate of supply of sediments allowing the preservation of these minerals otherwise very susceptible to weathering and selective destruction. Presence of angular and very well rounded varieties of zircon, tourmaline and rutile plus staurolite in the sandstones of the study area points towards a mixed provenance suggesting supply of sediments from Indian craton in the west, Naga Metamorphics in the east and also from the sediments formed in earlier depositional regime in the northeast. In addition to that, contributions from rising ophiolites in the east cannot be ruled out. Recycled nature of detritus from orogenic terrains may be interpreted by clustering of the points at the quartzose end of Q_mPK diagram (**Fig. 31**).

Presence of recycled quartz grains, schist rock fragments, tectonised mica, volcanic rock fragments and euhedral zircons, tourmaline and rutile also supports the above view. In addition, such a mixed detritus further suggests that these sediments were deposited during transitional and/or active phase of tectonic regime. Further, it may also be concluded that the deposition of these sediments through time kept pace with changing plate interaction. Rocks produced in the earlier tectonic regime might have also contributed detritus to the new tectonic regime. Mack (1984) suggested that, in such a condition, the derivation of detritus, in part, form the relict source rock of an earlier tectonic setting, and thus result in deposition of anomalous sandstones. However, error introduced in using the triangular plots of Dickinson and Suczek (1979) cannot be ruled out.

6.5 TRANSPORT MECHANISM AND DISPERSAL

Owing to the supply of sediments from mixed source terrain, the transportation and dispersal of the detritus during deposition of Barail sediments appear to be rather complex. The field observations coupled with laboratory investigations indicate that the clastics reached the site of deposition mostly through submarine distributory channels. The hydraulic processes that control the sediment dispersal patterns appear to have been:

i) net westward current related to easterly winds.
ii) onshore directional wave with increased intensity and decreasing water depth. (Curray, 1960)
iii) net offshore suspension transport of fine sand and silt derived from coastal areas perhaps through tidal inlets.

Textural analysis of Barail sediments clearly suggests a progressive basin ward decrease in the average grain size, degree of sediment sorting and also sand-mud ratio. Grain size distribution pattern and lithofacies distribution suggests a progressive decrease in energy across the shelf in response to increasing water depth and decreasing wave intensity, resulting in texturally graded shelf setting (Johnson and Baldwin, 1986).

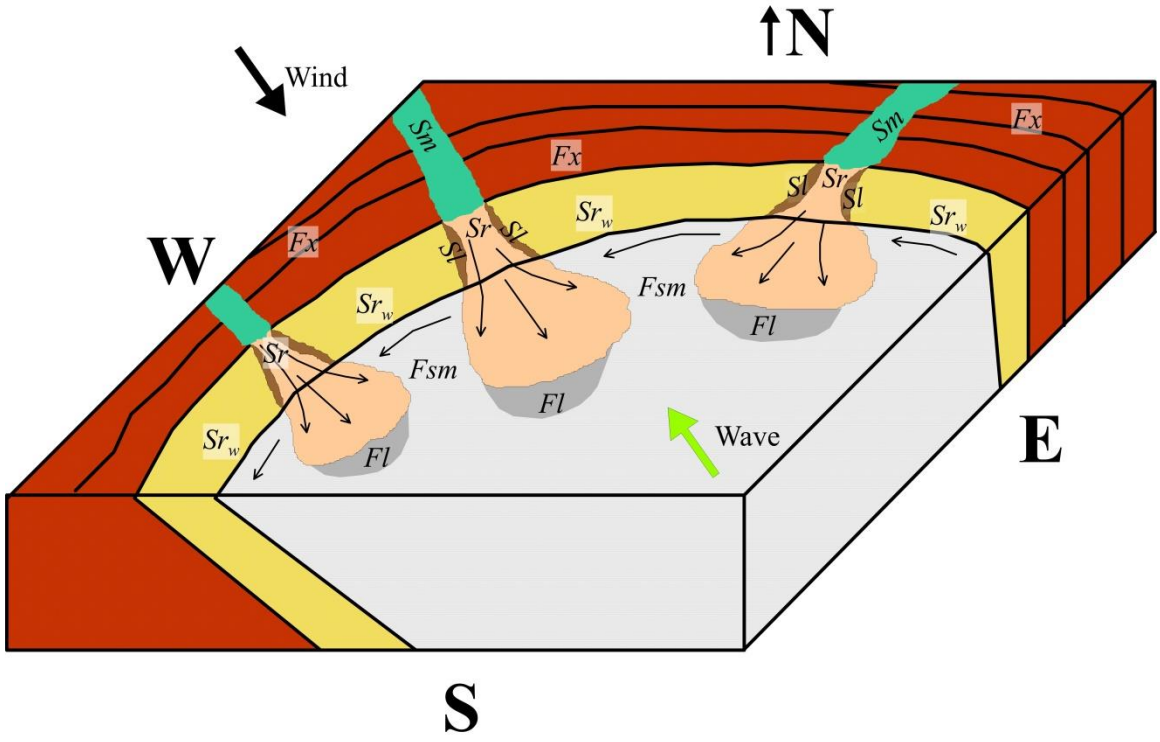

Fig. 46: Conceptual model envisaged for the study area

CHAPTER 7

SUMMARY AND CONCLUSION

The Oligocene Barail rocks, exposed towards the west of Kohima town (25°40'2.46"N, 94°6'9.74"E), provide a unique opportunity to study their evolution with respect to time and tectonics. Oligocene Barail sediments lie above the mixed lithology of Disang-Barail Transition (Pandey and Srivastava, 1998; Srivastava and Pandey, 2001). The Barail Group of rocks within Kohima Synclinorium, a part of Inner Fold belt, is unclassified and is represented by thickly bedded multistoried sandstones with occasional shale intercalations. So far, no detailed study was done on this dominantly arenaceous lithology except a few publications (Srivastava and Pandey, 2011, Kichu *et al.*, 2018). For the first time, through the present work, an attempt has been made to reconstruct the palaeoenvironment using facies analysis techniques, and also to search for the provenance of the Oligocene Barail sediments using petrographic and geochemical attributes.

To achieve the above objectives, 30 representative samples were studied for their grain size properties and more than 40 sandstones samples were studied for modal analysis. In addition to that, 20 sandstone samples were also analyzed for their major oxide composition. For understanding the diagenetic modifications of Barail sandstones, 12 samples were examined through XRD for clay mineral identifications along with 8 freshly broken sandstones samples for identification of their surface features through SEM. Altogether, nine vertical profile sections were constructed and carefully studied at various locations in the field and also more than 150 sandstone samples were collected in time and space. Sedimentary structures, including biogenic, have been recorded and photographed to supplement the field data.

A lithofacies scheme has been developed for simplifying and generalizing the observations made through the study of vertical profile sections. Based on the facies parameters (lithology including grain size, sedimentary structures, bed geometry and other aspects), altogether 7 lithofacies have been identified, namely i) Fine to medium massive sandstone facies (*Sm*) ii) Plane laminated fine to very fine sandstone facies (*Sl*)

iii) Fine cross laminated sandstone facies (*Fx*) iv) Shale-silt facies (*Fsm*) v) Mudstone facies (*Fl*) vi) Rippled sandstone facies (Sr) vii) Wave rippled fine to medium sandstones facies (Sr_w). A summary of characteristic features of all the lithofacies has been presented in **Table 10**.

The discrimination of depositional environments among the different lithofacies has been attempted using different bivariate statistical and textural parameters of grain size distribution. The C-M plot for the sediments corresponds to generally Class II, III and IV, suggesting that Barail sediments have been transported by both graded and uniform suspension with some sediment transported as bed load. The average values for CU and CS for Barail sediments correspond to 220 and 430 microns, respectively. The palaeobathymetric estimation using Passega's (1964) Cs-C depth diagram indicates that Barail sediments have been deposited under a shallow marine environment with some influence of fluvia processes. A depth range of very shallow to 60 /70 meters has been estimated for these sediments. The linear discriminant function and log-log plot of (σ_I^2) versus (SK_G/SM_z).$S(\sigma_I^2)$, after Sahu (1964), the multigroup discrimination and plot of V_1 and V_2 with $V_1 \Lambda V_2 = 74.4°$, after Sahu (1983), have also been employed for distinguishing broad aspects of depositional environments. A nearshore-shallow marine high energy environment has been inferred for the deposition of Barail sediments. Signatures of textural inversion have also been obtained through the study of textural maturity. Based on scalar properties, as well as data recorded at directional sedimentary structures wherever encountered, interpretation of palaeocurrents has also been attempted. The palaeocurrent analysis indicates that sediment supply was made from different directions and the basin was undulatory in nature. This also suggests that drainage in the vicinity was reorganized in response to changing plate interaction.

The average modal composition of different lithofacies may be seen in **Table 8**. The sandstones in the study area are dominantly arenite and sub-litharenite in composition. They exhibit the characteristics of early and deep burial diagenesis. The heavy mineral suit in conjunction with major oxide, indicate a mixed provenance with substantial contribution from igneous source especially at higher stratigraphic levels. Based on the quartz types; contributions from plutonic as well as metamorphic sources

have also been inferred. Compositionally, the sediments in the study area are mature to super mature. A humid climate has been envisaged for the weathering and erosion of sediments.

Ternary plots of QFL, Q_mFL_t, $Q_pL_vL_s$ and Q_mPK (Dickenson and Suczek, 1979) suggest that detritus were largely derived from recycled orogeny comprising all the three kinds of provenance *viz.* subduction complex provenance, collision orogenic provenance and foreland uplift provenance. Data points in these discriminatory diagrams also suggest that there had been some contribution from continental block province too. This is further supported by the presence of orthoclase and microcline along with euhedral zircons and tourmaline. Appearance of these mineral species at upper stratigraphic levels further suggests that there had been contributions either from Shillong plateau and/or Karbi Anglong massif (earlier known as Mikir Hills) lying immediately west of the basin. However, Imchen *et al.* (2014), while working with upper Disang Formation, have suggested that it was most probably Karbi Anglong massif rather than Shillong plateau, due to the presence of a graben adjacent to it. This also suggests that during upper Oligocene period, Indian plate owing to continued subduction beneath the Myanmar plate might have been very close to the basin contributing these minerals to the depocenter. Presence of these minerals in Barail sediments also points towards a basin of undulatory nature restricting long transport and facilitating the preservation of them. High rate of supply of sediments and/or quick burial could have also been responsible for the preservation of otherwise susceptible minerals. Presence of very well rounded zircon, tourmaline and rutile along with presence of sedimentary rock fragments also suggest their derivation from a sedimentary source. In addition, presence of such a mixed detritus suggest that deposition kept pace with changing plate interaction through time and sediments deposited under earlier regime could have also contributed sediments to depositional site. Geochemical analysis (major oxides) of these sediments also supports the above views and is in conformity with the inferences drawn from petrographic study.

The hydraulic processes that controlled the sediment dispersal pattern relate to

i) net westward current related to easterly winds.

ii) onshore directional wave with increased intensity and decreasing water depth. (Curray, 1960)

iii) net offshore transport of silt and silt enriched mud through suspension mechanism.

Lithofacies Sm, *Fx, Sr, Sr*$_w$ (upper shoreface) and *Sl* and *Fsm (*lower shoreface) have been considered to represent the mesotidal shoreface environment whereas *Fl* is considered to represent the offshore-transition.

A conceptual model for the deposition of various lithofacies of the Oligocene Barail sediments has been envisaged on the basis of lithofacies distribution within the study area. The depositional model depicts a near shore-shallow marine prograding beach face in a wave dominated ebb tidal delta. Cutting across the shoreface region (*Fx*) were the tidal channels (*Sm*) fetching the material from coast to the lower channels leading to the development of *Sl* and *Fsm* facies in lower shoreface region where wave effect is less. *Fl* is considered to represent the offshore transition. Lithofacies *Sr* and *Sr*$_w$ are considered to represent the upper shore face environment, where tidal and wave processes were dominant. On the basis of lithofacies distributions, a progressive decrease in the energy of the medium across the shelf in response to increasing water depth and decreasing intensity of wave disturbances has been visualized. Transgression and regression processes owing to thrust sheet loading seem to have developed a repetition of shoaling upward cycle in the study area.

Facies Code	Lithofacies	Sedimentary structures	Bed Geometry	Modal Composition	Texture	Suggested Environment
Sm	Sand - fine to medium	Vertical burrow marks, channels, leaf impression, intraclasts	Wedge shaped	Quartz 69.9% Feldspar 3.7% Rock frag 6.2% Others 20.2%	M_Z = 2.47 σ_I = 0.45 SK_I = -0.05	Upper shore face
Sl	Sand - very fine to fine	Plane laminations, ripples, Horizontal bedding showing colour variations, horizontal traces	Shoestring	Quartz 73.6% Feldspar 3.3% Rock frag 4.7% Others 17.4%	M_Z = 2.84 σ_I = 0.68 SK_I = 0.50	Lower shoreface
Fx	Sand - fine to medium	Fine cross laminations, small dimension channels, burrows	Sheet	Quartz 76% Feldspar 2.9% Rock frag 1.7% Others 19.4%	M_Z = 2.50 σ_I = 0.47 SK_I = -0.01	Upper shore face
Fsm	Silt, Shale	Laminations, Increased bioturbation	Shoestring			Low energy, lower shore face
Fl	Mud	Plane laminations, Bioturbation, intraclasts	Wedge shaped			Offshore transition
Sr	Sand – fine to medium	Interference and Linguoid ripples with mud drapes	Wedge shaped	Quartz 80.5% Feldspar 1% Rock frag 3.5% Others 15%	M_Z = 2.18 σ_I = 0.41 SK_I = -0.21	Upper shoreface
Sr_w	Sand – fine to medium	Wave ripples, bifurcating ripples	Tabular	Quartz 79.3% Feldspar 1.2% Rock frag 4.7% Others 14.8%	M_Z = 2.27 σ_I = 0.41 SK_I = -0.61	Upper shoreface

Table 10: Summary of the characteristic features of seven lithofacies of the Barail sediments, SW of Kohima

References

Acharyya, S. (1982): Structural framework and tectonic evolution of the Eastern Himalaya, *Himalayan Geology*. **10:**412-439.

Acharyya, S. (1990): Pan-Indian Gondwana Plate break up and evolution of the northern and eastern collision margins of the Indian Plate, *Jour. Him. Geol*. **1:**75-91.

Acharyya, S. (2007): Evolution of the Himalayan Palaeogene foreland basins, influence of its litho-packet on the formation of thrust related domes and windows in the Eastern Himalayas – A review, *Jour. Asian Earth Sci.* **31:**1-17.

Agarwal, O.P. and Ghose, N.C. (1986): Geology and stratigraphy of Naga Ophiolite between Meluri and Awankho, Phek District, Nagaland, India, *In*: Ophiolites and Indian Plate Margins, (*Eds.* N.C. Ghose and S. Vardharajan), pp.163-195.

Allen, J.R.L. (1966): Note on the use of plaster of Paris in flow visualization and some geological applications, *Journal of Fluid Mechanics*. **25:**331-335.

Allen, J.R.L. (1967): Depth indicators of clastic sequences, *Marine Geology*. **5:**429-446.

Allen, J.R.L. (1982): Simple models for the shape and symmetry of tidal sand waves: Dynamically stable symmetrical equilibrium forms, *Marine Geology*. **48:**51-73.

Allen, R.; Najman, Y.; Carter, A.; Barfod, D.; Bickle, M.J.; Chapman, H.J.; Garzanti, E.; Vezzoli, G.; Ando, S. and Parrish, R.R. (2008): Provenance of the Tertiary sedimentary rocks of the Indo-Burman Ranges, Burma – Burman arc or Himalayan derived?, *Jour. Geol. Soc. London*. **165:**1045-1057.

Basu, A.; Young, S.W.; Suttner, L.J.; James, W.C. and Mack, G.H. (1975): Re-evaluation of the use of undulatory extinction and poly-crystallinity in detrital quartz for provenance interpretation, *Journal of Sedimentary Petrology*. **45:**873–882.

Bhandari, L.L.; Fuloria, B.C. and Sastri, V.V. (1973): Stratigraphy of Assam Valley, *Bull. Am. Assoc. of Petrol. Geol.* **57(4):**642-654.

Bhatia, M.R. (1983): Plate Tectonics and Geochemical Composition of Sandstones, *The Journal of Geology*. **91(6):**611–627.

Bjorkum, P.A. and Gjelsvik, N. (1988): An isochemical model for formation of authigenic kaolinite, K- feldspar and illite in sediments, *Journal of Sedimentary Petrology*. **58:**506-511.

Blatt, H. and Christie, J.M. (1963): Undulatory extinction in quartz of igneous and metamorphic rocks and its significance in provenance studies of sedimentary rocks, *Journal of Sedimentary Research*. **33(3):**559–579.

Blatt, H.; Middleton, G. and Murray, R. (1980): Origin of Sedimentary Rocks, *Prentice Hall Inc., Englewood Cliffs, New Jersey*. 782p.

Boggs, S. Jr. (2012): Petrography of Sedimentary Rocks, 2nd Edition, *Cambridge University Press*. 600p.

Boles, J.R. (1982): Active albitization of plagioclase, Gulf Coast Tertiary, *Amer. Jour. Sci.* **282:**165-180.

Borak, B. and Friedman, G.M. (1981): Textures of sandstones and carbonate rocks in the world's deepest wells (in excess of 30,000 ft. or 9.1 km): Anadarko Basin, Oklahoma, *Sedimentary Geology*. **29:**133-151.

Brunnschweiler, R. (1966): On the geology of Indo-Burman Ranges. *Journal of the Geological Society of Australia*. **13:**137-194.

Burley, S.D.; Kantorowicz, J.D. and Waugh, B. (1985): Clastic diagenesis. *In*: Sedimentology: Recent and Applied Aspects (*Eds*: P. Brenchley and B.P.B. Williams). *Spec. Publ. Geol. Soc. London, Blackwell Scientific Publications, Oxford*. **18:**189–226.

Carozzi, A.V. (1960): Microscopic Sedimentary Petrography. *Wiley, New York-London*, 485 p.

Casshyap, S.M. and Khan, Z.A. (1982): Paleohydrology of Permian Gondwana streams in Bokaro basin, Bihar, *J. Geol. Soc. India.* **23**:419–430.

Chakravarti, D.K. and Banerjee, R.M. (1988): Evolution of Kohima Synclinorium – A reappraisal, GSI. 115 pts 2 & 4.

Chappell, J. (1967): Recognizing fossil strand lines from grain-size analysis, *Journal of Sedimentary Research*. **37(1):**157–165.

Chaudhary, A.R. (1993): Textural parameters of the Nagthat sediments of the Chakarata Hills, Kumaun Himalayas, *Ind. Jour. Earth Sci*. **20(3&4):**119-125.

Collinson, J.D. and Thompson, D.B. (1994): Sedimentary Structures, *CBS Publishers, New Delhi*. 198p.

Condie, K.C. (1967): Geochemistry of early Precambrian Greywacke from Wyoming, *Geochim. Cosmochim. Acta*. **321:**2136-2147.

Conner, C.W. and Frem, J.C. (1966): Precision on linear and aerial measurements in estimating grain size, *Jour. Sediment. Petro*. **36:**397-402.

Conolly, J.R. (1965): The occurrence of polycrystallinity and undulatory extinction in quartz in snadstones, *Jour. Sediment. Petrol*. **35:**116-135.

Crook, K.A.W. (1974): Lithofacies and geotectonics: the significance of compositional variations in flysch arenites (graywackes). *In*: Modern and Ancient Geosynclinal Sedimentation (*Eds*. R.H. Dott and R.H. Shaver), *SEPM sepc. Pub*. **19:**304-310.

Curray, J.R. (1960): Sediments and history of the Holocene transgression, Continental Shelf, Gulf of Mexico. *In*: Recent Sediments, NW Gulf of Mexico (*Ed*. R.L. Miller), pp.175-203.

Dapples, E.C. (1979): Diagenesis of Sandstones. *In*: Diagenesis in sediments and sedimentary rocks (*Eds*. G. Larsen and G.V. Chilingar), Elsevier, pp.31–97.

Dasgupta, A.B. (1977): Geology of Assam-Arakan region, *Quart. Jour. Min. Met. Soc. India*. **49:**1-50.

Desikachar, S.V. (1974): A review of the tectonic and geologic history of the Eastern India in terms of plate tectonic theory, *Jour. Geol. Soc. India*. **15(2):**137-149.

Dickinson, W.R. (1970): Interpreting detrital modes of greywacke and arkose, *Jour. Sediment. Petrol*. **40:**695-707.

Dickinson, W.R. and Rich, E.I. (1972): Petrologic intervals and petrofacies in the great valley sequence, Sacramento Valley, California, *Geol. Soc. Am. Bull*. **83:**3007-3024.

Dickinson, W.R. and Suczek, C.A. (1979): Plate tectonics and sandstone composition. *Am. Assoc. Petrol. Geol. Bull*. **63:**2164-2182.

Dickinson, W.R. and Valloni, R. (1980): Plate setting and provenance of sands in modern ocean basin, *Geology*. **8:**82-86.

Dickinson, W.R. (1982): Composition of sandstones in circumpacific subduction complexes and fore arc basins, *AAPG Bull*. **66:**121-137.

Dickinson, W.R.; Beard, L.S.; Brakenridge, G.R.; Erjave, J.L.; Ferguson, R.C.; Inman, K.F.; Knepp, R.A.; Lindberg, F.A. and Ryberg, P.P. (1983): Provenance of North American Phanerozoic sandstones in relation to tectonic setting, *Geol. Soc. Am. Bull*. **94:**222-235.

Directorate of Geology and Mining, Nagaland (1978): Himalayan Orogenesis.

Duane, D. B. (1964): Significance of skewness in recent sediments, western Pamlico Sound, North Carolina, *Journal of Sedimentary Petrology*. **34(4):**864–874.

Dutton, S.P. and Diggs, T.N. (1990): Of quartz cementation in the Lower Cretaceous Travis Peak Formation, East Texas History, *Journal of Sedimentary Petrology*. **60:**191-202.

Einsele, G. and Seilacher, A. (1982): Cyclic and Event Stratification. *Springer-Verlag Inc., Berlin*, 536pp.

Evans, P. (1932): Tertiary succession in Assam, *Trans. Min. Geol. Inst. India*. **37:**155-260.

Folk, R.L. (1951): Stages of textural maturity in sedimentary rocks. *Jour. Sediment. Petrol*. **21:**127-130.

Folk, R.L. and Ward, W.C. (1957): Brazos River bar: A study in the significance of grain size parameters, *Jour. Sediment. Petrol*. **27:**3-26.

Folk, R.L. (1966): A review of grain size parameters, *Sedimentology*. **6:**73-93.

Folk, R.L. (1974): Petrology of Sedimentary Rocks. *Hemphill Publishing Co., Austin, Texas*, 170p.

Folk, R.L. (1980): Petrology of Sedimentary Rocks. *Hamphill's, Austin, Texas*, 182p.

Frey, R.W. (1975): The realm of ichnology, its strengths and laminations. *In*: The Study of Trace Fossils, *Springer-Verlag*, pp.13-38.

Frey, R.W.; Pemberton, S.G. and Saunders, T.D. (1990): Ichnofacies and bathymetry – a passive relation, *Jour. Paleont*. **64:**8-155.

Friedman, G.M. (1961): Distinction between dune, beach and river sands from textural characteristics, *Jour. Sediment. Petrol*. **36:**514-529.

Friedman, G.M. (1962): On sorting, sorting coefficient and the log normality of the grain size distribution of sandstones, *Jour. Geol*. **70:**737-753.

Friedman, G.M. (1967): Dynamic processes and statistical parameters compared for size frequency distribution of beach and river sands, *Jour. Sediment. Petrol*. **37:**327-354.

Friedman, G.M. and Sanders, J.E. (1978): Principles of Sedimentology, *Wiley, New York*, 792p.

Ganju, J.L. and Khar, B.M. (1985): Structures, tectonics and hydrocarbon prospect of Naga Hills based on integrated remotely sensed data, *Petro. Asia Jour*. **8(2):**142-151.

Geological Survey of India, (1975): Unpublished report.

Ghosh, S.K. and Chatterjee, B.K. (1994): Depositional mechanism as revealed from grain size measures of the Palaeoproterozoic Kolhan siliclastics, Keonjhar district, Orissa, India, *Sediment. Geol.* **89:**181-196.

Gilbert, J.M. De and Benner, J.S. (2002): The trace fossil Gyrochorte; ethology and palaeoecology, *Revista Española de Paleontologia*. **17:**1-12.

Goldring, R. (1965): Sediments into rock, *New Scientist*. **26:**863-865.

Griffiths, J.C. (1967): Scientific Methods in Analysis of Sediments, *McGraw-Hill, New York*, 508p.

Grim, R.E. (1968): Clay Mineralogy, 2nd Edition, *McGraw-Hill, New York*, 596p.

Haentzschel, W. (1975): Treatise on Invertebrate Paleontology. *In*: Part W (*Ed.* C. Teichert), *Miscellania Geol. Soc. Amer. and Univ. Kansas Press*, pp.38-122.

Harris, S.A. (1958): Differentiation of various Egyptian aeolian microenvironments by mechanical composition, *Jour. Sed. Petrol*. **28:**164-174.

Hayes, M.O. (1975): Morphology of sand accumulation in estuaries – An introduction to the symposium. *In*: Estuarine Research v.II, Geol. and Engg. (*Ed*. L.E. Cronin), *Academic Press, London*, pp3-22.

Heald, M.T. and Lorese, R.E. (1974): Inference of coating on quartz cementation, *Jour. Sed. Pet.* **44:**1269-1274.

Heer, O. (1865): Die Urwelt der Schewiz, *F. Schulthess, Zürich*. 622p.

Herron, M.M. (1988): Geochemical classification of terrigenous sands and shales from core or log data, *J. Sediment. Petrol*. **58:**820–829.

Heward, A.P. (1981): A review of wave dominated clastic shoreline deposits, *Earth Science Reviews*. **17:**223-276.

Hubert, J.F. and Hyde, M.G. (1982): Sheet flow deposits of graded beds and mudstones on an alluvial sandflat playa system, Upper Triassic Blomidon Red Beds. St. Mary's Bay, Nova Scotia, *Sedimentology*. **29:**437-475.

Imchen, W.; Thong, G.T. and Pongen, T. (2014): Provenance, tectonic setting and age of the sediments of the Upper Disang Formation in Phek District, Nagaland, *Jour. Asian Earth Sciences*. **88:**11-27.

Ingersoll, R.V. (1974): Surface textures of first cycle quartz sand grains, *Jour. Sediment. Petrol*. **44:**151-157.

Ingersoll, R.V. and Suczek, C.A. (1979): Petrology and provenance of Neogene sand from Nicobar and Bengal fans, DSDP sites 211 and 218, *J. Sediment. Petrol*. **49:**1217–1228.

James, W.C. and Oaks, R.Q. Jr. (1977): Petrology of the Kinnikinic quartzite (Middle Ordovician), East Central Idaho, *Jour. Sediment. Petrol*. **47:**1491-1511.

Jequet, J.M. and Varnet, J.P. (1976): Moment and graphic size parameters in the sediments of Lake Geneva, Switzerland, *Jour. Sed. Pet.* **46:**305-312.

Johnson, H.D. and Baldwin, C.T. (1986): Shallow siliciclastic seas. *In*: Sedimentary Environments and Facies (*Ed*. H.G. Reading), 2nd Edition, *Blackwell Scientific Pub., Oxford*, pp.229-282.

Johnson, M.A. and Stride, A.H. (1969): Geological significance of North Sea and transport rates, *Nature*. **224:**1016:1017.

Kakul, Z. (1968): Origin, development and chemical classification of early Palaeozoic sandstone of central Bohemia, *Proc. Int. Geo. Cong.*, pp61-72.

Kichu, A.M. and Srivastava, S.K. (2018): Diagenetic environment of Barail sandstones in and around Jotsoma Village, Kohima district, Nagaland, India, *Journal of Geoscience Research*. **3(1):**31-35.

Kichu, A.M.; Srivastava, S.K. and Khesoh, K. (2018): Trace fossils from Oligocene Barail sediments in and around Jotsoma, Kohima, Nagaland - implications for palaeoenvironment, *Jour. Palaeo. Soc. India*. **63(2)**:197-202.

Korsch, R. J. (1984): Sandstone composition from the New England Orogen, Eastern Australia – Implications for tectonic settings. *Jour. Sed. Petrol*. **51:**212-220.

Krinsley, D.H. and Doornkamp, J.C. (1973): Atlas of Quartz Sand Surface Textures, *Cambridge University Press*, 90p.

Krishnan, M.S. (1982): Geology of India and Burma, *CBS Publishers, New Delhi*, 635p.

Krumbein, W.C. and Pettijohn, F.J. (1938): Manual of Sedimentary Petrology, *Appleton-Century Crofts, New York.*

Kumar, R. and Naik, G.C. (2006): Late Eocene to early Oligocene depositional system in Assam Shelf, *6th International Conference & Exposition on Petroleum Geophysics, Kolkata, 2006*, pp.904-910.

Lakhar, A.C. and Hazarika, I.M. (2000): Significance of grain size parameters in environmental interpretation of the Tipam Sandstones, Jaipur area, Dibrugarh District, Assam, *Jour. Ind. Assoc. Sedimentologists*. **19(1-2):**69-78.

Lambiase, J.J. (1982): Turbulance and the generation of grain size distribution (Abst.), 11th International Congress on Sedimentology, Hamilton, pp.80-81.

Leeder, M.R. (1982): Sedimentology, *George Allen and Unwin, London*, 344p.

LeBlanc, R.J. (1972): Geometry of sandstone reservoir bodies. In: Underground Waste Management and Environmental Implications (*Ed*. T.D. Cook), *Am. Assoc. Petrol. Geo. Mem*. **18:**133-187.

LeMaitre, R.W. (1976): The chemical variability of some common igneous rocks, *Jour. Petrol.* **17:**589-637.

Lundgren, S.A.B. (1891): Studier Öfver fossilförande lösa block, *Geol. Fören. Stockholm, Forhandl.* **13:**111-121.

MacEachern, J.A.; Pemberton, S.G.; Gingras, M.K. and Bann, K.L. (2007): The ichnofacies paradigm: a fifty year retrospective. *In*: Trace Fossils: Concepts, Problems, Prospects (*Ed*. W. Miller), Elsevier, Amsterdam, p.52-77.

Mack (1984): The sands and sandstones of Eastern Moray, *Edinburgh Geol. Soc. Trans*. **7:**148-172.

Mackenzie, D. B. (1972): Primary stratigraphic traps in sandstones. *In*: Stratigraphic Oil and Gas Fields (*Ed*. R.E. King), *Soc. Explore Geophys. Spec. Pub*. **10:**47-63.

Mahendar, K. and Banerji, R.K. (1989): Textural study and depositional environment of sand grains from rocks of Jaisalmer Formation, Jaisalmer District, Rajasthan, India, *Jour. Geol. Soc. India*. **33(3):**228-242.

Mallet, F.R. (1876): On the coal fields of Naga Hills bordering the Lakhimpur and Sibsagar Distict, Assam. *Geol. Survey of India*. **12(2):**286p.

Marzolf, J.E. (1976): Sand grain frosting and quartz overgrowth examined by SEM – the Najavo Sandstone, Utah, *Jour. Sediment. Petrol*. **46:**906-912.

Mason, C.C. and Folk, R.L. (1958): Differentiation of beach, dune and eolian flat environments by size analysis, Mustang Islands, Texas, *Jour. Sediments. Petrol*. **28:**211-226.

Mathur, L.P. and Evans, P. (1964): Oil in India, *22nd session, Int. Geol. Congress, New Delhi, India*. 85p.

McLennan, S.M.; Hemming, S.; McDaniel, D.K. and Hanson, G.N. (1993): Geochemical approaches to sedimentation, provenance and tectonics, *Geol. Soc. Amer. Spl. Paper*. **284:**21-40.

McLennan, S.M. (1989): REE in sedimentary rocks – Influence of provenance and sedimentary processes. *In*: Geochemistry and Mineralogy of REE (*Eds*. B.R. Lipin and G.A. McKey), *Min. Soc. Am., Washington*, 348p.

Miall, A.D. (1990): Hierarchies of architectural units in clastic rocks and their relationships to sedimentation rate. *In*: The Three Dimensional Facies Architecture of Terrigenous Clastic Sediments (*Eds*. A.D. Miall and Tyler), Soc. Econ. Palalo. And Mineralogist.

Middleton, G.V. (1976): Hydraulic interpretation of sand size distributions, *Jour. Geol*. **84:**405-426.

Moiola, R.J. and Weiser, D. (1968): Textural parameter – an evaluation, *Jour. Sediment. Petrol*. **38:**45-53.

Morad, S.; Bergan, M.; Knarud, R. and Nystuen, J.P. (1990): Albitization of detrital plagioclase in Triassic reservoir sandstones from the Snorre Field, Norwegian North Sea, *J. Sediment. Petrol.* **60:**411-425.

Moss, A.J. (1972): Bed load sediments, *Sedimentology*. **18:**159-219.

Naik, G.C. (1994): Subsurface geology and tectono-sedimentary evolution of pre-Miocene sediments of Upper Assam, India, *PhD thesis submitted to ISM, Dhanbad*.

Naik, G.C. (1998): Tectonostratigraphic evolution and paleogeographic reconstruction of NE India, *Proc. Indo-German Workshop on Border Strandlogy Magnetostratigraphy Pilot Project, Calcutta*.

Okada, H. (1971): Classification of sandstone – analysis and proposal. Jour. Geol. **79:**509-525.

Pandey, N. and Srivastava, S.K. (1998): A preliminary report on Disang-Barail Transition, NW of Kohima, Nagaland (Abst.), *Workshop on Geodynamics and Natural Resources of NE India, Dibrugarh*, p.24.

Passega, R. (1957): Textures as characteristics of clastic deposition, *Bull. Am. Assoc. Petrol. Geol.* **41:**1952-1984.

Passega, R. (1964): Grain size representation by CM patterns as a geological tool, *Jour. Sediment. Petrol*. **34:**830-847.

Passega, R. and Benarjee, R. (1969): Grain size image of clastic deposits, *Sedimentology*. **13:**233-252.

Passega, R. (1977): Significance of CM diagrams of sediments deposited by suspensions, *Sedimentology*. **24:**723-733.

Pettijohn, F.J.; Potter, P.E. and Siever, R. (1972): Sand and Sandstones, *Springer-Verlag*, 617p.

Pettijohn, F.J. (1975): Sedimentary Rocks, 3rd Edition, *Harper and Row*, 614p.

Pitman, E.D. (1972): Diagenesis of quartz in sandstone as revealed by SEM, *Jour. Sed. Petrol.* **42:**507-519.

Potter, P.E. and Pettijohn, F.J. (1977): Palaeocurrents and Basin Analysis, *Springer-Verlag, New York*, 425p.

Potter, P.E. (1978a): Significance and origin of big rivers, *Jour. Geol*. **86:**13-33.

Potter, P.E. (1978b): Petrology and chemistry of modern big rivers, *Jour. Geol*. **86:**423-449.

Prothero, D.R. (2004): Sedimentary Geology, *W.H. Freeman & Co., New York*, 557p.

Rangarao, A. (1983): Geology and hydrocarbon potential of a part of Assam-Arakan Basin and its adjacent region, *Petroleum Asia Jour.*, pp.127-158.

Reading, H.G. (1978): Sedimentary Environment and Facies, *Elsevier, North Holland, New York*, 464p.

Reading, H.G. (1986): Sedimentary Environment and Facies, *Elsevier, New York*, 464p.

Reineck, H.E. and Singh, I.B. (1980): Depositional Sedimentary Environments. *Springer-Verlag, New York*, 547p.

Roser, B.P. and Korsch, R.J. (1986): Determination of tectonic setting of sandstone-mudstone suites using SiO_2 content and Na_2O/K_2O ratio, *Jour. Geol*. 49:635-650.

Sagoe, K.O. and Visher, G.S. (1977): Population breaks in grain size distribution of sand – a theoretical model, *Jour, Sediment. Petrol*. **47:**285-310.

Sahu, B.K. (1964): Depositional mechanism from size analysis of clastic sediments, *Jour. Sediment. Petrol*. **34:**73-83.

Sahu, B.K. (1983): Multigroup discrimination of depositional environments using size discrimination statistics, *Ind. Jour. Earth Sci.* **10:**20-29.

Schwab, F.L. (1975): Framework mineralogy and chemical composition of continental margin-type sandstone, *Geology*. **3:**487-490.

Seilacher, A. (1967): Bathymetry of trace fossils, *Marine Geology*. **5:**413-428.

Selley, R.C. (1968): A classification of palaeocurrent models, *Jour. Geol*. **76:**349-368.

Selley, R.C. (1970): Ancient Sedimentary Environments, *Chapman and Hall, London*, 273p.

Selley, R.C. (1976): Subsurface environmental analysis of North Sea sediments, *Bull. Am. Assoc. Petrol. Geol.* **60:**184-195.

Sengupta, S.M. (1982): Interpretation of log probability graphs of grain sizes in the light of experimental studies (Abst.), *11th International Congress on Sedimentology, Hamilton*, p.81.

Sengupta, S.M. (1994): Introduction to Sedimentology, *Oxford and IBH Publishing Co.*, 314p.

Sevon, W.D. (1966): Distinction of New Zealand beach, dune and river sands by their grain size distribution characteristics, New Zealand, *Jour. Geol. and Geophys*. **19:**212-223.

Singh, B.P.; Pawar, J.S. and Karlupia, S.K. (2004): Dense mineral data from the north western Himalayan foreland sedimentary rocks and recent sediments - evaluation of the hinderland, *Jour. Asian. Earth Sci*. **23:**23-25.

Singh, H.S.; Rodriguez-Tovar, F.J. and Ibotombi, S. (2008): Trace fossils of the Upper Eocene-Lower Oligocene Transition of the Manipur Indo-Myanmar Ranges (Northeast India), *Turkish Journal of Earth Sciences*. **17:**821-834.

Smith, R. (1966): Grain size measurement in thin section and in grain mount, *Jour. Sediment. Petrol.* **36:**841-843.

Srivastava, S.K. and Pandey, N. (2001): Palaeoenvironmental reconstruction of Palaeogene Disang-Barail Transitional Sequences, NW of Kohima, Nagaland, NE India (Abst.), *Seminar on Contribution to Himalayan Geology, Dehra Dun*, p.7.

Srivastava, S.K. (2002): Facies architecture and depositional model for Palaeogene Disang-Barail Transition, North West of Kohima, Nagaland, *Unpub. PhD thesis, Nagaland University, Kohima*.

Srivastava, S.K.; Pandey, N. and Srivastava, V. (2004): Tectono-sedimentary evolution of Disang-Barail Transition, NW of Kohima, Nagaland, India, *Himalayan Geology*. **25(2):**121-128.

Srivastava, S.K. and Pandey, N. (2005): Depositional mechanism of Palaeogene sediments at Disang-Barail Transition, NW of Kohima, Nagaland, India, *Jour. Pal. Soc. India*. **50(1):**135-140.

Srivastava, S.K. and Pandey, N. (2008): Palaeoenvironmental reconstruction of Disang-Barail Transition using grain size parameters in Nagaland, *Nagaland Univ. Res. Jour.* **5:**164-176.

Srivastava, S.K. and Pandey, N. (2011): Search for provenance of Oligocene Barail sandstones in and around Jotsoma, Kohima, Nagaland, *Journal of the Geological Society of India*. **77:**433-442.

Srivastava, S.K. and Kesen, K. (2018): Tectonic-sedimentary evolution of Laisong sandstones exposed in and around pherima, Dimapur, Nagaland, *Journal of Applied Geochemistry*. **19(4)**:471-479.

Stauffer, P.H. (1966): Thin section size analysis – a further note, *Sedimentology*. **7:**261-263.

Stewert, H.B. Jr. (1958): Sedimentary reflections of depositional environments in San Miguel Lagoon, Baja California, Mexico, *Am. Assoc. Petrol. Geol. Bull*. **2:**2567-2618.

Suczek, C.A. and Ingersoll, R.V. (1985): Petrology and provenance of Cenozoic sandform in the Indus Cone and Arabian Basin (DSDP sites 221, 222, 224), *Jour. Sed. Petrol.* **55:**340-346.

Surdam, R.C. and Boles, R.J. (1979): Diagenesis of Volcanic Sandstones. *In*: (*Eds*. P.A. Scholle and P.R.Schluger).

Surdam, R.C.; Crosse, L.J.; Hagen, E.S. and Heasler, H.P. (1989): Organic inorganic interactions and sandstone diagenesis, *Amer.Asso. Petrol. Geol. Bull.* **73:**1-23.

Suttner, L.J.; Basu, A. and Mack, G.H. (1981): Climate and the origin of quartz arenites, *Jour. Sed. Petrol.* **51:**1235-1246.

Suttner, L.J. and Dutta, P.K. (1986): Alluvial sandstone composition and palaeoclimate framework mineralogy, *Jour. Sed. Petrol.* **56:**329-345.

Swan, D; Clague, J. J. and Luternauer, L. J. (1978): Grain size statistics II - Evaluation of grouped moment measures, *Jour. Sed. Pet.* **49(2):**487-500.

Swift, D.J.P. (1969): Inner shelf sedimentation: processes and products. *In*: The New Concepts of Continental Margin Sedimentation – Application to the Geological Records (*Ed*. D.J. Stanley), *Am. Geol. Instt., Washington*, pp.DS.5-1.

Swift, D.J.P.; Stanley, D.J. and Curray, J.R. (1971): Relict sediments on continental shelf – a reconsideration, *Jour. Geol*. **79:**322-346.

Tanner, W.F. (1964): Modification of sediment size distributions, *Jour. Sediment. Petrol*. **34:**156-164.

Textoris, D.A. (1971): Grain size measurement in thin section. *In*: Procedures in Sedimentary Petrology (*Ed*. R.E. Craver), *Wiley, New York*, pp.95-108.

Tiwari, R.P.; Rajkonwar, C.; Lalchawimawii, Malsawma, P. L. J.; Ralte, V. Z. and Patel, S.J. (2011): Trace fossils from Bhuban Formation, Surma Group (Lower to Middle Miocene) of Mizoram, India and their palaeoenvironmental significance, *Journal of Earth System Sciences*. **120(6):**1127-1143.

Tortosa, A.; Palomares, M. and Arribas J. (1991): Quartz grain types in Holocene deposits from the Spanish central system - some problems in provenance and analysis. *In*: Developments in Sedimentary Provenance Studies (*Eds*. A.C. Morton, S.P. Todd and P.D.W. Haughton), *Geological Society of America Special Publications, Bath, UK*. **57:**447-454.

Towe, K.M. (1962): Clay mineral diagenesis as a possible source of silica cement in sedimentary rocks, *Jour. sediment. Petrol*. **32:**26–28.

Tucker, R.W. and Vacher, H.L. (1980): Effectiveness of discriminating beach, dune and river sands by moments and the cumulative weight percentages, *Jour. Sed. Pet*. **50:**165-172.

Tucker, R.W. (1989): Techniques in Sedimentology, *Blackwell Scientific Publications, Oxford, London*.

Tucker, R.W. (1993): Carbonate diagenesis and sequence stratigraphy. *In*: Sedimentology Review (*Ed*. W.P. Wright). **1:**51-72.

Uddin, A and Lundberg, (1998): Cenozoic history of Himalayan-Bengal system, Bangladesh, *Bull. Geol. Soc. Amer*. **110(4):**497-511.

Uddin, A.; Kumar, P.; Sarma, N.J. and Akhtar, H.S. (2007): Heavy mineral constraints of the provenance of Cenozoic sediments from the foreland basins of Assam and

Bangladesh – erosional history of the Eastern Himalayas and the Indo-Burman Ranges, *Developments in Sedimentology*, **55:**823-847.

Visher, G.S. (1965): Fluvial processes as interpreted from ancient and recent fluvial deposits. *In*: Primary Sedimentary Structures and their Hydrodynamic Interpretation (*Ed*. G.V. Middleton), *Soc. Econ. Palaeont. Mineral*, Sp. Pub. **12:**265.

Visher, G.S. (1969): Grain size distribution and depositional processes, *Jour. Sed. Pet*. **39(3):**1074-1106.

Visher, G.S. (1970): Fluvial processes as interpreted from ancient and recent fluvial deposits, *Soc. Econ. Palaeont. Mineralogy*, Sp. Pub. **12:**116-132.

Walker, R. and James, N. (1992): Facies models: response to sea level change, *Geological Association of Canada*, 407p.

Walker, T.R. (1974): Formation of red beds in moist tropical climates - a hypothesis, *Geol. Soc. Am. Bull*. **85:**633-638.

Walther, J. (1894): Einleitung in die Geologic Alshistosische Wisenchaft, *Jena Verlag Von Gustav Fischer*. **3:**1055p.

Walton, E.K.; Stephens, W.E. and Shawa, M.S. (1980): Reading segmented grain –size curves, *Geol. Mag*. **117:**517-524.

Wentworth, C.K. (1922): A scale of grade and class terms for sediments, *Jour. Geol*. **30:**377-392.

Zuffa, G.G. (1980): Hybrid arenites: their composition and classification, *Journal of Sedimentary Research*. **50(1):**21–29.